Shp2 functions in postnatal skeletal muscle growth and regeneration

Inaugural-Dissertation

to obtain the academic degree

Doctor rerum naturalium (Dr. rer. nat.)

submitted to the Department of Biology, Chemistry and Pharmacy of Freie Universität Berlin

by

Joscha Griger

from Konstanz

July, 2015

This work was carried out at the Max-Delbrück-Center for Molecular Medicine from August 2010 to July 2015 under the supervision of Prof. Dr. Carmen Birchmeier.

1st Reviewer: Prof. Dr. Carmen Birchmeier
2nd Reviewer: Prof. Dr. Fritz Rathjen .

Date of defense: 06.11.2015

Acknowledgements

Table of Contents

I. Introduction

1. Embryonic and fetal skeletal muscle development

All vertebrate skeletal muscle of the trunk and limbs originates from somites. Somites are cell compartments of epithelial structures that lie on both sides along the neural tube and notochord. They derive from unsegmented paraxial mesoderm (PSM) that is progressively segmented in an anterior to posterior manner during early embryogenesis (overview in Hubaud & Pourquié, 2014, Maroto, 2012). Subsequently, signals from the adjacent tissue induce further differentiation of the somite (overview in Christ, 2007 & Maroto, 2012; Yusuf, 2006). Notochord-derived Shh induces the de-epithelialization of the ventromedial somite and formation of the sclerotome that will eventually give rise to the vertebral column. Wnt signals from the neural tube and dorsal ectoderm as well as Bmp signals from the lateral plate specify the formation of the dorsolateral dermomyotome (Wagner, 2000; Fan, 1997; Marcelle, 1997).

The first wave of myogenic differentiation starts around E8.5 when postmitotic myogenic precursor cells delaminate from the dorsomedial and ventrolateral lip of the dermomyotome to establish the primary myotome below the dermomyotome. These cells orient rostrocaudally and differentiate into primary myofibers that provide a scaffold for further muscle formation (Fig. 1.1, Tajbakhsh, 2000; Denetclaw, 2000; Kahane, 1998a &1998b). The dermomyotome expands along the dorsoventral axis, and epaxial and hypaxial dermomyotome can be discriminated (Denetclaw, 2000; Spörle, 2001). The epaxial dermomyotome will give rise to muscles associated with the vertebrae and ribs whereas the hypaxial part will form muscles distant from the dermomyotome, i.e. body wall, intercostal, diaphragm and limb musculature. The genetic hierarchies controlling myogenesis in these two compartments are different (see I.2). Around E11, the central part of the dermomyotome looses its epithelial structure and generates single cells, positive for the paired- and homeo-domain transcription factors Pax3 and Pax7 that enter the early myotome (Gros, 2005; Kassar-Duchossoy, 2005; Relaix, 2005). During embryonic as well as fetal muscle growth this population marks myogenic progenitor cells that do not express myogenic determination genes but are able to initiate the myogenic program. Pax3 and Pax7 are essential to maintain their identity as muscle stem cells. In Pax3/Pax7 double mutants embryonic and fetal muscle development is abrogated (details see I.2; Relaix, 2005). Notch signals are essential to maintain this progenitor cell population

and mutation of Rbp-J, the transcriptional mediator of the Notch signaling pathway, induces premature differentiation in muscle precursor cells (Vasyutina, 2007).
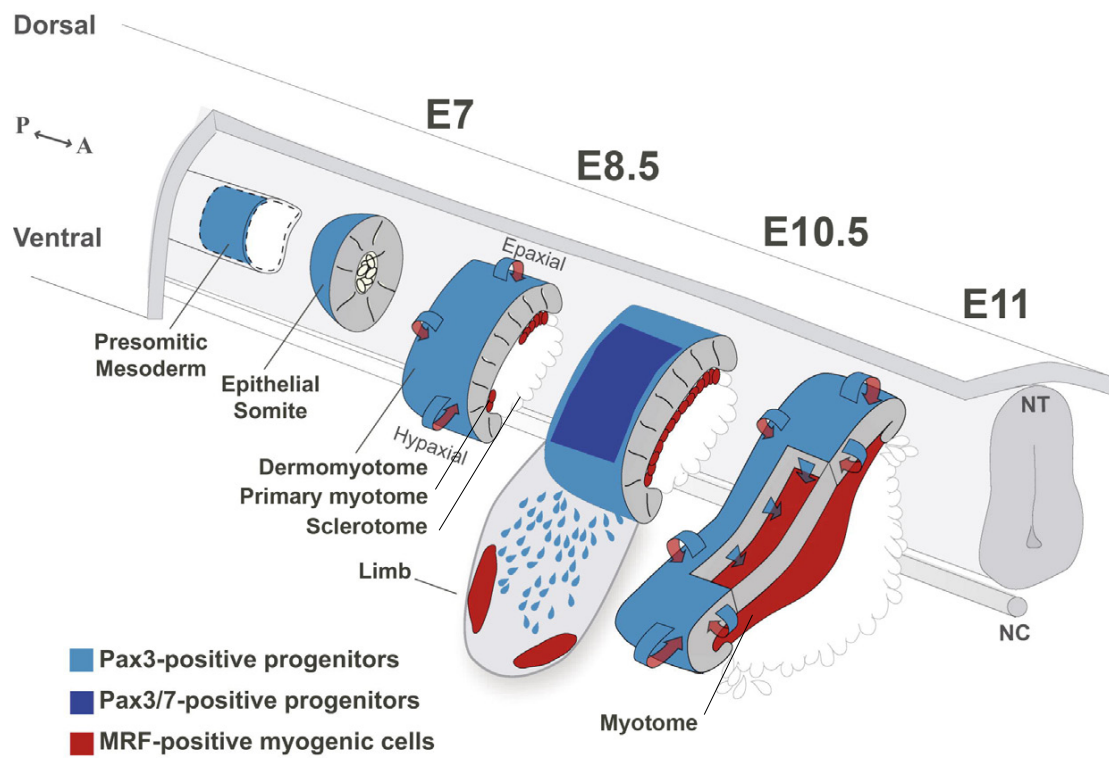
Fig. 1.1: Schematics of early somitogenesis and primary mouse myogenesis. Details see text (Adapted from Buckingham & Rigby, 2014)

On particular axial levels, Pax3+ cells delaminate from the hypaxial dermomyotome around E10 and migrate into the limbs, tongue and diaphragm anlage where they will form the progenitor pool and muscle. The receptor tyrosine kinase Met, a Pax3 target gene, and its ligand HGF are essential to initiate this migration (Bladt, 1995; Dietrich, 1999; Ginsberg, 1998; Epstein, 1996; Schienda, 2006). In Met or HGF mutant mice, myogenic precursor cells are unable to delaminate and to migrate to the sites distant from the dermomyotome, i.e. limb buds, tongue and diaphragm anlage. Furthermore, all migrating myogenic progenitors express the homeobox transcription factor Lbx1 (Mennerich, 1999; Brohmann, 2000). In mice lacking Lbx1, migratory precursors are specified normally but only few cells migrate to their targets. Cxcr4 is a G-protein coupled receptor expressed in migrating muscle precursor cells (Vasyutina, 2005). Its ligand SDF1 is expressed in the limb. Mutations of Cxcr4 or SDF1 have only mild effects on the migration of progenitor cells. Gab1 is an adaptor protein essential for signal transmission of Met, and Gab1 mutant mice show an impaired migration of

myogenic progenitors (Sachs, 2000). Cxcr4 and Gab1 cooperate to control migration of myogenic progenitors, and the combined mutation of Cxcr4 and Gab1 interferes very strongly with migration of myogenic progenitor cells (Vasyutina, 2005).

During fetal stages (starting from E14.5) a secondary myogenic phase takes place where progenitor cells that express Pax7 settle between primary myofibers. These cells extensively proliferate and fuse to primary myofibers or form secondary fibers (Relaix, 2005). Biressi et al. characterized fetal and embryonic myogenic progenitors and discovered that the transcriptional profile of embryonic (E11) and fetal (E16) Myf5+ cells differ from each other (Biressi, 2007). For instance, fetal progenitors cells up-regulate several cell surface proteins that can be used for their isolation by FACS, e.g. VCAM1, integrinα7 and Syndecan3 & Syndecan4 (Bröhl, 2012; Chakkalakal, 2014; Cornelison, 2001). Additionally, fetal and embryonic cells differ in differentiation capabilities, responsiveness to growth factors and Nfix expression (Messina, 2010). Nfix controls the activation of fetal gene expression in myogenic progenitors and skeletal muscle. Conditional mutation of Nfix using MyoD-Cre resulted in abrogated expression of fetal specific genes like β-enolase, muscle creatine kinase and persistent expression of genes specific for embryonic muscle, e.g. slowMyHC. Furthermore, overexpression of Nfix in embryonic muscle (E12.5) under the control of the Myosin light chain 1F promoter suffices to initiate the expression of fetal genes in embryonic muscle. Thus, Nfix is a master regulator that coordinates the switch from embryonic to fetal myogenic progenitor cells.

Before E16, myogenic progenitors are only loosely attached to the developing muscle fibers that do not yet possess a basal lamina. Starting from E15-E16, the progenitor cells assume a Satellite cell position, i.e. muscle progenitor cells begin to locate between the newly formed basal lamina and the muscle fiber (Rosen, 1992; Kassar-Duchossoy, 2005; Relaix, 2005). This process is completed around E17-E18. Homing of myogenic precursor cells to their niche is controlled by Notch signals. Satellite cells lacking Rbp-J and MyoD, which rescues premature myogenic differentiation of Rbp-J mutant precursor cells, do not localize beneath the basal lamina (Bröhl, 2012).

2. Genetic hierarchies defining myogenic progenitor cells

Myogenic differentiation of muscle precursor cells is controlled by myogenic regulatory factors (MRF), which comprise transcription factors of the MyoD family, i.e. myogenic factor 5 (Myf5), myogenic determination 1 (MyoD1), myogenic factor 6 (Myf6, also known as Mrf4) and myogenin (MyoG). Myf5 and MyoD act as determination factors whereas Mrf4 and MyoG have roles in the terminal differentiation of myogenic precursor cells. Nevertheless, Mrf4 also has a muscle-determining role during primary myogenesis. This core network is the same in all skeletal muscles of the trunk and limb. Upstream regulators that induce expression of the determination factors MyoD and Myf5 differ in the epaxial and hypaxial dermomyotome as well as different developmental stages, i.e. primary, secondary myogenesis and postnatal myogenesis.

Myf5 is the first MRF expressed in the epaxial dermomyotome and is subsequently activated in the hypaxial domain (Tajbakhsh, 2000). Besides a marked delay in epaxial myogenesis, Myf5 mutant mice do not show any overt skeletal muscle phenotype (Braun, 1992). MyoD is initially expressed in the hypaxial and subsequently in the epaxial domain. Similar to Myf5, loss of MyoD does not cause a dramatic phenotype during embryonic and fetal muscle development, except a delay in hypaxial myogenesis (Rudnicki, 1992). However, MyoD and Myf5 double mutant mice do not develop any skeletal muscle indicating that these genes act in a redundant manner, i.e. at least one of these factors is required to activate the myogenic determination program (Rudnicki, 1993). The Mrf4 locus is closely linked to the Myf5 locus. The mutation that eliminates Myf5 interferes also with expression of Mrf4. Experiments using different Myf5 mutant alleles that differentially affect the Mrf4 locus showed that Mrf4 suffices to initiate differentiation during primary myogenesis (Kassar-Duchossoy, 2004). Therefore, MyoD, Myf5 and Mrf4 can independently initiate myogenesis during early myogenesis. In later stages, myogenic determination depends only on Myf5 and MyoD and Mrf4 is expressed only in differentiating myogenic cells (Patapoutian, 1995; Zhang, 1995). MyoG is essential for the terminal myogenic differentiation. In MyoG mutant mice, muscle formation is initiated normally but terminal differentiation is completely abolished (Hasty, 1993; Nabeshima, 1993). Hence, MyoG functions downstream of MyoD and Myf5.

Upstream regulators of myogenic determination differ during primary and secondary myogenesis as well as postnatal muscle development. Pax3 and Pax7 are two paired- and homeo-domain transcription factors that emerged as important regulators

of myogenesis. Pax3 is expressed in the PSM and segmented somites and becomes restricted to the dermomyotome during subsequent development (Williams, 1994; Goulding, 1994). Pax3 and Pax7 positive cells from the central part of the dermomyotome delaminate and constitute a progenitor pool that is maintained throughout embryonic and fetal muscle development, which maintains the myogenic precursor pool. Embryos that lack both genes cannot form embryonic and fetal muscle, but form an early myotome (Relaix, 2005). Thus, primary myotome development is independent of Pax3 and Pax7. In the epaxial dermomyotome Shh and Wnt signals induce and maintain Myf5 expression (Gustafsson, 2002; Teboul, 2003; Borello, 2006). Initial experiments mutating Pax3 and Myf5(Mrf4) resulted in complete ablation of skeletal muscle (Tajbakhsh, 1997). This suggested that MyoD expression depends on either Pax3 or Myf5. Additionally, Pax3 regulates Myf5 expression in an indirect manner in the epaxial and the hypaxial domain (Sato, 2010; Bajard, 2006).

Hypaxial muscle formation depends on sine oculis homeobox homologue (Six) transcription factors and their transcriptional co-activators eyes absent (Eya). Both Six1-/-, Six4-/- and Eya1-/-, Eya2-/- double mutants loose Pax3 expression in the hypaxial domain and lack all limb muscles, indicating a role for Six/Eya complexes upstream of Pax3 in hypaxial muscles (Grifone, 2005). Moreover, Six/Eya complexes control MRF expression in the hypaxial dermomyotome, and Six1/Six4 double mutants down-regulate expression of Mrf4, MyoD and Myf5 (Grifone, 2005; Grifone, 2007; Relaix, 2013).
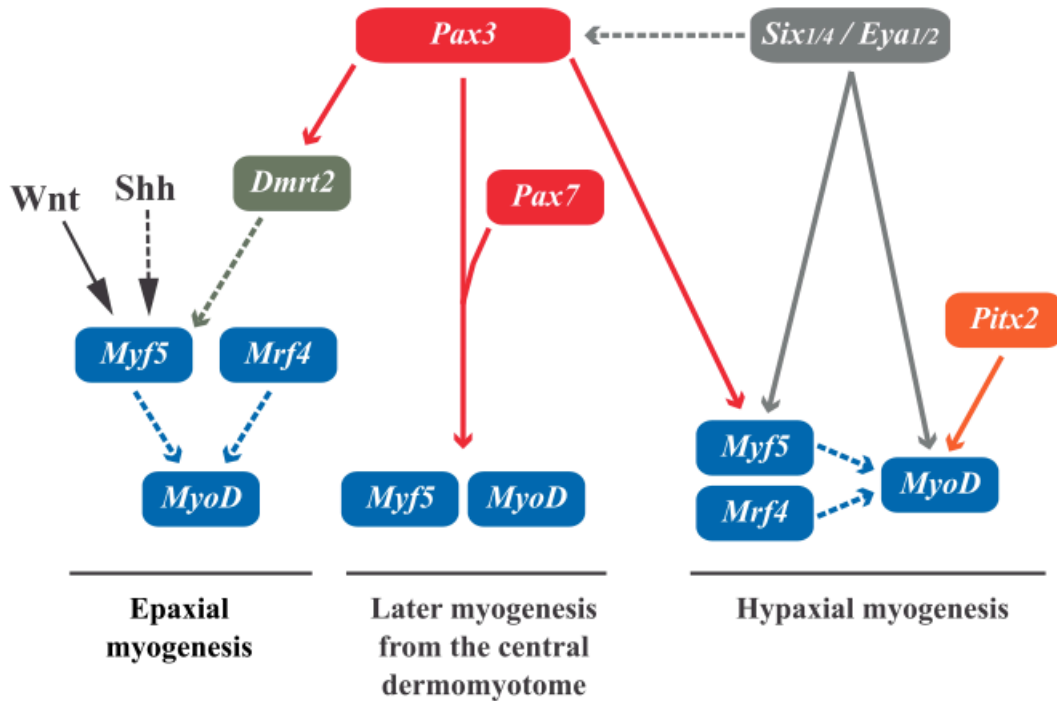
Fig. 1.2: Schematic representation of genetic transcription factor hierarchies controlling myogenic differentiation. Details see I.2 (adapted from Buckingham & Rigby, 2014).

In migrating myogenic progenitor cells Pax7 expression initiates when Pax3+ cells have settled in the limb muscle anlage (Hutcheson, 2009, Schienda, 2006). Pax3 becomes down-regulated in most limb myogenic progenitor cells in fetal development (Relaix, 2006). Pax7 mutant mice do not show any apparent muscle phenotype during embryonic and fetal muscle development probably due to functional compensation by Pax3 (Relaix, 2006). However, postnatal myogenesis is severely impaired due to cell death of Satellite cells suggesting that Pax3 and Pax7 have only partially redundant functions. Recent reports on Pax7 functions in Satellite cells suggested that Pax7 is only essential for early postnatal muscle growth but dispensable for adult muscle regeneration (Lepper, 2009). Later studies questioned this finding, since Pax7 mutation impaired long-term maintenance of Satellite cells (von Maltzahn, 2013; Günther, 2013). Günther and colleagues proposed that in Pax7^{-/-} Satellite cells, activated Satellite cells differentiate and are not lost by cell death, a distinct mechanism from the one observed in the early postnatal phase where Pax7^{-/-} Satellite cells undergo apoptosis.

3. Early postnatal skeletal muscle development

Skeletal muscle progenitors form muscle, but the shape of the muscle groups is determined by surrounding mesenchymal cells (Mathew, 2011; Kardon, 2003). This process is called muscle patterning and is completed at birth. Furthermore, fiber numbers do no longer increase in the first postnatal weeks (White, 2010). Nevertheless, mice increase dramatically in weight and size during the first weeks after birth, and all organs including skeletal muscle grow during this phase. Early postnatal muscle growth (P0-P21) is accomplished by fusion of new nuclei to already existing fibers. Satellite cells proliferate extensively in young postnatal muscle and provide the major source of myonuclei for postnatal fiber growth (Moss & Leblond, 1970, Moss & Leblond, 1971). After P21 the number of nuclei in fibers is stable, and muscle growth in subsequent stages is mainly accomplished by hypertrophy (Ontell, 1984; White, 2010).

About 30-35 % of nuclei in early postnatal mouse muscle are Satellite cells. During the first 3 weeks after birth Satellite cells proliferate to generate progeny that either self-renews to maintain the stem cell pool or differentiates to contribute to the growing muscle. However, the numbers of Satellite cells constantly decline until postnatal day 21 when they reach an equilibrium, and constitute less than 5% of all nuclei in the muscle (Albrook, 1971; Hellmuth, 1971; White, 2010). Satellite cells are thought to enter quiescence around P21, even though a fraction still expresses the cell cycle marker Ki67 at P28 (Schultz, 1978; Bröhl & Birchmeier, unpublished observation). Indeed, recent work demonstrates that Satellite cells still fuse to adult muscle fibers, even when the muscle is not damaged (Keefe, 2015).

Extracellular signals that regulate early postnatal proliferation and differentiation of Satellite cells are largely unknown. Several tyrosine kinase, cytokine and integrin receptors like the fibroblast growth factor receptors 1 & 4 (Fgfr1/4), the insulin-like growth factor receptor 1 (Igfr1), Met, Myostatin receptor and Integrinα6/α7/β1 are expressed in young postnatal Satellite cells (data from unpublished transcriptome analysis of FACS-isolated Pax3-GFP+ cells from the Relaix laboratory). But how Satellite cells are regulated by these receptors is not known.

Notch controls the expression of several bHLH factors in Satellite cells, like Hes1, Hey and HeyL and Notch signaling in Satellite cells is essential to enter quiescence in the early postnatal phase (overview Mourikis, 2014;). Hey1/HeyL double mutants or Hes1 single mutants Satellite cells up-regulate MyoD and Ki67 indicating that they remain in an active state (Fukada, 2011; Bröhl & Birchmeier, unpublished results).

Moreover, Rbp-J mutant Satellite cells cannot maintain quiescence and differentiate, whereas Notch activation by overexpression of the intracellular Notch domain (NICD) blocks proliferation and induces expression of markers typically expressed by mature/quiescent Satellite cells (Bjornson, 2012; Mourikis, 2012).

4. Satellite cells – stem cells of adult muscles

Adult skeletal muscle has a tremendous regeneration potential upon injury or exercise (Collins, 2005; Sadeh, 1985). For instance, when the *Tibialis anterior* muscle is destroyed by injection of toxin, it is regenerated within a period of two weeks (overview in Musarò, 2014). Satellite cells are the major stem cell population responsible for regeneration (Collins, 2005; Lepper, 2011; Sambasivan, 2011). These cells, first identified due to their characteristic location wedged in between the lamina and the muscle fiber, express a variety of nuclear and cell surface markers which can be used for their identification and isolation, amongst others Pax7, VCAM1 and Syndecan3/4 or Itgα7 (Mauro, 1961; Seale, 2000; Liu, 2013; Cornelison, 2001; Brack, 2007, Chakkalakal, 2014). In resting muscle, they are in a dormant or quiescent state but are quickly activated by injuries. Activation is characterized by up-regulation of MyoD and/or Myf5 and proliferation (Zammit, 2002). Activated Satellite either self renew to repopulate the Satellite cell pool or differentiate to repair injured muscle fibers (Lipton & Schultz, 1979; Collins, 2005; Zammit, 2004).

Activation of Satellite cells is a multi-step process that includes the disappearance of stress granules, initiation of protein synthesis from pre-existing mRNAs that were silenced (Myf5), down-regulation of the cell cycle inhibitor p27 and deactivation of the retinoblastoma tumor suppressor protein Rb as well as transcription/translation of MyoD (Crist, 2012; Zammit, 2002; Chakkalakal, 2014; Hosoyama, 2011). Subsequently, Satellite cells enter the cell cycle and express multiple cyclins and other cell cycle regulators (Fukada, 2007). Due to the complex changes during activation, the first cell cycle takes significantly longer than subsequent cycles (Siegel, 2011; Rocheteau, 2012). Injuries of muscle fibers and the surrounding extracellular matrix release mitogens that activate Satellite cells (Bischoff, 1986 & 1990). An elegant study identified a pre-activation state of Satellite cells, termed G_{Alert}, which is induced by systemic factors. These factors are released by injured muscle tissue and act on muscle tissue distant from the site of injury, i.e. the contralateral *Tibialis anterior*. G_{Alert} Satellite cells initiated phosphorylation of the ribosomal protein S6 by mTORC1, have increased metabolic activity and up-regulate

cyclins but do not incorporate BrdU (Rodgers, 2014; Ma & Blenis, 2009). Met and its ligand HGF were implicated in this process. Met mutant Satellite cells distant from the sites of injury lacked up-regulation of phospho-S6 and showed a delayed first division in culture. Conversely, HGF injections in resting muscle leads to aberrant Satellite cell activation (Tatsumi, 1998).

Signals regulating the eventual cell cycle entry are not well analyzed *in vivo*. Several mitogens, including HGF, Igf1 and Fgf's, were shown to be present in regenerating muscle and capable of activating Satellite cells. Satellite cells express the according receptors and respond to these factors in culture (overview in Bentzinger, 2010). Furthermore, p38 Mapk signaling was described to be essential for cell cycle entry and Mapk/Erk signaling seems to be crucial for the G_1 to S phase transition of cultured Satellite cells (Jones, 2001 & 2005). However, the underlying signaling pathways that activate Satellite cells *in vivo* are not understood.

Satellite cells undergo several rounds of symmetric divisions to generate enough myogenic precursor cells for repair of injured muscle. All activated Satellite cells express the non-canonical Wnt receptor Fzd7. Its ligand Wnt7a is secreted by regenerating myofibers and activation of Fzd7 drives the symmetric expansion of Satellite cells by activation of the planar-cell-polarity pathway (Le Grand, 2009; Bentzinger, 2013).

Satellite cells up-regulate myogenic transcriptions factors to progress towards differentiation. The p38 Mapk signaling pathway was suggested to play a role in activation of the myogenic program and differentiation. In asymmetric divisions, activated p38 was distributed to the committed daughter cells by the Par complex and induced MyoD expression (Troy, 2012). Another study reported that p38 activity regulates repressive epigenetic marks on the Pax7 promoter thought the polycomb complex (Palacios, 2010).

Satellite cell heterogeneity in the adult

Several groups described that adult subpopulations of Pax7+ cells differ in regards to their stemness, i.e. ability to self renew. How these different populations are related to each other is so far not fully understood.

Lineage tracing of Myf5+ cells (using a Myf5[Cre] transgene and a YFP reporter) identified a small subset of Satellite cells that never expressed Myf5 until adulthood (Kuang, 2007). These Pax7+Myf5- cells were able to divide asymmetrically and are

thought to be particularly stem cell-like, i.e. the balance between self-renewal and differentiation is shifted towards self-renewal. In contrast, Pax7+Myf5+ Satellite cells are more committed to the myogenic lineage and are more likely to differentiate. Picard and colleagues independently demonstrated the occurrence of two distinct progenitor lineages, i.e. Pax7+Myf5- & Pax7+Myf5+, in embryonic and fetal muscle of the chick (Picard, 2013).

Recently, pulse-chase experiments using an inducible GFP-tagged Histone H2B identified two populations of myogenic precursor cells, a slowly proliferating/label retaining (LRC) and a fast proliferating/non-label retaining (NLRC) VCAM1+Itga7+ population, which separate after birth (Chakkalakal, 2014). Until postnatal day 7 these lineages were indistinguishable by their expression of myogenic determination genes. The NLRC population showed a slightly higher expression level of the cell cycle marker Ki67, whereas the LRC fraction expressed higher levels of the cyclin-dependent kinase inhibitor p27. At later stages, the LRC fraction was characterized by higher expression of Pax7 and reduced expression of myogenic determination genes. Both populations were present and persisted in the adult Satellite cell pool (Chakkalakal, 2012 & 2014).

Furthermore, Rocheteau and colleagues described a population of Satellite cells expressing high levels of Pax7 (Pax7[High]) that is able to retain a template DNA strand during divisions (Rocheteau, 2012). They already observed this label-retention in young animals. The daughter cells receiving the newly synthesized strand expressed higher levels of myogenic determination genes and lower levels of Pax7. This indicates that the Pax7[High] population is a more stem cell-like population.

5. The Mapk/ Erk signaling pathway

Receptor tyrosine kinases (RTK) transmit extracellular growth factor signals into the cytoplasm. Binding of the growth factor promotes RTK dimer formation, activation of the tyrosine kinase activity, autophosphorylation of the receptors and transphosphorylation of effector proteins. This activates intracellular signaling pathways (overview in Katz, 2007; Lemmon & Schlesinger, 2010; Schlessinger, 2000).

One major intracellular signaling pathway activated by RTKs is the mitogen activated protein kinase pathway (Mapk). Four different Mapk pathways exist: Erk1/2, p38, Jnk and Erk5. These pathways are similar in the sense that they consist of a linear three-layer kinase cascade. The most upstream mitogen-activated protein kinase kinase

kinase (Mapkkk) activates a Mitogen-activated protein kinase kinase (Mapkk) by phosphorylation. Mapkk subsequently activates the Mapk, which phosphorylates further targets in the cytoplasm and/or nucleus.

Activation of the Mapk/Erk cascade by growth factors involves recruitment and phosphorylation of the adaptor proteins Grb2, Shc and Shp2. Grb2 constitutively interacts with the guanine exchange factor Sos and recruits it to the membrane (overview in McKay & Morrison, 2007). Membrane-bound Sos interacts with the G-protein Ras and catalyzes a GDP-GTP exchange that is crucial for further downstream activation. Activation of RTKs (and Ras) is initiated on the cell surface, and continues in intracellular membrane compartments after RTK internalization. Ras-GTP activates kinases of the Raf family, the Mapkkk (overview in Wellbrock, 2004; McKay & Morrison, 2007). Subsequently, activated Raf phosphorylates Mek1/2 and phospho-Mek1/2 in turn phosphorylates the extracellular regulated kinase (Erk1/2) (overview in McKay & Morrison, 2007). Several adaptor proteins recruit all three proteins, Mapkkk/Mapkk/Mapk, in close proximity to each other, for instance KSR and MP1 at the plasma and endosomal membranes, respectively (overview in Kolch, 2005). These complexes are thought to modulate signaling strength and duration and are responsible for activation of Erk in the cytoplasmic vs. nuclear compartments.

Activated Erk phosphorylates several cytoplasmic and nucleic targets including transcription factors like c-fos, Elk1 and c-myc or the Mitogen and stress-activated kinases 1/2 (Msk1/2), p90 ribosomal S6 kinase (Rsk) and Mapk interacting kinase 1 (Mnk1/2) that indirectly regulate translation (Gille, 1996; Deak, 1998; Sears, 2000; Deak, 2000; Chen, 1991; Waskiewicz, 1997). In addition, Erk phosphorylates growth promoting transcription factors, i.e. c-Fos, Elk1 and Myc, leading to their stabilization (Janknecht, 1993; Gille, 1996; Janknecht, 1993; Murphy, 2002; Sears, 2000). Continuous activation of the pathway results in the expression of growth promoting genes and seems to be essential for cells to enter the cell cycle. In particular, passage through the G_1 phase of the cell cycle dependents on Erk signaling (reviewed in Meloche & Pouysségur, 2007).

Erk1 and Erk2 have a 90 % sequence homology in mammals and have similar functions (Boulton, 1990 & 1991). Hence, Erk1 mutant mice have no overt phenotype besides impaired thymocyte development (Pagès, 1999). Erk2 mutant embryos die during early embryogenesis (Saba-El-Leil, 2003) due to impaired trophoblast development. However, Erk1/2 double mutations have strong phenotypes in many cell types that are not affected by the mutation of the single genes (Srinivasan, 2009;

Satoh, 2011; Chan, 2013). Together, the data indicate that overlapping and specific functions for the two Erks exist.

Several studies implicated Mapk/Erk signaling in maintenance of myogenic progenitors at different stages of development, but downstream effectors of Erk signaling in myogenesis are not well understood. Erk appear to be dispensable in regulation of myogenic genes and differentiation. Studies with developing myogenic progenitors and cultured Satellite cells revealed a function of Erk in maintenance of the undifferentiated state, and pharmacological inhibition of Erk activation increased the expression of myogenic marker like Myosin heavy chain (Michailovici, 2014). Blocking nuclear translocation of Erk and pharmacological inhibition of Erk activity had similar effects, indicating that nuclear Erk effectors are important. Le Grand and colleagues mutated Erk1 in Satellite cells and found a decreased re-occupation of the Satellite cell compartment after regeneration (Le Grand, 2012). Sprouty proteins are negative regulators of Mapk/Erk signaling and are induced by active RTKs, providing a negative feedback loop. Modestly elevated Erk activity in Sprouty1$^{-/-}$, Sprouty2$^{-/-}$ embryos increased numbers of Pax7+ cells in the dermomyotome, and reduced numbers of MyoD+ and MyoG+ cells. Sprouty1 is highly expressed in quiescent Satellite cells but quickly down-regulated upon activation (Shea, 2010). When Satellite cells re-enter quiescence they up-regulate Sprouty1 expression again. A subset of Sprouty1 mutant Satellite cells were unable to re-enter quiescence. Down-regulation of Mapk/Erk signaling might therefore be necessary in activated Satellite cells to return to quiescence or differentiate.

6. The Src-homology 2-domain containing tyrosine phosphatase (Shp2)

Several groups identified mammalian Shp2 (PTPN11) independently in the early 1990s in mammals (Adachi, 1992; Ahmad, 1993; Feng, 1993; Freeman, 1992; Vogel, 1993). The Drosophila homologue is called Corkscrew (csw), and its genetic analysis showed that it is an essential component of RTK signaling cascades (Perkins, 1992). Gain- and loss-of function mutations of Shp2 in humans were found to be a major cause for two developmental disorders, Noonan and LEOPARD syndrome, and for Juvenile myelomonocytic leukemia (JMML), respectively. Mutation of Shp2 in mice further emphasized the importance of the protein as Shp2$^{-/-}$ embryos die before implantation (Yang, 2006).

Shp2 contains a central phosphatase (PTP) domain as well as two SH2 domains (N-SH2 & C-SH2). In addition, the protein contains two tyrosine residues (Tyr542 & Tyr

580) that can be phosphorylated, and a proline rich motif in the C-terminus. In the basal state, the catalytic phosphatase activity of Shp2 is low. Stimulation by a phospho-tyrosine peptide ligand (containing one or two phospho-tyrosines) increased the catalytic activity (Pluskey, 1995; Eck, 1996). Structural studies by Neel and colleagues identified an elegant mechanism how phospho-tyrosine binding to the SH2 domains controls the phosphatase activity (Neel, 1998). In its inactive form, the N-SH2 domain is wedged into the PTP domain and blocks substrates from entering the PTP domain. Binding of a phosphorylated tyrosine by the C-SH2 domain induces conformational changes. The N-SH2 domain is subsequently released from the PTP domain and can bind a second phospho-tyrosine residue. This step "activates" the PTP domain and allows substrates to enter. Functions of the tyrosine residues in the C-terminus are less clearly understood. Several activating proteins have been identified, including platelet-derived growth factor receptor (PDGFR), the cytokine receptor gp130, adaptor proteins like members of the Gab/Dos family and fibroblast growth factor receptor/insulin-like receptors tyrosine kinase substrates (FRS/ IRS). All of these proteins can bind to Shp2 when they are phosphorylated on tyrosines (Klinghoffer, 1995; Stahl, 1995; Schaper, 1998; Maroun, 2000; Schaeper, 2007; Hadari, 1998; Hanke, 2009).
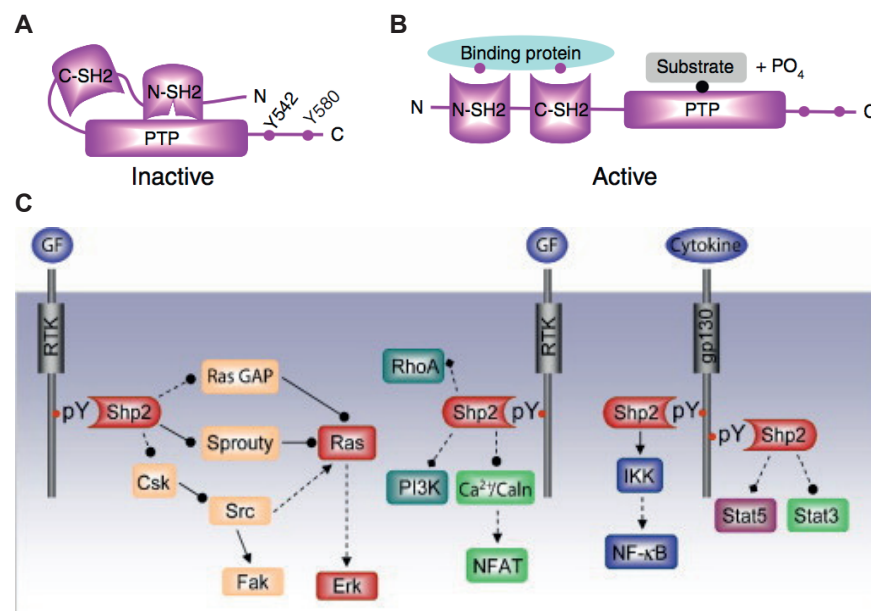
Fig.1.3: Structure and function of Shp2. A) Schematic depiction of inactive Shp2 **B)** Activated Shp2 bound to a phosphorylated substrate by its SH2 domains. **C)** Signaling pathways regulated by Shp2. Full lines: direct interaction, dashed lines: indirect interact; arrowheads: positive regulation, circle heads: negative regulation. Adapted from Grossmann, 2010

Shp2 regulates signaling pathways activated by receptor tyrosine kinases, cytokine and integrin receptors (overview in Grossmann, 2010). Mapk/Erk signaling is the major pathway controlled by Shp2. In most cases when this was analyzed carefully, the initial Mapk/Erk activation is not impaired when Shp2 is lacking, but Erk activation cannot be maintained and is quickly down-regulated (Grossmann, 2009; Araki, 2003; Li; 2014). Several molecular mechanisms have been proposed to explain how Shp2 promotes sustained Erk activation, and these depend on the receptor and/or cell types analyzed.

Bennett and colleagues found increased phosphorylation of Tyr542 in Shp2 upon PDGF receptor stimulation (Bennett, 1994). This phosphorylation site lies in a potential Grb2-binding consensus site. Shp2 directly interact with the PDGF receptor indicating a potential scaffolding function for Shp2 in the recruitment of the Grb2-SOS complex to the membrane. Another study by Vogel et al. identified phosphorylated Tyr580 of Shp2 as a major Grb2 binding site essential for Ras activation (Vogel, 1996). Nevertheless, Tyr542 and Tyr580 are only phosphorylated by some but not all stimuli, indicating that the postulated adaptor function cannot explain all Shp2 functions.

Regulation of a negative Mapk/Erk feedback-loop by Shp2 was also reported. Sprouty proteins are feedback inhibitors of the Mapk/Erk cascade and block Grb2-SOS recruitment to the activated RTK. Activated RTK phosphorylate Sprouty proteins, which regulates their signaling activity. Shp2 can inactivate Sprouty by dephosphorylation, thereby disrupting the Sprouty/Grb2 complex (Hanafusa, 2002 & 2004; Teft, 2002 & 2005). Recently, a substrate-trapping variant of corkscrew identified Sprouty as a substrate in the developing drosophila eye. This suggests that Sprouty proteins are in vivo targets of Shp2 (Jarvis, 2006). Shp2 also regulates the activity of the cytoplasmic focal adhesion kinase (Fak) that controls the Mapk/Erk cascade via the Src kinase (Ren, 2004; Zhang, 2004; Grossmann, 2009; Lan, 2015).

Besides Mapk/Erk signaling, Shp2 was also shown to regulate the activities of Jak/Stat and PI3K/Akt signaling pathways. Positive and negative effects on these signaling pathways were reported. Furthermore, Shp2 regulates several other signaling pathways in a cell type and/or receptor dependent manner including FAK, JNK-, NFAT-, NF-κB, Mapk/p38 and Rho GTPase signaling (overview in Grossmann, 2010). Shp2 is preferentially located in the cytoplasm and most studies address the molecular function of Shp2 in this compartment; nuclear functions of Shp2 have been little addressed. In a Shp2 substrate-trap screen, Hatakeyama and colleagues identified parafibromin as a novel nuclear Shp2 substrate (Takashi, 2012).

Parafibromin binds the nuclear ß-catenin/TCF complex and modulates Wnt target gene expression. A more recent study identified interactions of Shp2 with Yap and Taz, the transcriptional activators of the Hippo pathway (Tutsumi, 2013). Nevertheless, *in vivo* analyses indicate that the regulation of Mapk/Erk signaling is the major function of Shp2 (Li, 2014; Heuberger, 2014; Yang, 2013; Sheean, 2014)

7. Shp2 in development and disease

Ubiquitous expression of Shp2 throughout embryonic development and in postnatal stages indicated that this tyrosine phosphatase could have broad functions. Shp2$^{-/-}$ mice died before implantation, a very early stage of embryonic development (Yang, 2006). Furthermore, several gain- and loss-of-function point mutations in humans cause developmental defects and are associated with the progression of certain types of cancers.

Several gain-of-function mutations in Shp2 have been identified that cause the developmental disorder Noonan syndrome. With varying penetrance, Noonan syndrome patients develop craniofacial, cardiac and skeletal defects, and display mental retardation (Turner, 2014). Additionally, Shp2 gain-of-function mutations are one of the major causes of myelomonocytic leukemia (Tartaglia, 2005). JMML is characterized by massive expansion and tissue infiltration of myeloid cells and macrocytic anemia (overview in Emanuel, 1996). Mutations responsible for the phenotype are mainly present in the N-SH2 domain and interfere with the autoinhibitory interface. These are thought lead to enhanced Shp2 catalytic activity and subsequent increased Ras/Erk signaling (Araki, 2004; Fragale, 2004; Krenz, 2008; Mohi, 2005; O'Reilly, 2000).

Shp2 loss-of-function mutations are associated with the LEOPARD syndrome, which is characterized by facial abnormalities, cardiac defects, retardation of growth and deafness (overview in Noonan, 2006; Ogata, 2005; Tartaglia, 2005). Most loss-of-function mutations occur in the PTP domain of Shp2 and impair its catalytic activity (Hanna, 2006; Kontaridis, 2006).

The introduction of conditional Shp2 mutations in several tissues has shed light on the role of Shp2 in later developmental processes. Studies in T-cells showed that Shp2 controlled the balance between proliferation and expansion of CD4+ cells, and resulted in defective Mapk/Erk signaling regulated by the TCR receptor (Qu, 1997 &1998 & 2001; Alberola-Ila, 1995; Crompton, 1996; Swat, 1996). Mutations of Shp2 in the central nervous system impair the self-renewal of neural progenitor cells and

change the balance between neurogenesis and astrogenesis (Gauthier, 2007; Ke, 2007; Yamamoto, 2005). Schwann cells are peripheral myelinating glial cells derived from the neural crest. Shp2 mutation in the neural crest interfered with Schwann cell proliferation, migration and terminal differentiation (Grossmann, 2009). Several other studies have shown that Shp2 functions also in other tissues and cell types, for instance in liver regeneration, pancreatic insulin production, branching of kidney tubules and cardiomyopathy (overview in Grossmann, 2010).

Shp2 functions in muscle development and regeneration were incompletely analyzed. Mutation of Shp2 with by the MCK-Cre allele, which introduces mutations into myoblasts and myotubes, interferes with myotubes formation in culture and fiber type specification (Fornaro, 2006). These defects were contributed to impaired NFAT signaling. Studies analyzing Gab1 and Shp2 interactions in embryos and in culture highlighted the importance of Shp2 in the Met dependent migration of myogenic precursor cells (Schaeper, 2007). Mutating Shp2 at the onset of myogenesis by a Pax3[Cre] allele phenocopied the deficits reported by Schaeper and verified the importance of Shp2 for migration of myogenic precursors (Vasyutina & Birchmeier, unpublished results). Initial analysis of fetal and early postnatal myogenic precursor cells indicated a strong postnatal muscle growth defect (Schneider, doctoral thesis, FU Berlin, 2011). This showed that Shp2 mutant Satellite cells are not maintained and progressively disappeared during the first two weeks after birth. This analysis identified decreased proliferation as the major cause for the impaired muscle growth, but did not address the mechanisms of Shp2 in any depth.

8. Aim of the study

The molecular mechanisms of Shp2 functions in skeletal muscle development, is not fully understood. Shp2 functions in Satellite cells of adult muscle were not yet addressed. In this study, I analyzed the effects of Shp2 mutation in Pax7 expressing progenitor cells. Additionally, I analyzed the effects of Shp2 mutation in adult Satellite cells in non-injured muscle, a state where Satellite cells are quiescent, and in regenerating skeletal muscle, when Satellite cells are activated. My data indicate Shp2 is indispensible for proliferation of Satellite cells during postnatal development and muscle regeneration.

II. Material & methods

1. Materials

1.1 Chemicals & enzymes

All chemicals, enzymes, oligonucleotides, solutions, whole transcriptome arrays and antibodies were obtained from the following companies: Ambion (Austin, USA), Illumina (San Diego, USA), Biozym (Hess. Oldendorf), Dianova (Hamburg), Invitek (Berlin), Merck (Darmstadt), MWGBiotech (Ebersberg), Roche (Mannheim), Roth (Karlsruhe), Serva (Heidelberg), Sigma-Aldrich (München), Thermo Fisher Scientific (Waltham, USA), Partec (Görlitz), Ferak (Berlin), Pan Biotech (Aidenbach), Biochrom AG (Berlin), US biological (San Antonio, USA), Perkin Elmer (Waltham, USA), TH.Geyer (Renningen), R&D systems (Minneapolis, USA), Santa Cruz Biotechnology (Dallas, USA), Beckton Dickinson BD (Franklin Lakes, USA), Biorad (Hercules, USA), Leica (Wetzlar), Millipore (Billerica, USA), Abcam (Cambridge, UK), MP biomedicals (Santa Ana, USA), Bioline (London, UK), MRC Inc. (Cincinnati, USA), EURx (Gdansk, Poland), Sakura (Alphen aan den Rijn, Netherlands), Polysciences (Eppelheim), Vector laboratories (Burlingame, USA)

1.2 Buffers & media

1.2.1 Genotyping buffer

Tissue lysis buffer

Tris pH8.5	100	mM	(Roth #4855)
EDTA	5	mM	(Roth #8043)
SDS	0.2	% (w/v)	(Serva #20765)
Proteinase K	100	µg/mL	(Sigma #P6556)

PCR mix

Sucrose	15.3	% (w/v)	(Roth #4621)
β-Mercaptoethanol	0.012	‰	(Ferak #31012)
10x PU-buffer	1	x	
Dilut	0.2	%	
DMSO	0.4	‰	(Merck)
dNTPs (5mM)	0.625	mM	(Invitek)

Aliquote and store at -20°C

10x PU buffer

Tris-HCl pH8.8	450	mM	
Cresol red solution	50	% (v/v)	
H_2O	1.5	mL	
$MgCl_2$	35	mM	(Roth #A537)
$(NH_4)SO_4$	12.74	mM	(Roth #3746)
Aliquote and store at -20°C			

Dilut

T0.1E	50	% (v/v)
Cresol red solution	0.054‰	(v/v)
NaOH	1.33	mM
Aliquote and store at -20°C		

Cresol red solution

Dissolve a small amount of o-Cresol red (Roth #KK15.1) in T0.1E and adjust pH to 8.8. Aliquote and store at -20°C.

T0.1E

Tris-HCl pH 8.8	10	mM
EDTA	0.1	mM

TAE

Tris	40	mM
EDTA	1	mM
Acetic acid	0.1	% (v/v)

1.2.2 Media & solutions for Cell/ fiber isolation and culture

NB4 digest medium

DMEM (Glc 1g/L)	1	x	(Gibco #21885)
HEPES	25	mM	(Pan Biotech #P05-01100)
Gentamycin	0.5	% (v/v)	(Gibco #15710)
Store at 4°C			

FACS sorting buffer

HBSS (-Ca^{2+} -Mg^{2+})	1	x	(Gibco #14175)
HEPES	25	mM	
BSA	1	% (w/v)	(Roth #8076)
Gentamycin	0.5	% (v/v)	

Sterile filter and store at 4°C for up to one month

Fiber isolation medium

DMEM (Glc 1g/L)	1	x	
L-Glutamax	2	% (v/v)	(Gibco #35050)
Penicillin/ Streptomycin	1	% (v/v)	(Sigma #4333)

DMEM+

DMEM (Glc 1g/L)	1	x	
FCS	20	%	(Sigma #/Lot F7524/041M3397)
Penicillin/ Streptomycin	1	% (v/v)	

Heat inactivate FCS once for 30 min at 55°C before use

DMEM/F12+

DMEM/ F12	1	x	(Gibco #31331)
FCS	15	%	
Gentamycin	0.5	% (v/v)	

Fiber differentiation medium

Fiber isolation medium			
Horse serum	10	% (v/v)	(Biochrom AG # 59135)
Chick embryo extract	0.05	% (v/v)	(US biologicals #C3999)

Heat inactivate horse serum once for 30 min at 55°C before use

1.2.3 Buffers for immunohistochemistry

DPBS

DPBS	10	x
MQ-H2O		

4% PFA/PBS

p-Formaldehyde	4	%	(Merck)
DPBS (10x)	1	x	
NaOH	0.64	mM	

Dissolve p-formaldehyde in heated MQ-H2O (80°C) and add NaOH. Stir until PFA is dissolved. Add DPBS afterwards. Filter solution, aliquot and store at 4°C for up to a week or at -20°C.

Zambonis's fixative

p-Formaldehyde	2	% (w/v)	
Saturated picric acid	15	% (v/v)	(Merck #100623)
0.1M PO$_4$ buffer			

adjust pH to 7.3, filter and aliquote. Store at -20°C

IF blocking buffer

DPBS			
Horse serum	10	%	
TSA blocking reagent	0.5	g	(Perkin Elmer #FP1012)

Dissolve BSA and horse serum in DPBS and sterile filter

Add TSA and stir on a heating plate (80°C) until the powder is dissolved (1-2h). Store at 4°C for 2-3 days or at -20°C

Staining buffer

DPBS (10x)	1	x	
BSA	0.3	%	
Horse serum	3.0	%	
Triton-X-100	0.1	%	(Sigma #T9264)

PBX

DPBS (10x)	1	x
Triton-X-100	0.1	%

1.2.4 Buffers for protein biochemical analysis

RIPA

Tris-HCl pH 8.0	10	mM
EDTA	1	mM
EGTA	0.5	mM	(Roth #3054)
Triton-X-100	1	%
Na-Deoxycholat	0.1	%	(Serva #18330)
SDS	0.1	%
NaCl	140	mM	(Roth #3957)

RIPA+

RIPA	1	x
Complete protease		
Inhibitor cocktail	1:50	(Roche #14653600)
Phosphatase inhibitor		
Cocktail 2	1:100	(Sigma #5726)
Phosphatase inhibitor		
Cocktail 3	1:100	(Sigma #0044)

4x protein loading buffer (containing b-mercaptoethanol)

Tris-HCl pH 6.8	240	mM
Glycerol	40	%	(Roth #3783)
SDS	8	%
Bromphenol blue	0.04	%	(Sigma #114405)
β-mercaptoethanol	5	%

SDS-running buffer

Tris-Base	25	mM
Glycine	192	mM	(Merck #104201)
SDS	0.1	% (w/v)
MQ-H_2O		

Prepare a 10x stock without SDS and adjust to pH 8.3. Add SDS to 1x working solution.

Nitrocellulose membrane blotting buffer

Glycine	192	mM
Tris-base	25	mM
SDS	0.01	% (w/v)
Methanol	20	% (v/v) (Chem.Solute #1437)

Prepare a 5x stock solution without Methanol. Add cold methanol just before use. Store both solutions at RT. 1x blotting buffer can be used twice.

PBST

DPBS (10x)	1	x
Tween-20	0.5	% (v/v) (Sigma #P9416)

PBST+

DPBS (10x)	1	x
Tween-20	0.5	%
BSA	5	%

1.3 Mouse strains

1.3.1 Pax7^{ICNm}

(Mario Capecchi, University of Utah, USA)

An IRES-Cre-FRT-neo-FRT cassette was inserted into the 3' UTR following the stop codon in exon 10 of Pax7. Crossing with mice expressing FLP-e excised the neo cassette (Keller, 2004).

1.3.2 Pax7^{CreERT2}

(Cheng-Ming Fan, Carnegie institution for Science, Maryland, USA)

Beginning with the Pax7$^{tm1.2Sjc}$ allele in which exon 2 was knocked out leaving a single loxP site, parts of exon 1 was replaced with a cre/ERT2 (ESR1) fusion followed by an IRES-DsRed and an frt flanked neo cassette. Germ line, flipase mediated recombination removed the neo cassette (Lepper, 2009).

1.3.3 Shp2^{flox}

(Walter Birchmeier, Max-Delbrück-Centre for Molecular Medicine, Berlin, Germany)

A loxP site was inserted upstream of exon 3 and an frt flanked neo cassette with a 5' loxP site was inserted downstream of exon 4. The neo cassette was removed by germ line, flipase mediated recombination (Grossmann, 2009). Cre mediated recombination deletes exon 3 & 4 and results in a frame shift mutation of the Shp2 gene. The protein product is 45 amino acids long and non-functional.

1.3.4 Rosa-flox-stop-flox-YFP (RYFP)

(Phillipe Soriano, Mount Sinai School of medicine, New York, USA)

A construct containing a floxed PGK-neo cassette and an enhanced yellow fluorescent protein (EYFP) gene was inserted into the Gt(ROSA)26Sor locus via homologous recombination. The floxed neo cassette contains a strong tpA stop sequence which prevents the transcription of EYFP (Srinivas, 2001).

1.3.5 Rosa-flox-stop-flox-MEK1DD (MEK1DD)

(Klaus Rajewsky, Max-Delbrück-Centre for Molecular Medicine, Berlin, Germany)

A targeting vector designed with (from 5' to 3') a splice acceptor site, a loxP-flanked Neo-STOP cassette, a cDNA sequence encoding rat MEK1DD (a mutant form of MAPKK1 rendered constitutively active by two serine->aspartic acid substitutions (S218D/S222D) within the catalytic domain), an frt-flanked internal ribosomal entry site-enhanced green fluorescent protein cassette (IRES-EGFP), and bovine polyadenylation signal was inserted between exons 1 and 2 of the Gt(ROSA)26Sor locus (Srinivasan, 2009). Cells expressing Cre recombinase the stop cassette is deleted and MEK1DD expression initiated.

1.4 Antibodies

Primary antibodies were diluted in staining buffer. Dilutions are shown in the table below.

		Dilution						
Antigen	Host species	IHC-Frozen	IF cell culture	Western Blot	Flow cytometry	Antigen retrieval	provider	#
anti-Desmin	goat	500	500	-	-	-	R&D	AF3844; Lot:YIL0208071
anti-Pax7	mouse	1000	1000	-	-	citric acid + heat (IHC)	DHSB	Pax7-a
anti-Pax7	guinea pig	2500-5000	2500-5000	-	-	-	generated by J.Griger	
anti-Myogenin (M-20)	rabbit	-	150	-	-	-	Santa Cruz	SC-576; Lot: E0710
anti-Shp2 (C-18)	rabbit	-	-	800	-	-	Santa Cruz	SC-280; Lot:E1309
anti-Laminin	rabbit	500		-	-	-	Sigma	L9393
anti-VCAM1	goat	100	100	-	100	-	R&D	AF643
anti-CD31-PE	rat	-	-	-	200	-	BD Pharmingen	553373
anti-CD45-PE	rat	-	-	-	200	-	BD Pharmingen	553081
anti-Sca1-PE	rat	-	-	-	200	-	BD Pharmingen	553336
anti-BrdU	rat	300	300	-	-	HCl (IF+IHC)	AbD Serotec	OBT0030
anti-Ki67	rabbit	500	500	-	-	-	Leica	F032531; Lot: 6019624
anti-Col IV	goat	500	-	-	-	-	Millipore	AB769; Lot: 2515446
anti-phospho Histone H3 (Ser10)	rabbit	-	1000	-	-	-	Abcam	AB5176; Lot: GR6832-1
anti-phospho-p44/p42 (Thr202/ Tyr 204)	rabbit		200	2000	-	90 % MetOH (IF)	cell signaling	4370
anti-p44/p42	rabbit	-	-	3000	-	-	cell signaling	9102
anti-phospho-Akt (Ser473)	rabbit	-	-	1000	-	-	cell signaling	9271
anti-Akt	rabbit	-	-	1000	-	-	cell signaling	9272
anti-phospho-p38 (Thr180/Tyr182)	rabbit	-	-	1000	-	-	cell signaling	4511
anti-p38	rabbit	-	-	1000	-	-	cell signaling	8690
anti-β-actin	rabbit	-	-	1000	-	-	cell signaling	4967
anti-Gapdh	mouse	-	-	1000	-	-	Abcam	AB9484; Lot: GR24304
anti-MyoD	guinea pig	-	-		-		generated by J.Griger	
anti-phospho-S6 (Ser235/Ser236)	rabbit	-	100	-	-		cell signaling	4858

Primary antibodies were detected with Cy2/Cy3/Cy5-conjugated, species-specific secondary antibodies (0.5 µg/µL, Dianova). By default, the stock solutions were diluted 1:500 in staining buffer.

1.5 Oligonucleotides

1.5.1 Oligonucleotides for genotyping

Allele	Primer	Sequence	$T_{Annealing}$
Pax7^{ICNm}	For-wt	5'-gct ctg gat aca cct gag tct-3'	
	For-mut	5'-gga tag tga aac agg ggc aa-3'	55°C
	Rev-mut	5'-tcg gcc ttc ttc tag gtt ctg ctc-3'	
Shp2^{flox}	For	5'-atg act cct gga gcc cat tg-3'	60°C
	Rev	5'-ttc cca tca cct cag act cc-3'	
Pax7^{CreERT2}	For	5'-act agg ctc cac tct gtc ctt c-3'	64°C
	Rev	5'-gca gat gta ggg aca ttc agt g-3'	
RYFP	For	5'-aaa gtc gct ctg agt gt tat-3'	
	Rev-wt	5'-gga gcg gga gaa atg gat atg-3'	60°C
	Rev-mut	5'-gcg aag agt ttg tcc tca acc-3'	
MEK1DD	For	5'-gtc aat gag cct cct cca aa-3'	55°C
	Rev	5'-gca ata tgg tgg aaa ata ac-3'	

1.5.2 Oligonucleotides for qPCR

Primers were designed to detect unrecombined Shp2 transcripts in Satellite cells by detecting exon 3 or 4. Exon 3 and 4 are deleted after Cre mediated recombination. Both primer pairs span an exon-exon-junction. Primer Shp2 (exon3) binds in exon 2 and 3; primer Shp2 (exon 4) binds in exon 4 and 5.

Transcript	Primer	Sequence	$T_{Annealing}$
Shp2 (exon3)	For	5'-gac aaa ggg gag agc aac ga-3'	60°C
	Rev	5'-tac gag ttg tgt tga ggg gc-3'	
Shp2 (exon4)	For	5'-ttc acc cca aca tca ctg gt-3'	60°C
	Rev	5'-gca cag ttc agc ggg tac t-3'	

2. Methods

2.1 Animal experiments

2.1.1 Labeling of proliferating cells *in vivo*

Labeling of replicating cells in pre- or postnatal tissue was done with BrdU. Animals were intraperitoneally injected with BrdU (75 µg/g body weight, Sigma #B5002). Animals were sacrificed 2 hours later.

2.1.2 Intraperitoneal Tamoxifen injections

To induce recombination with the Pax7^{CreERT2} allele 5-6 week old animals were injected intraperitoneally with 100 µL of a Tamoxifen/sunflower oil solution (20 mg/mL, MP Biomedicals #156738) for 5 consecutive days.

2.1.3 Intramuscular Cardiotoxin injections

Muscle regeneration was induced by intramuscular injection of 30 µL sterile-filtered Cardiotoxin/PBS solution (10 µM, Sigma #C9759) into the *Tibialis anterior* (TA) muscle. The contralateral TA muscle was injected with the same volume of sterile PBS. Verena Schöwel (AG Spuler, Muscle research Unit, ECRC, Charité, Berlin, Germany) performed the intramuscular Cardiotoxin injections.

2.2 Cell culture

All cells were kept at 37°C/5% CO_2 in a cell culture incubator (Binder).

C2C12 were cultured with DMEM+ and split 1:10 every other day. 75.000 cells were seeded in 6-well plates and cultured 18-20 hours for inhibitor experiments. GS493 (Grosskopf, 2015) was added to the culture medium for 1 hour. Control cells were treated with the according volume of DMSO.

FACS-sorted young primary myoblasts were cultivated with DMEM/F12+ medium. 80.000/350.000 events were seeded per well in 16/8-well chamber slides (Nunc #178599/177445) and cultured for approx. 16-20 hours before fixation/lysis.

To detect proliferating cells in cultured cells or muscle fibers, cultures were incubated with BrdU (10 µM) for the according time frames.

Extensor digitorum longus floating fiber culture

Carefully isolated *Extensor digitorum longus* (EDL) muscles were incubated in 3 mL fiber isolation medium containing 0.2% (w/v) Collagenase I (Sigma #C0130) at 37°C in a water bath for 120 min. Every 20 min the suspension was gently agitated. After the digestion step the muscles were incubated for 20 min in pre-warmed fiber isolation medium in a cell culture incubator at 37°C/5% CO_2. Subsequently the muscle was gently triturated with blunt Pasteur pipettes until sufficient numbers of single fibers dissociated from the muscle. Dead fibers and debris were carefully removed with a pipette and the single muscle fibers carefully transferred to fiber differentiation medium. Fibers were cultured for up to 72 hours. Approx. 50-100 fibers were kept in one 6 cm cell culture dish (Sterilin #124). All cell culture dishes used for trituration and culture were pre-coated with 5% BSA/PBS solution (heat-inactivated for 30 min at 55°C and 0.2 µm sterile filtered).

Extensor digitorum longus floating fiber culture

2.3 Molecular biological methods

2.3.1 DNA isolation from tissue biopsies

Tissue biopsies were digested in 50 µL of tissue lysis buffer at 55°C o/N. After digestion Proteinase K was inactivated in a heating block at 95°C for 5 min. Samples were diluted with 300 µL of MQ-H$_2$O. 1 µl of the solution was used for PCR reactions.

2.3.2 Polymerase chain reaction (PCR)

Genotyping PCRs were performed in a Biometra Thermal cycler. The PCR conditions were the following:

PCR reaction

Allele	Pax7[ICNm]		Shp2[flox]		RYFP		Pax7[CreERT2]		Mek1DD	
	[µL]	final conc.	[µL]	final conc.	[µL]	final conc.	[µL]	final conc.	[µL]	final conc.
10x reaction buffer (Invitrogen)	-		-		2.00	1x	2.00	1x	3.0	1x
50 mM MgCl$_2$ (Invitrogen)	-		-		1.20		1.00	2.5 mM	1.2	2 mM
DMSO (Merck)	-		-		-	-	0.66	3.33 % (v/v)	-	-
dNTPs (5 mM, Invitek)	-		-		1.00	0.25 mM	1.32	0.33 mM	3.0	0.5 mM
MQ-H2O	1.30	-	1.30	-	12.00	n/a	8.82	n/a	21.4	n/a
PCR-Mix (see 1.2.1)	15.59	-	15.59	-	-	-	-	-	-	-
each primer (10 µM)	1.00		1.00		1.00	0.2 mM	2.00	1 µM	0.5	0.17 µM
Taq DNA polymerase (5 U/µL; Invitrogen)	0.125		0.125		0.133	0.05 U/µL	0.20	0.05 U/µL	0.2	1 U
Notes	all three primers in one reaction		-		primer combinations in seperate PCR reactions		-		2 µL gDNA template	

PCR condition

Allele	Pax7[ICNm]	cycles	Shp2[flox]	cycles	RYFP	cycles	Pax7[CreERT2]	cycles	Mek1DD	cycles
Denaturation [95 °C]		1	120 s	1	240 s	1	120 s	1	300 s	1
Denaturation [95 °C]	30 s		40 s		60 s		45 s		30 s	
Extension [72 °C]	30 s	30	30 s	40	60 s	36	60 s	35	30 s	35
Annealing [see 1.5.1]	60 s		30 s		60 s		45 s		60 s	
Final extension [72 °C]	420 s		120 s	1	300 s	1	90 s	1	120 s	1
Band size wt [bp]	465		220		600		780			
Band size mut [bp]	340		350		320		250		420	

Applied annealing temperatures are shown in 1.5.1. PCR reactions were mixed with 5x loading buffer (Bioline #BIO-37045) and loaded onto a 1.5 % (w/v) Agarose gel (LE Agarose, Biozym #840004 in TAE buffer) containing propidium iodide (1 µg/µL) in an electrophoresis chamber filled with TAE buffer. DNA fragments of different size were separated by applying a voltage of 180V. Bands were visualized with a UV imaging system (Vilber Lourmat). Hyperladder I (Bioline #H4-215101) was used as a DNA standard.

2.3.4 Total RNA extraction

Cells were lyzed in 1600 µL TRIzol® (Ambion #15596) and stored at -80°C until further processing. Total RNA was isolated according to manufacturers instruction. Briefly, 3 µL of Polyacrylcarrier (MRC Inc. #PC152) was added and samples incubated at RT for 5 min. To separate the aqueous phase containing the total RNA 300 µL Chloroform were added, the sample mixed vigorously and centrifuged at 10.000 g at 4°C for 15 min (Eppendorf 5417R centrifuge). The upper phase was mixed with 600 µL of Isopropanol, incubated at RT for 10 min or -20°C o/N, respectively. The RNA was pelleted by centrifugation at 12.000 g for 10 min at 4°C followed by 3 washing steps with 75 % EtOH. The pellet was air-dried at RT for approx. 10 min and dissolved in RNAse-free H_2O.

2.3.5 First-strand cDNA synthesis

First-strand cDNA synthesis was performed using the SuperscriptIII cDNA synthesis kit (Life technologies #18080) according to manufacturers instructions. After the first strand cDNA synthesis the volume was adjusted to 100 µL with TE buffer.

2.3.6 Quantitative polymerase chain reaction (qPCR)

qPCR was performed on a Biorad C1000 Thermal cycler using the 2x SG qPCR Master Mix (EURx #E0401). The primers were always used at a final concentration of 1 µM. 1 µL of cDNA was used for the reaction. Annealing temperatures for the specific primers can be found in 1.5.2. Primer amplification efficiencies were determined using the method introduced by Pfaffl et al. (Pfaffl, 2001). Only primer pairs with an amplification efficiency E > 1.9 were used for qPCR experiments. Anticipated PCR products were validated by melting curve analysis and by band size analysis with an agarose gel. The standard amplification protocol used was as follows:

Denaturation	95°C	15 min
denaturation	95°C	30 sec
annealing	see 1.5.2	30 sec
extenion	72°C	30 sec
Melting curve	65 to 95°C	0.5°C/10s

C_t values were normalized to Gapdh C_t values. Relative expression differences in between control and mutant were calculated with the $2^{\wedge}(-\Delta\Delta Ct)$ method (Winer, 1999).

2.3.7 cRNA synthesis for Microarray hybridization

RNA was isolated from 200-300.000 FACS-sorted VCAM1+CD31-CD45-Sca1- cells according to 2.3.4. The pellet was dissolved in 11µL of RNAse-free H_2O and the concentration determined using a Nanodrop 1000 UV-spectrophotometer (Thermo scientific). 500 ng RNA were used for double strand cDNA synthesis and subsequent in vitro transcription of biotinylated cRNA using the Illumina® TotalPrep RNA amplification kit (Ambion, AMIL1791). The cRNA size distribution was analyzed on a 1.5 % Agarose gel containing prodidium iodide.

2.3.8 cRNA hybridization and chip analysis

Gabriele Born (AG Hübner, Genetics of cardiac disease, MDC Berlin) performed the hybridization of the cRNA to Mouse-Ref8 v2.0 Expression bead chips (Illumina #-202-0202) and the readout. The obtained raw data was imported into Genome studio (Illumina), normalized by quantile normalization and exported to Partek genomics suite (V6.6, Partek). To correct for processing and littermate batch effects a batch removal algorithm was applied on the data files. Prior to analysis of deregulated genes a principal component analysis was performed to analyze the homogeneity of the samples of each genotype. Samples of one genotype that did not cluster within their genotype group were excluded from the data set and the remaining samples were reassessed by the methods described above. The samples were then analyzed for differentially expressed genes by an ANOVA variance analysis and further processing by a multiple test correction algorithm (Benjamini & Hochberg, 1990). Genes that passed though the following criteria: fold-change > ±1.5 and a false discovery rate FDR < 0.05 were considered deregulated and statistically significant. The retrieved gene sets were analyzed for enriched Gene Ontology (GO) terms with the functional annotation-clustering tool of the DAVID bio database (Huang, 2009).

2.4 Flow cytometry

2.4.1 Single cell isolation from skeletal muscle

Isolated limb (muscle) tissue was minced with scissors and digested in 2 mL (E14.5-P0) or 10 mL (adult) of NB4 digest medium containing 14 mU/mL NB4 Collagenase (Serva, #17465, 0.726 U/mL stock) and 2.5 U/mL Dispase II (Roche #10887800, 100U/mL stock) in a Multitron II (HT instruments) incubator at 37°C and gentle shaking at 120 rpm for 60 min. Every 20 min (2x) the tissue suspension was pipetted up-and down for 25 times. After 60 min Trypsin (Gibco #15090-046, 0.2% (w/v) stock) was added to yield a concentration of 0.006% (w/v), the sample pipetted up-and down for 25 times and the suspension mixed with 6 mL of cold Satellite cell growth medium supplemented with 2 mM EDTA. Subsequently, the suspension was filtered with a CellTrics® 100 µM cell strainer (Partec #04-0042-2318) to remove larger debris. The filtrate was centrifuged at 500g at 4°C for 15 min and the pellet resuspended in 1mL cold FACS sorting buffer.

2.4.2 Staining of live cells for fluorescence activated cell-sorting (FACS)

The filtered cell suspension was centrifuged at 500g for 5 min at 4°C and the pellet resuspended in 500 µL of FACS sorting buffer containing VCAM1, CD31-PE, CD45-PE and Sca1-PE antibodies in the according dilutions. The cells were incubated for 15 min at 4°C under gentle shaking. Subsequently, the cells were washed with 900µL of FACS sorting buffer two times and resuspended in 500 µL FACS sorting buffer that contained goat-Cy5 antibody for 15 min at 4°C under gentle mixing. The cells were washed two times and filtered trough a 35 µm cell strainer into 5 mL FACS tubes (BD Falcon #352235). Mice carrying a RYFP allele were immediately after the first filtering step in 2.9.1 filtered through a 35 µm strainer into 5 mL FACS tubes and analyzed/processed by FACS. To identify dead or damaged cells propidium iodide (1 µg/mL) was added shortly prior to further processing. VCAM1+CD31-CD45-Sca1- or YFP+/YFP- cells were isolated with a FACS Aria 2 or Aria 3 (Beckton Dickenson) equipped with 405, 488, 561 and 635 nm lasers. Examples of the FACS isolation strategies are depicted in appendix Fig.A1/2/5.

2.4.3 Propidium iodide cell cycle analysis

500.000 YFP+ events isolated from E18 fetuses according to 2.9.1 and 2.9.2 were centrifuged at 500g for 10 min at 4°C. The pellet was resuspended in 500 µL cold

0.1M PO_4 buffer (pH 7.4) and the cell suspension transferred dropwise to 500 µL of cold 1% PFA/ PO_4 solution (final PFA concentration 0.5%) under constant gentle vortexing in a 15 mL tube. After exactly 10 min on ice 14 mL of cold PO_4 buffer were added and the suspension centrifuged at 500g for 15 min at 4°C. The pellet was washed once in 10 mL of cold PO_4 buffer and centrifuged one more time at 500g for 15 min at 4°C. To stain DNA with propidium iodide the pellet was resuspended in 500 µL of pre-warmed PBX containing 30 µg/mL propidium iodide and 3 mg/mL DNase-free RNase (Roth #7156, heat-inactivated DNase: 95°C for 10 min). This suspension was incubated in a water bath at 37°C for 15 min protected from light. Every 5 min the suspension was vortexed gently. Analysis was performed directly in the staining solution on a LSRFortessa flow cytometer equipped with 405, 488, 561 and 635 nm lasers (Beckton Dickenson). An example of the sorting strategy is shown in appendix Fig.A4.

2.4.3 Cytospin preparation of FACS-sorted cells

Between 50.000 and 100.000 events isolated by FACS were pipetted in the plastic funnel of an assembled cytospin cassette containing a coated glass slide (Marienfeld). The cassette was centrifuged at 500 rpm for 5 min at RT in a Cytospin 3 centrifuge (Shandon). The cells were fixed with 4% PFA/PBS for 10 min at RT and washed 3x with PBS at RT before further processing.

2.5 Histological methods

2.5.1 Cryoconservation of tissue specimen

Embryonic and postnatal tissue up to P14 was fixed using Zambonis fixative for 2 h at 4°C. After extensive washing in PBS tissue specimen were incubated in a 30% Sucrose/DPBS solution at 4°C o/N, embedded in OCT compound (Sakura, #2017) with peel-away plastic molds (Polysciences #18986/18646), and subsequently snap-frozen in $N_2(l)$.

Postnatal tissue older than two weeks was snap-frozen with $N_2(l)$ in OCT compound. Samples were stored at -80°C until further processing.

2.5.2 Tissue sectioning

Tissue specimen were sectioned on a cryostat (Microtom HM560, Walldorf) at a thickness of 12 μm, respectively, and mounted on adhesive glass slides (Marienfeld #08 100 00). Sections were dried at 37°C for 30 min.

2.6 (Immuno-)histochemical methods

2.6.1 Hematoxilin & Eosin staining

PFA-fixed sections were incubated in Mayer's hematoxylin (Sigma #HT109/HT107) for 10 min at RT and washed three times with tap water. After a short dip in Ethanol/HCl solution (1,1% HCl, freshly prepared) the sections were washed under running tap water for 5 min followed by 40s incubation in Eosin Y (Roth #CI45380) solution (1% in 0.05% Acetic acid). The slides were incubated in 70% EtOH for 10s and subsequently incubated in 80% EtOH/ 96% EtOH/ Isopropanol for 1 min at RT. Finally the slides were incubated in Xylol (Roth #8713) for 15s and air-dried. The slides were mounted with Entellan (Merck).

2.6.2 Oil Red O staining

Immediately prior to use an Oil Red O working solution (stock solution/ distilled water 3:2, 10 min incubation at RT and subsequently filtered) was prepared (stock solution: 0.5% (w/v) Oil Red O in Isopropanol). PFA fixed sections were rinsed with 60% Isopropanol. The sections were incubated with Oil red O working solution of 15 min at RT in the dark and washed once with 60% Isopropanol. To lightly stain the nuclei they were dipped 5 times into hematoxylin solution. Afterwards the slides were shortly washed with distilled water and mounted with Shandon immunomount.

2.6.3 Immunohistochemical analysis of cryosections and cell cultures

Cell cultures and fiber cultures were fixed with 4% PFA/DPBS for 10 min at RT and washed 3x in PBS (fiber cultures in PBST). Fresh postnatal tissue was post-fixed after sectioning with Zambonis fixative for 20 min at RT followed by 3 PBS washing steps.

Fixed sections/cells were blocked and permeabilized using TSA blocking buffer for 1h at RT and subsequently incubated with the according primary antibodies in staining buffer at 4°C o/N. After 3x washing steps with PBX for 10 min at RT the

sections were incubated with species-specific secondary antibody-fluorophore conjugates in staining buffer for 1 h at RT followed by 3 PBX washing steps. Nuclei were counterstained with DAPI (Sigma #09542). Stained sections were mounted with Shandon immuno-mount (Thermo scientific, #9990412) and sealed with nail polish.

Antigen retrieval for Pax7 staining of cryosections was performed by incubating in Vector antigen unmasking solution (Vector laboratories, H-3300) at 80°C for 30 min. Slides were washed with PBS before further processing (postfixation, blocking, etc.).

Antigen retrieval for BrdU detection was accomplished by incubating slides in 1M HCl at 37°C for 30 min and subsequent PBS washing before further processing.

Detection of phospho-p44/p42 was done by incubating muscle fibers in 90 % MetOH at -20°C for 5 min after fixation and subsequent PBST washing.

2.7 Proteinbiochemical analysis

2.7.1 Cell lysis

Cells were lysed in RIPA (CSH) buffer by resuspending the cells directly in RIPA and gentle shaking for 30 min at 4°C. Insoluble components were separated by centrifugation at max speed for 30 min at 4°C (Eppendorf 5417R centrifuge).

2.7.2 EZQ protein quantitation

Protein concentration of lysed cells was determined using the EZQ protein quantitation kit according to manufacturers instructions (Life Technologies, R-33200). Briefly, 1 μL of protein sample was applied to Whatman paper in the supplied 96-well plate, fixed on the membrane with MetOH and stained with EZQ staining solution for 30 min at RT. After 2 washing steps with washing buffer (10% MetOH, 7% acetic acid). The Whatman paper was reinserted in the 96-well plate and the fluorescence intensities measured on an Infinite M200 Pro microtiter plate reader (Tecan) with an excitation/emission wavelength of 485/590 nm. Samples concentrations were interpolated from fluorescence values obtained with a chicken hemoglobin standard of known concentration.

2.7.3 SDS-polyacrylamide gel electrophoresis (SDS-PAGE)

Protein samples were mixed with 4x protein loading buffer and the volume adjusted with RIPA. Protein denaturation was achieved by incubation of the samples at 95°C

for 5 min. Discontinuous SDS-polyacrylamid gel electrophoresis was used to separate proteins by their molecular weight (Laemmli, 1970). A Mini-gel casting form (Protean 3, Biorad) was used to prepare the gel consisting of a separation (12% poly-acrylamide) and stacking (5% poly-acrylamide) gel. The gel was placed in an electrophoresis chamber (Protean 3, Biorad) containing cooled SDS-running buffer. Until the samples had passed the stacking gel a continuous voltage of 75 V was applied and subsequently elevated to 160 V until the loading buffer front had reached the bottom of the separation gel. PageRuler™ Plus prestained protein ladder (life technologies, #26619) was used as a size indicator.

2.7.4 Transfer of proteins to Nitrocellulose membranes

After removal of the SDS-gel from the glass form the gels were equilibrated in 1x blotting buffer for 5 min. A tank blot system (Mini trans-blot electrophoretic transfer cell, Biorad) with cold blotting buffer was used to transfer proteins from the SDS-gel to a nitrocellulose membrane (0.45 µm pore size; Millipore #IPVH00010) by applying 75 or 25 V for 2 h or o/N under continuous cooling. The membrane was kept in PBS until further processing.

2.7.5 Immunological detection of proteins on Nitrocellulose membranes

The nitrocellulose membranes were blocked with PBST+ for 1 hour at RT. Primary antibodies were diluted PBST+ and incubated with the membrane o/N at 4°C. To wash off unbound antibody the membranes were washed 3x in PBST for 10 min at RT. Primary antibodies were detected with Horseradish peroxidase (HRP)-conjugated secondary antibodies diluted in PBST+ (1h at RT). After 3 washing steps in PBST for 10 min at RT. The HRP activity was detected with Super signal West Pico chemiluminescene substrate (Life technologies #34080) and documented with a Chemismart 5100 imaging station (Vilber Lourmat).

2.8 Image acquisition and processing

2.8.1 Documentation of histological data

All images were acquired with a confocal laser-scanning microscope (LSM 700, Zeiss) equipped with 405, 488, 561 and 639 nm lasers and ZEN V8.1.3 software. All files were saved as lsm5.files.

2.8.2 Image quantification

lsm5-files were opened with ImageJ V1.45S (NIH). All image quantifications were performed by manual counting of positive signals. A minimum of 500 cells was counted for each animal.

Minimal Feret's diameters were obtained by manually measuring the shortest possible distance in between two parallel planes on the opposite sides of a muscle fiber in ImageJ. A minimum of 1000 fibers was measured for each animal.

For quantification of phospho-Erk1/2 levels in VCAM1+ cells the cell area was marked according to the membrane marker VCAM1 and the phospho-Erk1/2 pixel intensities of this area quantified. Background fluorescence was determined by integrating the pixel intensities of an area adjacent to the cells. The average background intensity per pixel was multiplied by the amount of pixels per VCAM1+ area and subtracted from the Erk1/2 signal. To further normalize the fluorescence intensities for cell size the background subtracted Erk1/2 signals were divided with the number of VCAM1+ pixels yielding average fluorescence intensities per VCAM1+ pixel per cell. A minimum of 50 cells was quantified per animal.

2.8.3 Image processing

Lsm5 files obtained from confocal microscopy experiments were opened in ImageJ and the according false colors assigned. The image was exported as an RGB file and saved as tif-file for further image processing with Adobe Photoshop CS5 (Adobe).

2.9 Statistical analysis

Cell counts were performed on muscle tissue or cell cultures of at least three animals per genotype. The statistical significance was determined using unpaired Student's two-tailed t-test in Microsoft Excel.

III. Results

1. Shp2 recombination in fetal and neonatal myogenic progenitor cells

Shp2 mutant animals die during gastrulation, which precludes an analysis of Shp2 functions in muscle development (Yang, 2006). To analyze Shp2 functions in muscle, I used the Cre-loxP system, which allows the introduction of a mutation in a particular cell lineage (Gu, 1994). I used the Pax7^{Cre} line (Pax7^{ICNm}) to introduce conditional mutations into the myogenic lineage (Keller, 2004). Pax7 is expressed in myogenic precursor cells of the limb starting around E10.5 and in particular domains of the nervous system (Jostes, 1990; Mansouri, 1996). The strain used contains an IRES-Cre cassette in the endogenous Pax7 locus, and thus leaves the Pax7 coding sequences intact. Recombination is introduced in the myogenic lineage in the limb starting around E12 (Keller, 2004; Hutcheson, 2009; Biressi 2013). Cre-mediated recombination of the Shp2^{flox} locus deletes exon 3 and 4, which results in a frame-shift mutation and expression of a non-functional protein containing only 45 amino acids (Grossmann, 2009).

To verify the loss of Shp2, I purified myogenic progenitor cells from limbs at an early fetal stage (E14.5) and after birth (P0) by FACS and performed a western blot on these cells. Previously, FACS had been used to isolate progenitor cells from E17 mice (VCAM1+CD31-CD45-Sca1- cells or Vcam1+Integrinα7+ cells (Bröhl, 2012; Chakkalakal, 2014)). However, these proteins are not highly expressed in myogenic progenitor cells prior to E15 (Rosen, 1992, data from unpublished transcriptome analysis of FACS-isolated Pax3-GFP+ cells from the Relaix laboratory). I therefore used a different strategy, i.e. a Rosa26-flox-stop-flox-YFP (RYFP) allele that was introduced into the Pax7^{ICNm}; Shp2^{flox} mutant background to sort the cells. The Rosa26-flox-stop-flox-YFP expresses the fluorescent reporter YFP after removal of the translational STOP cassette (Srinivas, 2001). Cells that express the Cre recombinase delete the stop cassette and start to express YFP. I purified the YFP+ cell population by FACS, using a single-cell suspension obtained after collagenase/dispase-digestion of the limb (Fig. 3.1a, d). The entire gating strategy is depicted in appendix Fig.A1. I detected 430.000 and 850.000 events after sorting cells from limbs of E14.5 and P0 mice, respectively (Fig. 3.1g). To verify the cell purity and identity, I analyzed Pax7 and MyoG expression in cytospin preparations (Fig. 3.1b, e, h). This distinguishes between myogenic precursors (Pax7+MyoG-) and

postmitotic myoblasts (Pax7-MyoG+). Additionally, I purified the YFP- fraction to verify that the YFP+ population contains the myogenic cell population (Fig. 3.1c, f, h).
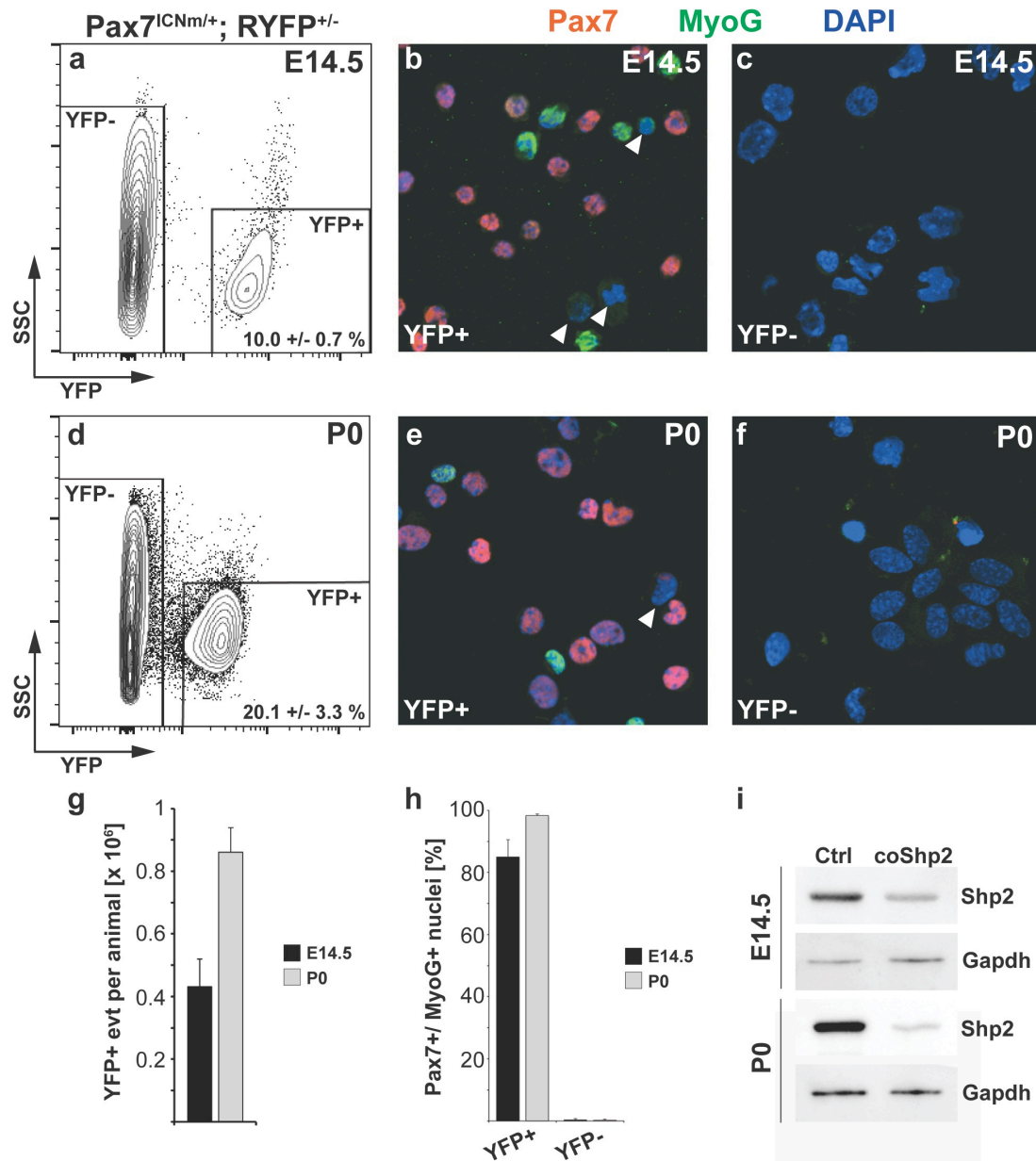
Fig. 3.1: Recombination of Shp2 in myogenic progenitor cells. (a & d) Contour plots showing fluorescence intensities for YFP (x-axis) and side scatter properties (y-axis) of cells isolated from limbs of Pax7$^{ICNm/+}$, RYFP$^{+/-}$ animals at **a)** E14.5 and **d)** P0. Average gate frequencies +/- SD are depicted in the plot. **(b-c, e-f)** Immunohistological analysis of isolated YFP+ and YFP- cells stained with anti-Pax7 and anti-MyoG antibodies from **(b-c)** E14.5 and **(e-f)** P0 animals, as indicated. Arrowheads depict Pax7-MyoG- nuclei. **g)** YFP+ events per animal at E14.5 and P0. **h)** Quantification of myogenic progenitors (Pax7+MyoG-) and postmitotic myoblasts (Pax7-MyoG+) cells in the YFP+ and YFP- populations. **i)** Western blot analysis of Shp2 protein in YFP+ populations of Pax7^{ICNm}; Shp2^{flox} animals at E14.5 and P0.
Ctrl: control, Pax7$^{ICNm/+}$; Shp2$^{flox/+}$; RYFP$^{+/-}$
**coShp2:** mutant, Pax7$^{ICNm/+}$; Shp2$^{flox/flox}$; RYFP$^{+/-}$

The isolated YFP+ cells were highly enriched in myogenic cells i.e. 85 % of the cells isolated from E14.5 mice, and 97% of the cells isolated from P0 animals expressed Pax7 and/or MyoG. In comparison, less than 1% of YFP-negative cells were myogenic. Thus, the majority of myogenic cells had undergone Cre-dependent recombination, and expressed YFP+.

To test for the depletion of Shp2, I analyzed Shp2 protein levels by western blot using FACS sorted myogenic cells (YFP+ cells) from control (Pax7$^{ICNm/+}$; Shp2$^{flox/+}$; RYFP$^{+/-}$) and conditional Shp2 mutant (coShp2, Pax7$^{ICNm/+}$; Shp2$^{flox/flox}$; RYFP$^{+/-}$) mice (Fig. 3.1i). This showed a marked reduction of Shp2 protein in mutant compared to control myogenic cells at E14.5 and P0. The reduction of Shp2 was less pronounced at E14.5, which might be partly due to impurities.

2. Postnatal muscle growth deficit in coShp2 mice

Previous analysis performed by Robin Schneider in the laboratory showed that coShp2 animals did not display any apparent phenotype immediately after birth, for instance a difference in weight or size (Schneider, doctoral thesis, 2010). However, coShp2 animals gained less weight in the first two postnatal weeks and started to display changes in motor behavior. In addition, Robin Schneider and I observed a severely compromised muscle growth during the first two weeks after birth (Fig. 3.2a-d). To quantify the impaired muscle growth I measured the minimal Feret's fiber diameter of *Extensor carpi radialis longus* (ECRL) muscle fibers (Fig. 3.2e, f). The minimal Feret's diameter describes the shortest possible distance in between two parallel planes along a muscle fibers and corrects thus for errors that are introduced when the fiber is not sectioned transversally (Merkus, 2009). At birth the minimal Feret's fiber diameters were similar in control and coShp2 muscle. However, one week after birth the diameter was decreased by 17% and 19% when coShp2 (Pax7$^{ICNm/+}$; Shp2$^{flox/flox}$) and wild type (Pax7$^{+/+}$; Shp2$^{flox/flox}$) muscle was compared at P7 and P14, respectively. Similarly, the numbers of nuclei/fiber were reduced in the coShp2 muscle (Schneider, doctoral thesis, FU Berlin, 2011).
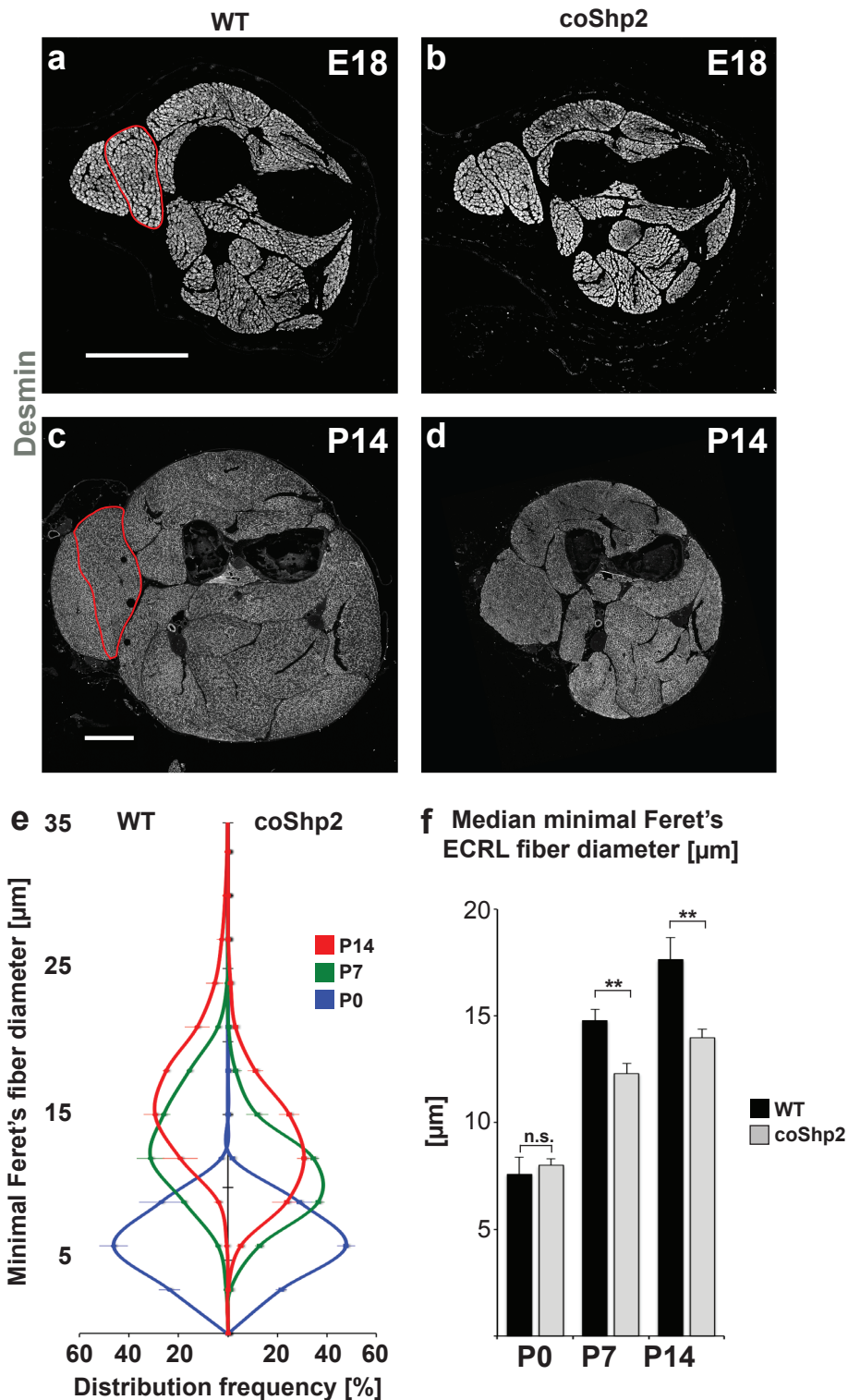
Fig. 3.2: Postnatal muscle growth deficit of coShp2 mice. a-d) Immunohistological analysis of lower forelimbs using an anti-Desmin antibody at **(a-b)** E18 and **(c-d)** P14; the *Extensor carpi radialis longus* muscle (ECRL) is indicated by a red line in a) & c). **e)** Distribution of minimal Feret's fiber diameter of ECRL fibers from control and coShp2 mutants at P0 (blue), P7 (green) and P14 (red). **f)** Quantification of the median minimal Feret's fiber diameter. Scale bar: 500 μm.

WT: wild type, Pax7$^{+/+}$; Shp2$^{flox/flox}$

coShp2: mutant, Pax7$^{ICNm/+}$; Shp2$^{flox/flox}$

3. The pool of myogenic progenitor cells is not maintained in coShp2 mice

Fetal and early postnatal skeletal muscle grows primarily by the addition of myonuclei to existing myofibers (White, 2010). Pax7+ myogenic precursor cells provide the cellular source for the muscle growth. Robin Schneider had observed that the myogenic progenitor pool declined after birth in coShp2 mutants. I verified this and tested whether the heterozygous mutation affects Pax7+ cells, i.e. I compared wild type animals (Pax7$^{+/+}$; Shp2$^{flox/flox}$), Shp2 heterozygous (Pax7$^{ICNm/+}$; Shp2$^{flox/+}$) and Shp2 mutant (Pax7$^{ICNm/+}$; Shp2$^{flox/flox}$) animals (Fig. 3.3a-f, j). At E16, I did not observe significant differences. At subsequent stages (E18), the number of Pax7+ myogenic precursors was reduced in coShp2 muscle. After birth, the numbers declined further, but I did not find significant differences in the number of Pax7+ cells in Shp2 heterozygous animals. To verify the decrease in myogenic precursor cell numbers at P0, I used flow cytometry (Fig. 3.3g-i). The percentage of myogenic VCAM1+CD31-CD45-Sca1- cells was decreased by 50% in coShp2 animals compared to wild type and Shp2 heterozygous animals (Fig. 3.3k, appendix Fig.A2). This was similar to the decrease of Pax7+ cells per 100 fibers.
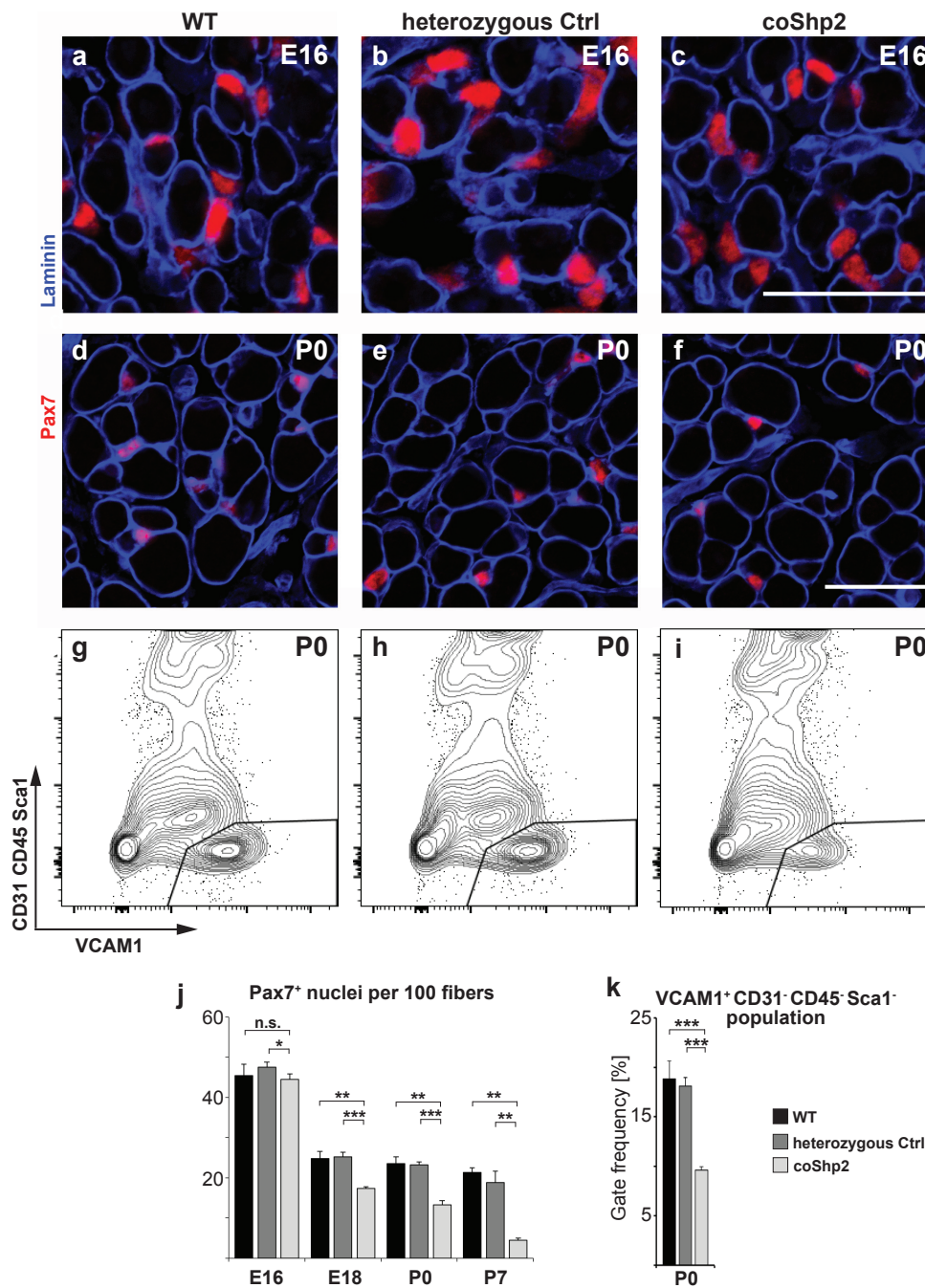
Fig. 3.3: **Postnatal loss of Satellite cells in Shp2 mutant muscle.** Immunohistological analysis of muscle in the lower forelimb using antibodies against Pax7 and Laminin at E16 **(a-c)** and P0 **(d-f)**. **(g-i)** Contour plots showing relative fluorescence intensities for VCAM1 (x-axis) and CD31, CD45 and Sca1 (y-axis) of FACS sorted cells from limb muscle at P0. The indicated gate was used to sort VCAM1+CD31-CD45-Sca1- cells. **j)** Quantification of Pax7+ cells per 100 muscle fibers in muscle of lower forelimbs at indicated developmental stages. **k)** Percentage of VCAM1+CD31-CD45-Sca1- cells isolated from muscle of wildtype, heterozygous controls and homozygous coShp2 mutants. Scale bar: 30 μm

WT: wild type, Pax7$^{+/+}$; Shp2$^{flox/flox}$

Heterozygous Ctrl: Cre-positive heterozygous control, Pax7$^{ICNm/+}$; Shp2$^{flox/+}$

coShp2: mutant, Pax7$^{ICNm/+}$; Shp2$^{flox/flox}$

4. Proliferation of coShp2 myogenic progenitor cells

Next I verified the cellular mechanisms that cause the decline in numbers of myogenic progenitors. Apoptosis, premature differentiation or decreased proliferation might account for this. Robin Schneider had already found that cell proliferation but not apoptosis was affected in coShp2 mutant muscle.

I verified the change in BrdU incorporation of Pax7+ cells. In addition, I analyzed the expression of the cell cycle marker Ki67, and quantified cells in the different phases of cell cycle to characterize the impaired proliferative capacity. Since I did not detect differences between wildtype and heterozygous control mice in initial experiments, I did not continue to analyze the heterozygote animals in immunohistological experiments. At E16, wildtype (Pax7$^{+/+}$; Shp2$^{flox/flox}$) and coShp2 (Pax7$^{ICNm/+}$; Shp2$^{flox/flox}$) animals showed similar rates of BrdU+ incorporation, but the rates declined at subsequent developmental stages (Fig.3.4a-c, d, e, g, h). The onset of the change in proliferation coincides approximately with the time at which myogenic progenitor cells assume a Satellite cell position (Kassar-Duchossoy, 2005; Relaix, 2005).

I therefore also analyzed Satellite cells inside and outside of their niche, and defined their proliferative activity using BrdU. At E16.5, around half of the Pax7+ cells locate to the interstitial space, and the other half colonized the niche below the lamina of the muscle fiber (Fig. 3.5a,b & f; Satellite cell homing appendix Fig. A3). Proliferation of Pax7+ cells was similar in the interstitial space of control and coShp2 mutant muscle. When located in the niche, Pax7+ cells showed a mild but significant decrease in proliferation in coShp2 muscle.
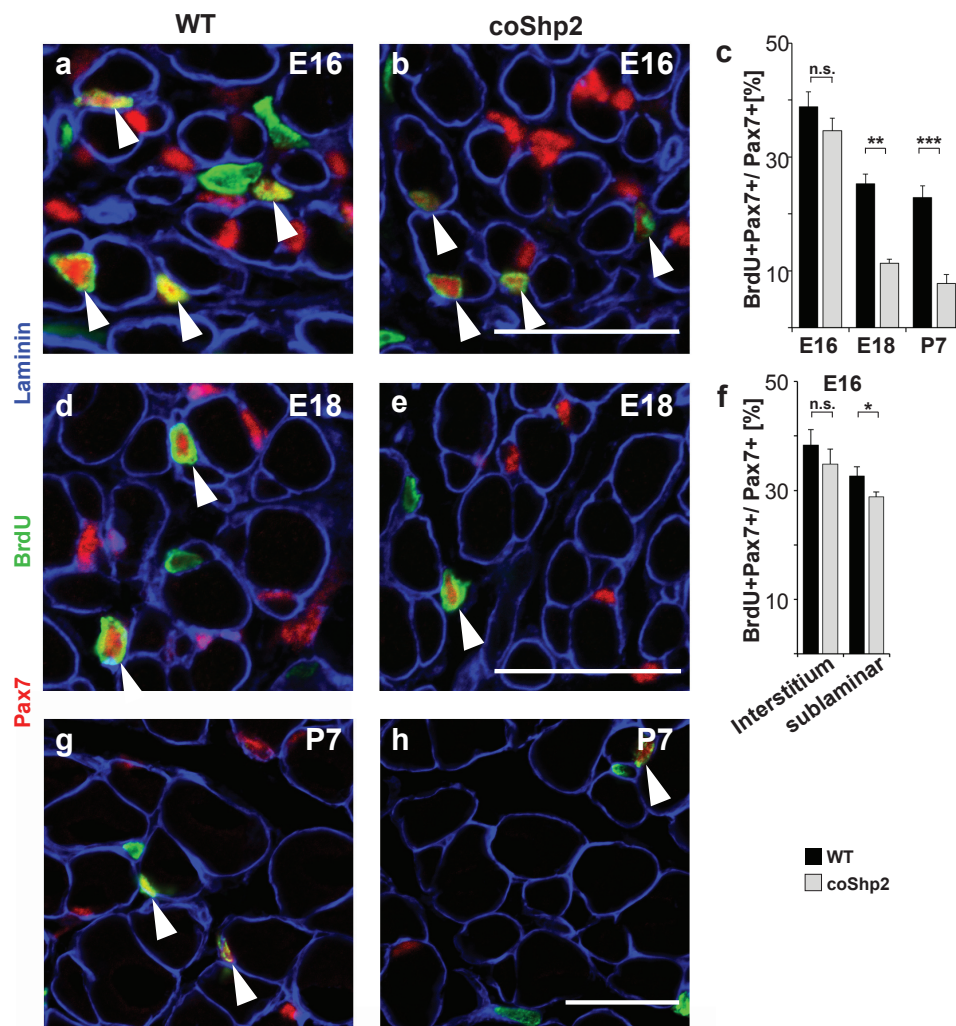
Fig. 3.4: **Proliferation is impaired in coShp2 myogenic progenitor cells at postnatal stages.** Immunohistological analysis of lower forelimbs using anti-Pax7, anti-BrdU and anti-Laminin antibodies at **(a-b)** E16, **(d-e)** E18 and **(g-h)** P7. Animals were pulse-labeled with BrdU for 2 hours. Arrowheads indicate Pax7+BrdU+ nuclei. **c)** Quantification of BrdU+Pax7+ cells at indicated developmental stages. **f)** Quantification of BrdU+Pax7+ cells in the interstitial space and in a sublaminar position at E16. Scale bar: 30 µm

WT: wild type, Pax7^{+/+}; Shp2[flox/flox]

coShp2: mutant, Pax7[ICNm/+]; Shp2[flox/flox]

BrdU labels S-phase cells. To define all Satellite cells that are in the cell cycle, I stained for Ki67 (Fig. 3.5, (Lopez, 1991)). At E16 all myogenic precursor cells proliferate, i.e. express Ki67 in coShp2 and control mice. Interestingly, at E18, despite the fact that BrdU incorporation was decreased (50% decrease in mutants), Ki67 expression was little affected. Directly after birth more than 50 % of Pax7+ cells had exited the cell cycle in coShp2 animals, i.e. were Ki67 negative, whereas most control Satellite cells were still cycling. This difference between Ki67 expression coShp2 and control mice became more pronounced by P7.
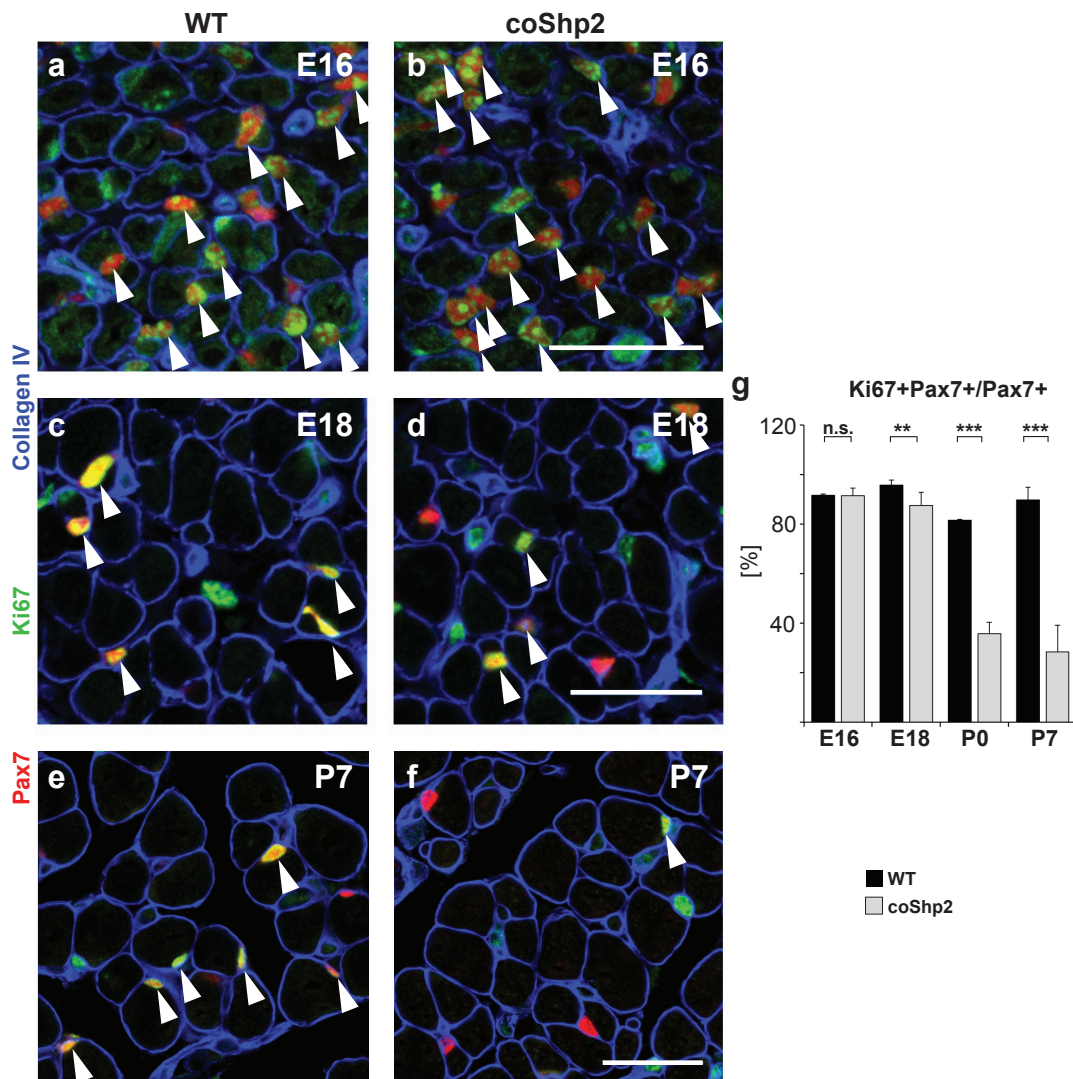
Fig. 3.5: **Early postnatal coShp2 myogenic progenitor cells exit the cell cycle. (a-f)** Immunohistological analysis using antibodies directed against Pax7, Ki67 and Collagen IV on lower forelimbs at **(a-b)** E16, **(c-d)** E18 and **(e-f)** P7. **g)** Quantification of Ki67+Pax7+ cells of all Pax7+ cells at different developmental stages.

WT: wild type, Pax7$^{+/+}$; Shp2$^{flox/flox}$

coShp2: mutant, Pax7$^{ICNm/+}$; Shp2$^{flox/flox}$

The difference between BrdU incorporation and Ki67 expression in Satellite cells at E18.5 might indicate that cell cycle progression is impaired and that the cells accumulate at a certain phase of the cell cycle (Fig.3.6a, b). Alternatively, mutant Satellite cells might have already stopped to proliferate but not yet reached quiescence. To assess their DNA content, I isolated YFP+ cells and stained them with the double strand DNA/RNA intercalator propidium iodide. This dye has been widely used to quantify the distribution of cells in different cell cycle phases (overview in Darzynkiewicz, 2010). The full gating strategy for this assay is shown in appendix Fig.A1&4.

The histogram in Fig.3.6d showed an accumulation of Shp2 mutant Satellite cells in the population that corresponds to cells in the G_0/G_1 phase of the cell cycle. Quantification of the relative distribution of cells in the different phases was performed in FloJo vX10.0.7 using an algorithm of the cell cycle analysis tool (Watson Pragmatic algorithm; Watson, 1987). CoShp2 myogenic progenitor cells (Pax7$^{ICNm/+}$; Shp2$^{flox/flox}$; RYFP$^{+/-}$) were enriched in the G_0/G_1 phase of the cell cycle compared to the cells obtained from the control (Pax7$^{ICNm/+}$; Shp2$^{flox/+}$; RYFP$^{+/-}$) mice (Fig.3.6c).
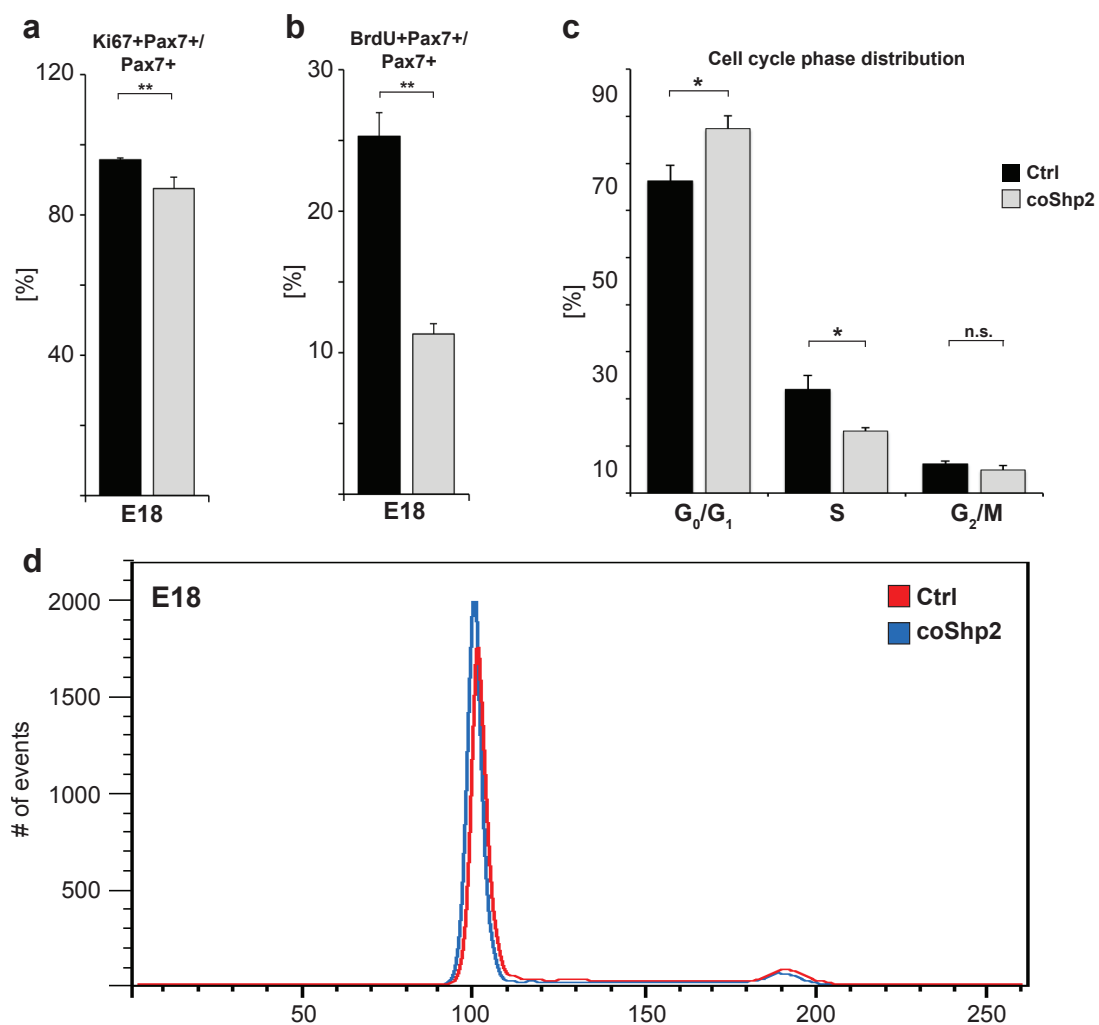
Fig. 3.6: **Cell cycle profile of fetal myogenic progenitor cells.** Quantification of **(a)** BrdU incorporation and **(b)** Ki67 expression in Pax7+ cells in limb muscle at E18. **c)** Quantification of cell cycle phase distribution for histogram shown in d). **d)** Flow cytometric analysis of propidium iodide stained YFP+ cells isolated from limb muscles at E18.
Ctrl: control, Pax7$^{ICNm/+}$; Shp2$^{flox/+}$; RYFP$^{+/-}$
coShp2: mutant, Pax7$^{ICNm/+}$; Shp2$^{flox/flox}$; RYFP$^{+/-}$

5. Proliferation of cultured myogenic progenitor cells

The transcription factor Pax7 is expressed in myogenic progenitor cells. Pax7^{ICNm} mediated recombination in myogenic precursors leads to a loss of Shp2 in the growing muscle fiber, as well, which might affect progenitor proliferation indirectly. To assess whether proliferation is affected in a cell-autonomous manner, I analyzed Shp2 mutant myogenic progenitor cells in culture. For this, YFP+ cells were isolated at E14.5 and P0 and cultivated over night in growth medium. I analyzed proliferation using BrdU incorporation and for expression of the cell cycle marker Ki67. BrdU incorporation was not significantly changed in early fetal Shp2 mutant myogenic progenitors (Pax7$^{ICNm/+}$; Shp2$^{flox/flox}$; RYFP$^{+/-}$), but was severely impaired in neonatal Shp2 mutant cells compared to control cells (Pax7$^{ICNm/+}$; Shp2$^{flox/+}$; RYFP$^{+/-}$) (Fig.3.7a-c). Thus, BrdU incorporation was decreased by 80% in neonatal coShp2 Satellite cells. Analysis of the cell cycle marker Ki67 showed that more than 97 % cells of controls and coShp2 mutants at E14.5 remained in the cell cycle. In neonatal Satellite cells, the number of Ki67+ cells was reduced by 40 % compared to control cells (Fig.3.7d-f).
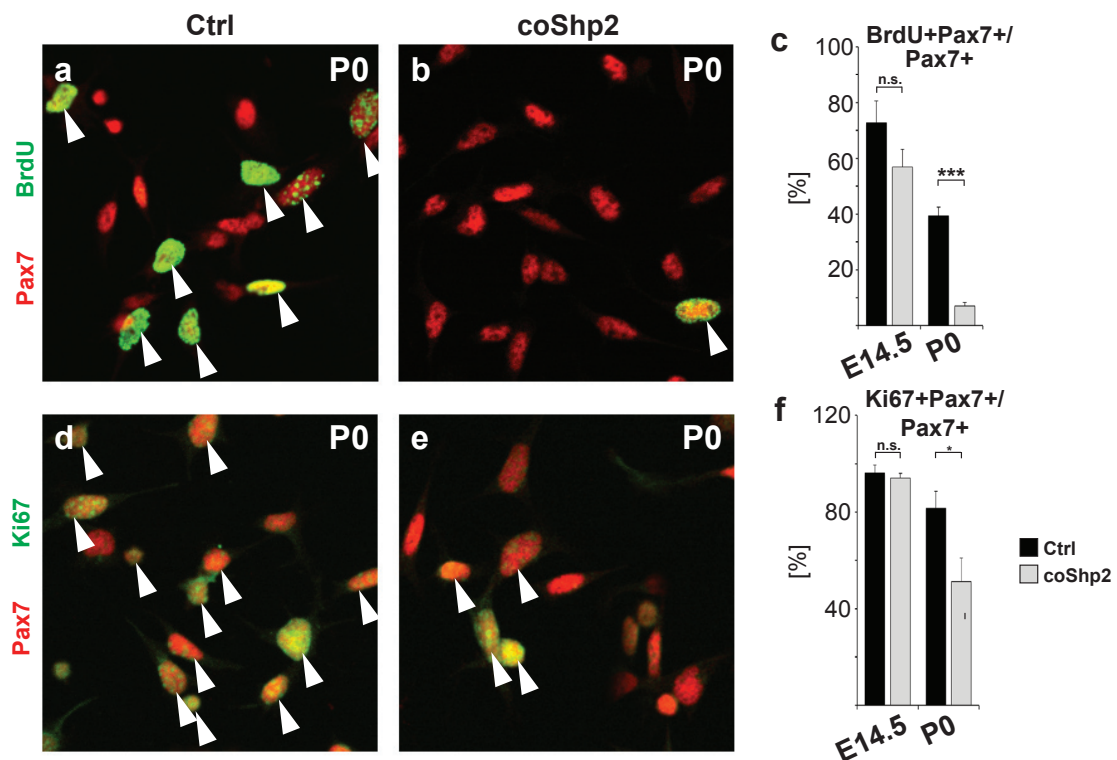
Fig. 3.7: Cultured neonatal coShp2 myogenic progenitor cells do not proliferate. Immunohistological analysis of cultured myogenic progenitors isolated at P0 stained with an anti-Pax7 and **(a-b)** anti-BrdU, and **(d-e)** anti-Ki67 antibodies. Cells were incubated with BrdU for 1 hour. Quantification of **(c)** BrdU+Pax7+ and **(f)** Ki67+Pax7+.
Ctrl: control, Pax7$^{ICNm/+}$; Shp2$^{flox/+}$; RYFP$^{+/-}$
coShp2: mutant, Pax7$^{ICNm/+}$; Shp2$^{flox/flox}$; RYFP$^{+/-}$

6. Genome-wide expression analysis of neonatal coShp2 myogenic progenitor cells

To gain further insights in the molecular mechanism by which Shp2 interferes with neonatal Satellite cell proliferation, I performed a genome-wide transcription analysis using microarrays. VCAM1+CD31-CD45-Sca1- cells were isolated by FACS from newborn mice, and analyzed. Gabriele Born performed the hybridization and reading of the microarrays (MDC Berlin, AG Prof. Hübner, Experimental genetics of cardiac disease). After importing the raw data into Partek Genomics suite v6.6 I retrieved a list of differentially expressed genes. To exclude false-positives, the p-values have to be corrected by a multiple test correction algorithm, e.g. false discovery rate FDR (Benjamini-Hochberg, 1990). The number of genes that passed with a fold-change > + 1.5/< -1.5 and a false discovery rate FDR < 0.05 as significance criteria in Shp2 mutant VCAM1+CD31-CD45-Sca1- cells (Pax7$^{ICNm/+}$; Shp2$^{flox/flox}$) was small compared to control cells (Pax7$^{ICNm/+}$; Shp2$^{flox/+}$) (34 significantly down- and 50 significantly up-regulated genes). Therefore, I also analyzed differentially expressed genes using a FDR < 0.075 as a cut-off. This yielded a list of each about 100 up- and down-regulated genes that is listed in appendix Tab.A1&2. It should be noted that differences of expression using both methods had p-values below 0.001. I used a GO term enrichment analysis and the functional annotation-clustering tool of the D.A.V.I.D. database to analyze these genes further (Huang, 2009).

Among the deregulated gene genes associated with cell cycle (e.g. CyclinD1, Polo-like-kinase 2, PCNA; enrichment p = 5.5×10^{-6}, Tab.3.1), extracellular matrix proteins (e.g. Col1a1, Col12a1, Col14a1, Col6a1, TenascinXb; enrichment p = 2.9×10^{-12}, Tab.3.2) and proteases that process and remodel the extracellular matrix (Adamts2, Mmp23, Tab.3.2) as well as proteins that bind growth factors (Igf-binding protein Igfbp4/6/7, Decorin; enrichment p=1.5×10^{-9}, Tab.3.2) were enriched. I also noted that several transcription factors that correspond to immediate early genes (Egr2, Egr4, and Erm, Tab.3.1) were present on the list. Receptor tyrosine kinase signaling controls expression of these factors (overview in Sukhatme, 1990; Pérez-Cadahía; 2011; O'Donnell, 2012). This is in accordance with the impaired proliferation that I observed *in vivo*, and indicates that RTK signaling might be impaired. Moreover, coShp2 Satellite cells appear to re-model their niche by up-regulating genes encoding components of the extracellular matrix and proteases.

Tab.3.1: Down-regulated genes in neonatal Shp2 mutant Satellite cells. Differentially expressed transcripts in FACS-sorted VCAM1+CD31-CD45-Sca1- coShp2 (Pax7$^{ICNm/+}$; Shp2$^{flox/flox}$) and control (Pax7$^{ICNm/+}$; Shp2$^{flox/+}$) cells were analyzed for enriched GO terms. Displayed are genes that were associated with the enriched GO terms cell cycle (p=5.5x10^{-6}), cell division (p=2.1x10^{-5}) and transcriptional activity (p=7.3x10^{-2}; not significant).

	Gene symbol	Definition	Fold change	p-value	FDR
Cell-cycle & cell division associated proteins	Ccnd1	cyclin D1	**-2.78**	0.0003	0.0550
	Clspn	claspin homolog	**-2.67**	0.0002	0.0479
	Plk2	polo-like kinase 2	**-2.62**	0.0000	0.0067
	Plk4	polo-like kinase 4	**-2.44**	0.0002	0.0492
	Dek	DEK oncogene	**-2.44**	0.0003	0.0548
	Ndc80	NDC80 homolog, kinetochore complex component	**-2.44**	0.0000	0.0298
	Ccnb1	cyclin B1	**-2.22**	0.0003	0.0537
	Cenpl	centromere protein L	**-2.11**	0.0008	0.0744
	Cenpl	centromere protein L	**-2.11**	0.0008	0.0744
	Ranbp1	RAN binding protein 1	**-2.11**	0.0001	0.0434
	Pcna	proliferating cell nuclear antigen	**-2.02**	0.0007	0.0713
	Dbf4	DBF4 homolog	**-1.97**	0.0002	0.0477
	Siah2	seven in absentia 2	**-1.78**	0.0006	0.0669
	Timeless	timeless homolog	**-1.74**	0.0006	0.0692
	Eed	embryonic ectoderm development	**-1.72**	0.0006	0.0706

	Gene symbol	Definition	Fold change	p-value	FDR
Transcriptional activity	Egr4	early growth response 4	**-3.02**	0.00068	0.07128
	Egr2	early growth response 2	**-2.59**	0.00077	0.07435
	Zfp367	zinc finger protein 367	**-2.23**	0.00012	0.04451
	Zfp131	zinc finger protein 131, transcript variant 1	**-2.11**	0.00048	0.06483
	Etv5	ets variant gene 5 (Erm)	**-2.01**	0.00022	0.05301
	Psip1	PC4 and SFRS1 interacting protein 1	**-1.82**	0.00002	0.02746
	Sertad1	SERTA domain containing 1	**-1.80**	0.00025	0.05367
	Pknox1	Pbx/knotted 1 homeobox	**-1.80**	0.00064	0.07058
	Sdpr	serum deprivation response	**-1.76**	0.00038	0.05893
	Maff	v-maf musculoaponeurotic fibrosarcoma oncogene family, protein F	**-1.76**	0.00034	0.05496
	Taf5	TAF5 RNA polymerase II, TATA box binding protein (TBP)-associated factor	**-1.66**	0.00028	0.05480
	Nup62	nucleoporin 62	**-1.62**	0.00010	0.04340
	Smad5	MAD homolog 5 (Drosophila)	**-1.54**	0.00018	0.04815

Tab.3.1: Up-regulated genes in neonatal Shp2 mutant Satellite cells. Differentially expressed transcripts in FACS-sorted VCAM1+CD31-CD45-Sca1- coShp2 (Pax7[ICNm/+]; Shp2[flox/flox]) and control (Pax7[ICNm/+]; Shp2[flox/+]) cells were analyzed for enriched GO terms. Displayed are genes associated with the highly enriched GO terms extracellular matrix associated proteins ($p = 2.9 \times 10^{-12}$), secreted proteins ($p = 3.4 \times 10^{-8}$) and growth factor binding ($p = 1.5 \times 10^{-9}$).

	Gene symbol	Definition	Fold change	p-value	FDR
Extracellularmatrix-associated proteins	Adamts2	a disintegrin-like and metallopeptidase with thrombospondin type 1 motif, 2	2.90	0.0002	0.0537
	Fmod	fibromodulin	2.82	0.0002	0.0534
	Mfap2	microfibrillar-associated protein 2	2.62	0.0004	0.0614
	Tnxb	tenascin XB	2.55	0.0005	0.0657
	Dcn	decorin	2.49	0.0005	0.0651
	Kera	keratocan	2.43	0.0004	0.0597
	Col12a1	collagen, type XII, alpha 1	2.23	0.0000	0.0280
	Col1a2	collagen, type I, alpha 2	2.18	0.0001	0.0420
	Mmp23	matrix metallopeptidase 23	2.13	0.0001	0.0452
	Loxl1	lysyl oxidase-like 1	2.07	0.0001	0.0445
	Vtn	vitronectin	1.99	0.0004	0.0614
	Col14a1	collagen, type XIV, alpha 1	1.88	0.0008	0.0744
	Postn	periostin, osteoblast specific factor	1.82	0.0001	0.0383
	Eln	elastin	1.77	0.0002	0.0524
	Col6a1	procollagen, type VI, alpha 1	1.71	0.0003	0.0548
	Kazald1	Kazal-type serine peptidase inhibitor domain 1	1.59	0.00050	0.06568

	Gene symbol	Definition	Fold change	p-value	FDR
secreted proteins & growth factor binding capability	Htra1	HtrA serine peptidase 1	2.32	0.0002	0.0477
	Igfbp7	insulin-like growth factor binding protein 7	1.90	0.0005	0.0648
	Igfbp6	insulin-like growth factor binding protein 6	3.06	0.0000	0.0275
	Igfbp4	insulin-like growth factor binding protein4	2.32	0.0003	0.0548
	Ngfr	nerve growth factor receptor (TNFR superfamily, member 16)	2.05	0.0008	0.0744
	Pdgfra	platelet derived growth factor receptor, alpha polypeptide	2.97	0.0001	0.0377
	Cxcl14	chemokine (C-X-C motif) ligand 14	2.31	0.0003	0.0548
	Scg3	secretogranin III	1.50	0.0006	0.0667
	C1qtnf6	C1q and tumor necrosis factor related protein 6	1.83	0.0000	0.0067
	Bmper	BMP-binding endothelial regulator	2.24	0.0005	0.0656

7. Molecular characterization of coShp2 myogenic progenitors

7.1 Signaling pathways influenced by loss of or inhibition of Shp2 in C2C12 cells and cultured primary myogenic progenitors

Shp2 was shown to regulate a variety of signaling pathways including Mapk/Erk, PI3K/Akt and p38 signaling (Araki, 2003; Grossmann, 2009; Zhang, 2002; He, 2013). GS493 is a competitive inhibitor of the phosphatase activity of Shp2 (Grosskopf, 2015). To investigate the effects of Shp2 inhibition, I used myogenic C2C12 cells, a cell line that derives from Satellite cells and is able to differentiate into myotubes. I used increasing GS493 concentrations on C2C12 cells in growth medium, and analyzed effects on phosphorylation of Mapk/Erk, PI3K/Akt and Mapk/p38 by western blot (Fig. 3.8a).

Neither Akt nor p38 showed a reduction in phosphorylation with all tested concentrations. However, increasing GS493 concentrations strongly decreased Erk1/2 phosphorylation. 5 µM GS493 decreased Erk1/2 activation by 60 % compared to cells incubated with DMSO, higher concentrations decreased the phosphorylation by more than 90 %.
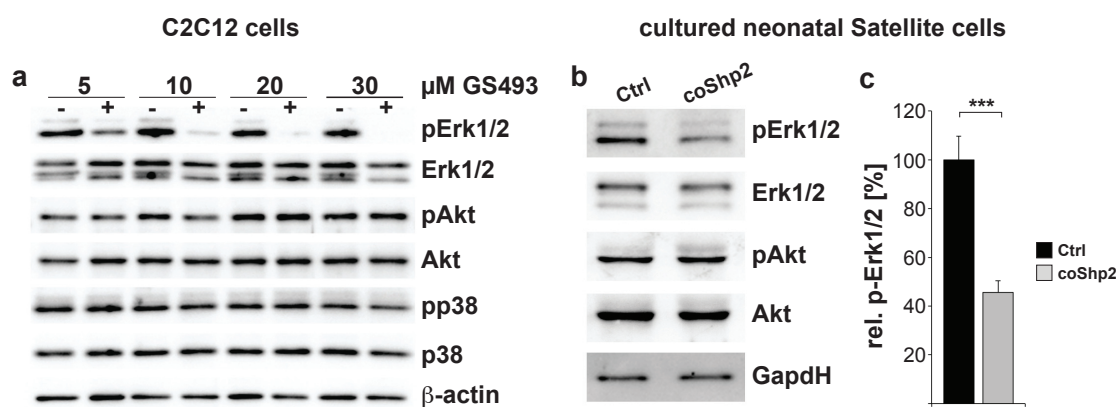
Fig. 3.8: Shp2 is essential for full Erk1/2 activation in C2C12 cells and neonatal myogenic cells. a) Western Blot analysis of C2C12 cells for pErk1/2, pAkt, pp38 and pStat3 levels cultivated in growth medium and incubated with GS493 for 1 h. **b)** Western Blot for analysis of pErk1/2 levels in coshp2 myogenic progenitors cells cultivated in growth medium for 18 hours after FACS isolation of YFP+ cells from limbs of neonatal pubs at P0. **c)** Quantification of b)
Ctrl: control, Pax7$^{ICNm/+}$; Shp2$^{flox/+}$; RYFP$^{+/-}$
coShp2: mutant, Pax7$^{ICNm/+}$; Shp2$^{flox/flox}$; RYFP$^{+/-}$

The data obtained from C2C12 cells suggests impaired Mapk/Erk activation upon pharmacological inhibition of Shp2. To verify if Shp2 is necessary for full Mapk/Erk activation I isolated YFP+ cells from extremities of control (Pax7$^{ICNm/+}$; Shp2$^{flox/+}$; RYFP$^{+/-}$) and coShp2 (Pax7$^{ICNm/+}$; Shp2$^{flox/flox}$; RYFP$^{+/-}$) animals by FACS from P0 animals. I cultured the cells in growth medium overnight and I analyzed Erk and Akt phosphorylation by Western Blot (Fig.3.8b, c). Similar to C2C12 cells Erk1/2 activation in cultured neonatal Satellite cells was impaired. Quantification of the western blot signal indicated that phospho-Erk1/2 levels were reduced by 60%.

7.2 Mild changes in myogenic differentiation in coShp2 mutant Satellite cells

Premature differentiation of myogenic progenitor might account for the cell cycle exit of coShp2 Satellite cells. To test this, I isolated YFP+ cells from neonatal P0 animals by FACS and analyzed them for expression of myogenic markers (MyoD and MyoG) and cell cycle inhibitors (p21 and p57) that are up-regulated during myogenic differentiation (Zalc, 2014; Chakkalakal, 2014; Pajcini, 2010; Carlson, 2008). Analysis of cytospin preparations of YFP+ cells from control mice (Pax7$^{ICNm/+}$; Shp2$^{flox/+}$; RYFP$^{+/-}$) demonstrated that 38 % of all Pax7+ cells co-expressed MyoD (Fig.3.9a-c). In coShp2 (Pax7$^{ICNm/+}$; Shp2$^{flox/flox}$; RYFP$^{+/-}$) cells, the number of Pax7+MyoD+ cells was slightly but significantly decreased to 23 % and I noted that the MyoD staining intensity appeared to be reduced. Similarly, MyoG expression was mildly down-regulated (Fig.3.9d-f). Analysis of MyoD and MyoG mRNA expression in FACS-isolated YFP+ cells showed a down-regulation in coShp2 cells (Fig.3.9g). Only the change in MyoG transcripts reached significance. Additionally, transcripts levels of p21 and p57 were unaffected.
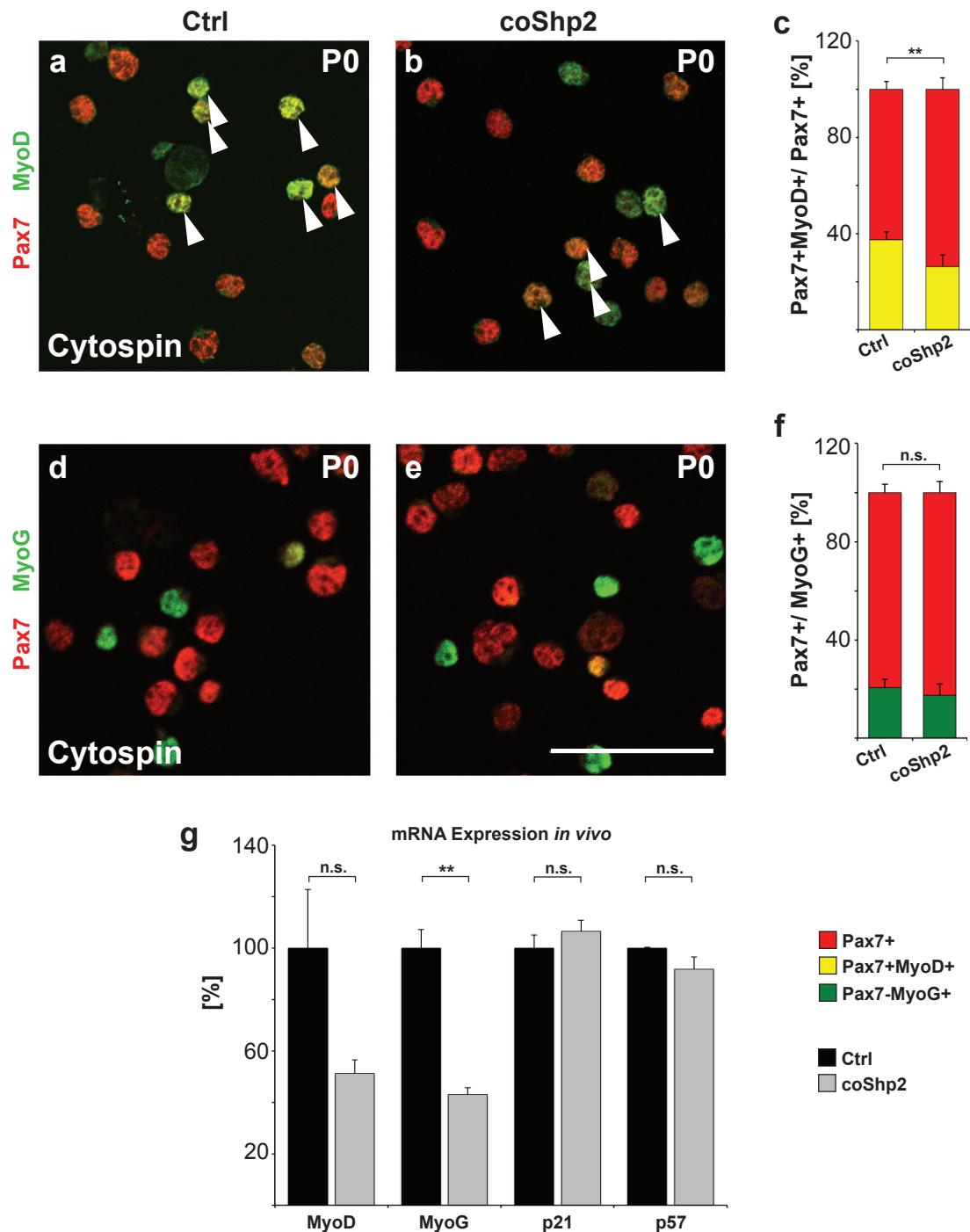
Fig. 3.9: Expression of myogenic regulatory factors and cell cycle inhibitors. YFP+ fraction of neonatal Pax7^{ICNm}; Shp2^{flox}; RYFP$^{+/-}$ animals were FACS-isolated and immediately fixed. Pax7 and **(a-b)** MyoD and **(d-e)** MyoG expression was analyzed by immunohistology. **c)** Quantification of Pax7 and MyoD expression in FACS-isolated YFP+ cells. **f)** Quantification of Pax7 and MyoG expression in YFP+ cells directly after isolation. **g)** mRNA expression levels of MyoD, MyoG, p21 and p57 in YFP+ cells was analyzed by qPCR.

Ctrl: control, Pax7$^{ICNm/+}$; Shp2$^{flox/+}$; RYFP$^{+/-}$

coShp2: mutant, Pax7$^{ICNm/+}$; Shp2$^{flox/flox}$; RYFP$^{+/-}$

8. Shp2 mutation in quiescent Satellite cells

Mutation of Shp2 with the constitutive Pax7^{ICNm} allele impairs muscle growth and interferes with survival of the mice. I therefore used an inducible Pax7^{CreERT2} allele to define Shp2 functions in adult Satellite cells and muscle regeneration (Lepper, 2009). Satellite cells in the adult are quiescent and become activated after muscle injury. I investigated non-injured and regenerating muscle in adult animals after Shp2 mutation. The outlines of these experiments are depicted schematically in Fig. 3.10a & 3.10b.
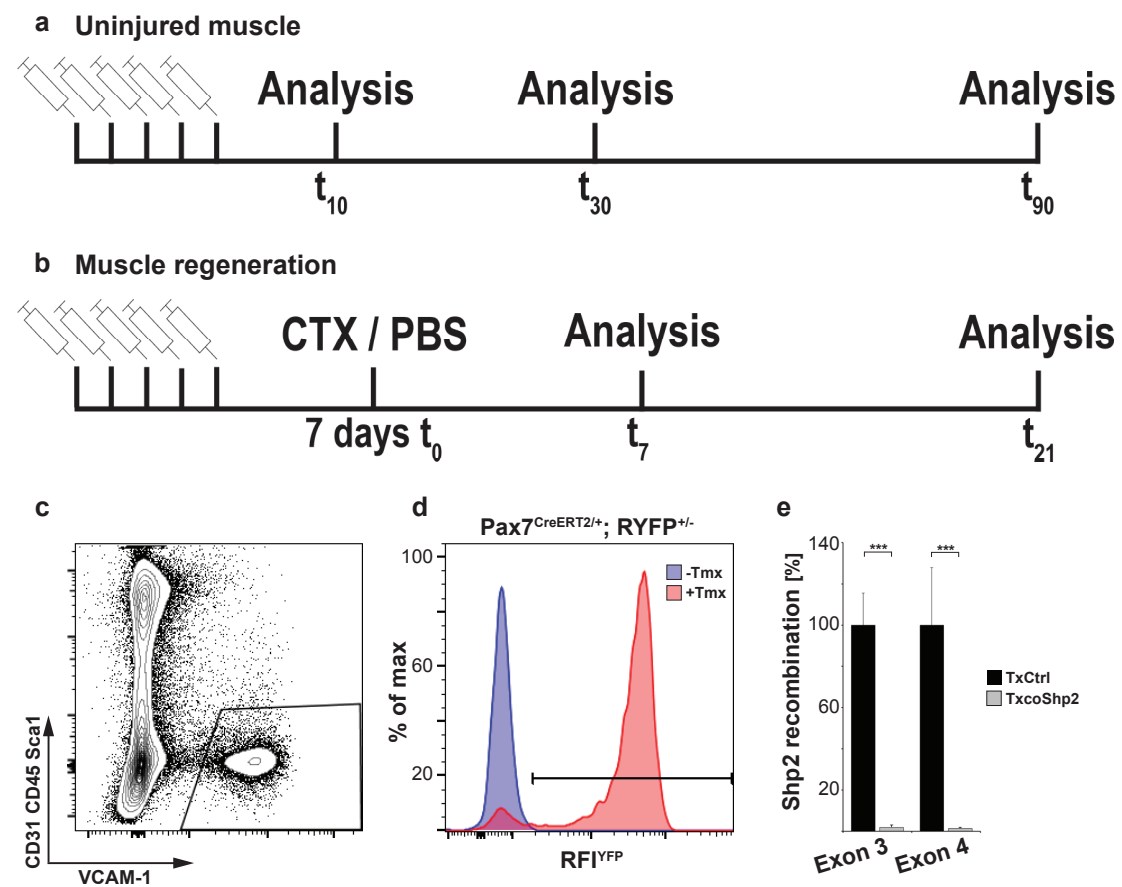
Fig. 3.10: Tamoxifen-induced recombination with the Pax7^{CreERT2} allele. a) Intraperitoneal injections of Tamoxifen to mutate Shp2 and to analyze maintenance of Satellite cells in sedentary muscle. **b)** Experimental scheme for the analysis of muscle regeneration. Muscle fiber injury was induced by intramuscular CTX injections. **c)** Flow cytometric identification of adult Satellite cells isolated from non-injured TA muscle. The gate depicts VCAM1+CD31-CD45-Sca1- cells **d)** YFP fluorescence of VCAM1+CD31-CD45-Sca1- cells of Pax7$^{CreERT2/+}$; RYFP$^{+/-}$ animals was analyzed 10 days after the last Tamoxifen injection. Blue/ red histogram: -/+ Tamoxifen. RFI^{YFP}: rel. YFP fluorescence intensity **e)** Relative mRNA expression from non-recombined Shp2 allele indicates that the majority of Satellite cells have undergone Shp2 recombination 10 days after the last Tamoxifen injection.

TxCtrl: control, Pax7$^{CreERT2/+}$; Shp2$^{flox/+}$

TxcoShp2: mutant, Pax7$^{CreERT2/+}$; Shp2$^{flox/flox}$

To test the recombination efficiency, I introduced a RYFP reporter into the Pax7^{CreERT2} background and injected 5 week old Pax7$^{CreERT2/+}$; RYFP$^{+/-}$ animals with a Tamoxifen solution intraperitoneally for 5 consecutive days. 10 days after the last Tamoxifen injection, I isolated VCAM1+CD31-CD45-Sca1- Satellite cells from TA muscles and tested the cells for YFP expression (Fig. 3.10c-d, appendix Fig.A5). 93 % of all VCAM1+CD31-CD45-Sca1- cells expressed YFP, indicating that the protocol I used allows efficient recombination. To test for recombination of the Shp2^{flox} allele, I generated Pax7$^{CreERT2/+}$; Shp2$^{flox/flox}$ mice and isolated RNA from VCAM1+ Satellite cells 10 days after the last Tmx injection. Recombination of the Shp2 gene deletes exon 3 and 4 (Grossmann, 2009). To quantify the levels of non-recombined Shp2, I designed two qPCR primer pairs that bind in either exon 3 or 4, and quantified mRNA that contains these exons in Satellite cells from *Tibialis anterior* muscle. 2% of the levels of unrecombined mRNA were observed in TxcoShp2 Satellite cells (Pax7$^{CreERT2/+}$; Shp2$^{flox/flox}$) compared to control cells (Pax7$^{CreERT2/+}$; Shp2$^{flox/+}$) (Fig. 3.10e).

9. Maintenance of Satellite cells in resting muscle depends on Shp2

In non-injured adult muscle, the majority of Satellite cells are quiescent. To assess whether Shp2 is required in quiescent Satellite cells, I defined the number of Pax7+VCAM1+ cells in control (Pax7$^{CreERT2/+}$; Shp2$^{flox/+}$) and mutant (Pax7$^{CreERT2/+}$; Shp2$^{flox/flox}$) animals after Tamoxifen treatment (Fig. 3.11). It should be noted that both, control and mutant mice, were treated with Tamoxifen. 10 days after treatment, Satellite cell numbers in control and mutant animals were similar. After 1 and 3 months, Satellite cells of in TxcoShp2 animals had declined by 32% and 50% in comparison to control animals, respectively (Fig. 3.11a-c). Surprisingly, 3 months after the Tamoxifen treatment the number of Satellite cells in control animals was also significantly lowered (Fig. 3.11d). Thus, the presence of a heterozygous Shp2 mutation already changes Satellite cell maintenance. In contrast, the heterozygous mutation had no effect on postnatal muscle development (Fig. 3.3).
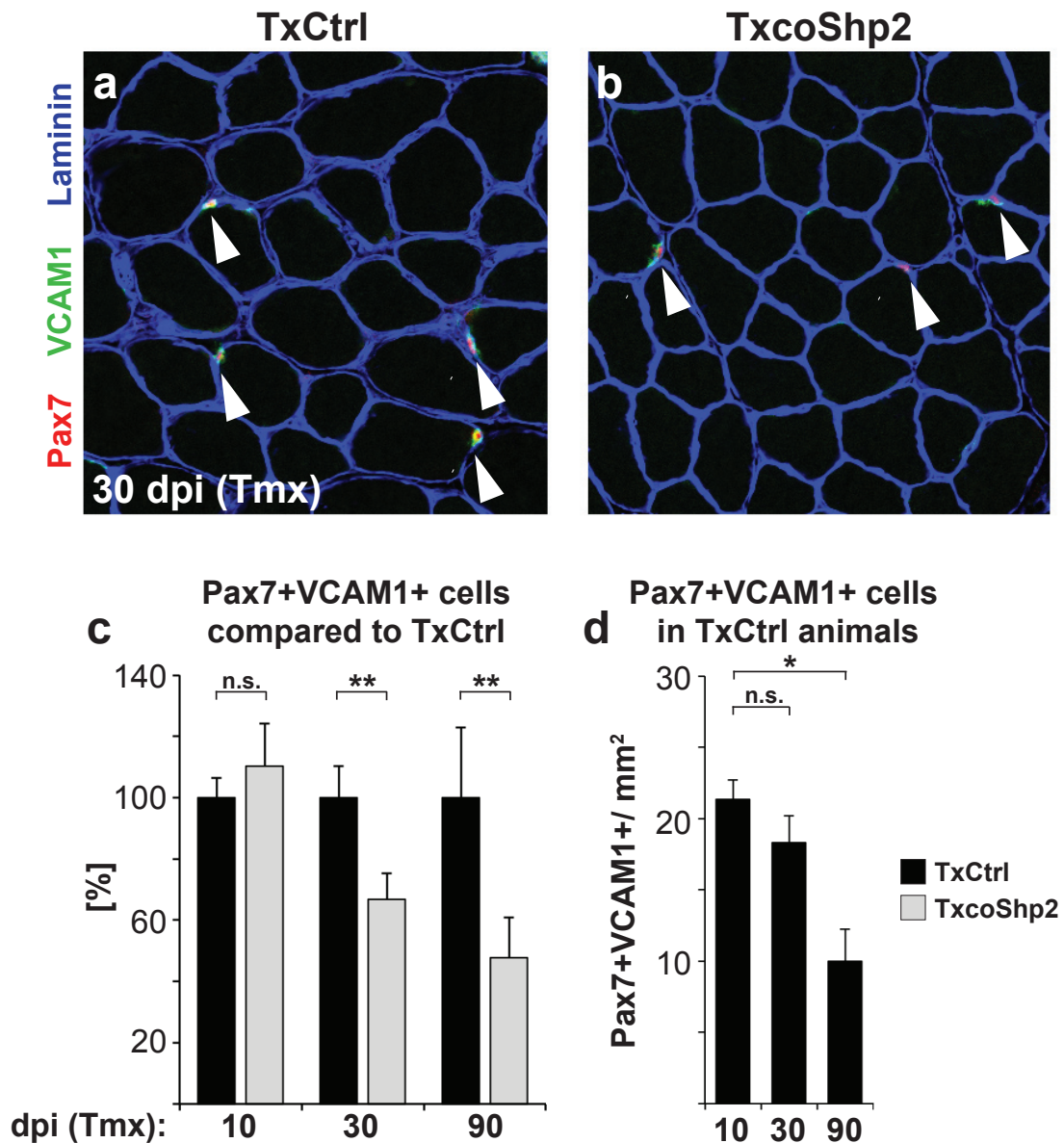
Fig. 3.11: **Long-term maintenance of Satellite cells depends on Shp2.**
(a-b) Immunohistological analysis of resting TA muscle with anti-Pax7, anti-VCAM1 and anti-Laminin antibodies after Tamoxifen-induced mutation of Shp2. **c)** Relative Quantification of Pax7+VCAM1+ Satellite cells resting TA muscle 10, 30 and 90 after Tamoxifen treatment (dpi (Tmx)). Controls were normalized to 100%. **d)** Quantification of Pax7+VCAM1+ Satellite cells resting TA muscle 10, 30 and 90 dpi(Tmx) in control animals.
TxCtrl: control, Pax7[CreERT2/+]; Shp2[flox/+]
TxcoShp2: mutant, Pax7[CreERT2/+]; Shp2[flox/flox]

10. Muscle regeneration is severely impaired in Shp2 mutant Satellite cells

Satellite cells are quiescent in non-injured muscle and quickly activate upon injury of the muscle fiber. The majority of the Satellite cell progeny will differentiate and fuse to regenerate the damaged tissue, but a subpopulation will self-renew and replenish the stem cell pool (Collins, 2005; Zammit, 2004). Cardiotoxin (CTX) injections induce severe muscle damage and can be used to study regeneration. CTX, a mixture of snake toxins from the cobra *Naja mossombica mossombica*, induces depolarization of the myofiber sarcolemma, which leads to fibers necrosis and initiation of muscle regeneration (Lin Shiau, 1976). Regenerating muscle fibers can be identified because they contain central nuclei. Verena Schöwel (Prof. Simone Spuler, Muscle research Unit; ECRC Berlin) injected TA muscles of TxCtrl (Pax7$^{CreERT2/+}$; Shp2$^{flox/+}$) and TxcoShp2 (Pax7$^{CreERT2/+}$; Shp2$^{flox/flox}$) mice with CTX on the experimental side, and PBS on the contralateral control side. The injury was induced 7-10 days after Tamoxifen treatment, i.e. at a time point when the number of Satellite cells was not yet affected (see Fig. 3.11c). Immunohistological analysis of the muscle using laminin antibodies (to visualize matrix around the fiber) and DAPI (to visualize nuclei) showed that muscle regeneration in TxcoShp2 mutants was severely impaired (Fig. 3.12a,b,g,h). Seven days after CTX injection, newly formed fibers were barely identifiable, and most fibers were necrotic. Also twenty-one days after CTX injection, only few new fibers had formed, demonstrating that regeneration was not only delayed (Fig. 3.12c,d). The deficit in fiber regeneration was also apparent when I used hematoxylin/eosin to stain the tissue, which revealed in addition fibrotic tissue and large, apparently empty areas in the injured muscle (Fig3.12i,j). I reasoned that these might correspond to fat tissue, which is known to form when muscle regeneration is impaired (Joe, 2010; Uezumi, 2010 & 2011). Indeed, Oil Red O staining demonstrated the presence of fat depositions (Fig. 3.12e,f). In conclusion, muscle regeneration was severely impaired when Shp2 is lacking, and instead of new muscle fibers fat deposits and fibrotic tissue were formed.
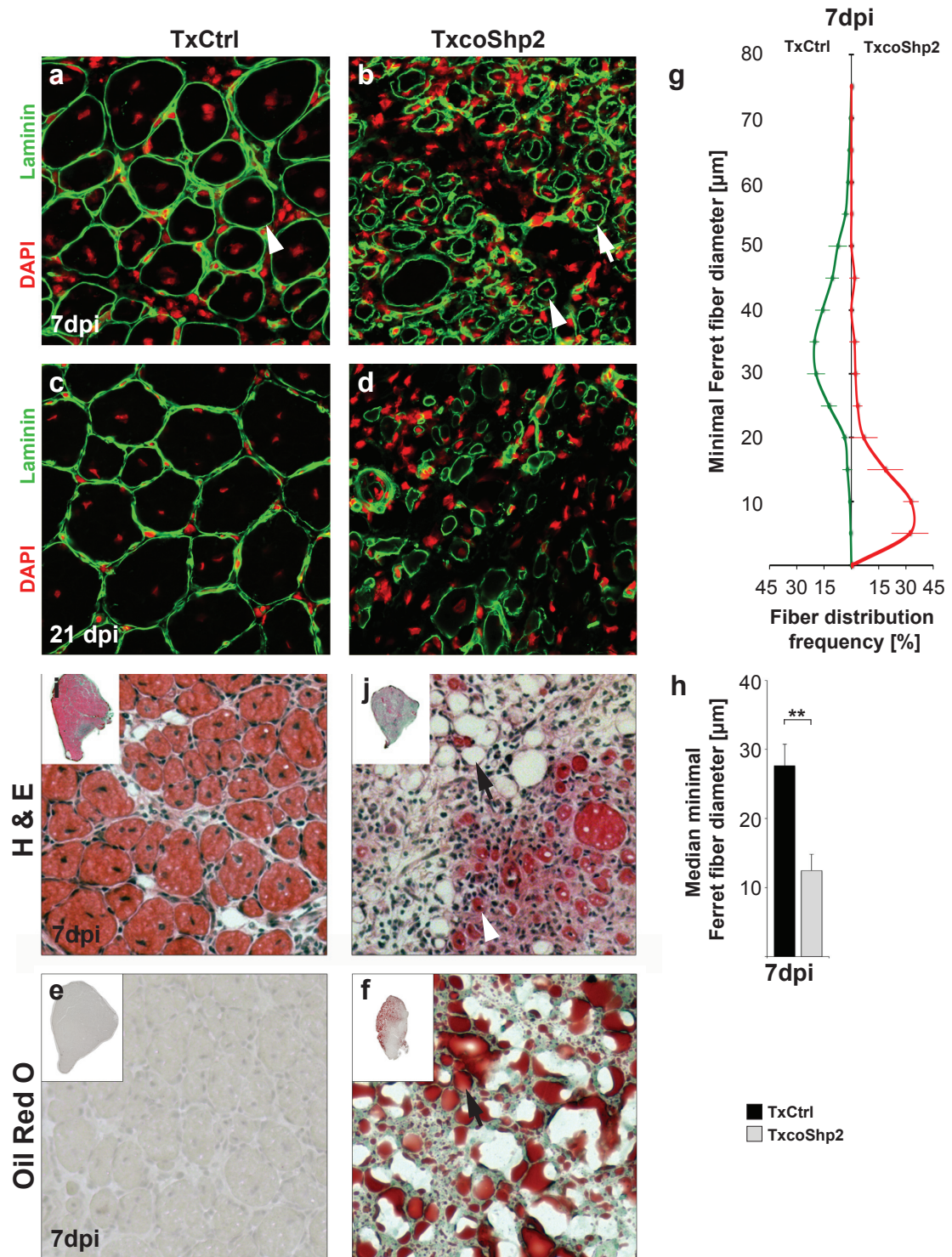
Fig. 3.12: Shp2 mutant Satellite cells cannot regenerate injured muscle. Histological analysis of TA muscle 7 dpi by **(a-b)** Oil Red O and **(c-d)** hematoxylin/eosin staining. Immunohistological analysis of TA muscle using an anti-Laminin antibody **(e-f)** 7 and **(i-j)** 21 dpi. **g)** Minimal Ferret fiber diameter distribution of regenerating TA muscle fibers 7 dpi. **h)** Median minimal Ferret fiber diameters of regenerating fibers 7 dpi. White arrowheads: regenerating muscle fibers, white arrows: necrotic fibers, black arrows: fat vacuoles.

TxCtrl: control, Pax7[CreERT2/+]; Shp2[flox/+]

TxcoShp2: mutant, Pax7[CreERT2/+]; Shp2[flox/flox]

I next analyzed whether Satellite cells were maintained in TxcoShp2 mutant muscle (Fig.3.13). Regenerating muscle of control animals showed 146 Pax7+VCAM1+ cells per mm^2 and thus a strong increase in Satellite cell numbers compared to resting muscle. Satellite cells numbers in injured TxcoShp2 muscle however had decreased to 5 Pax7+VCAM1+ cells per mm^2. Thus, in the damaged TxcoShp2 mutant muscle, the Satellite cell pool is not re-established.
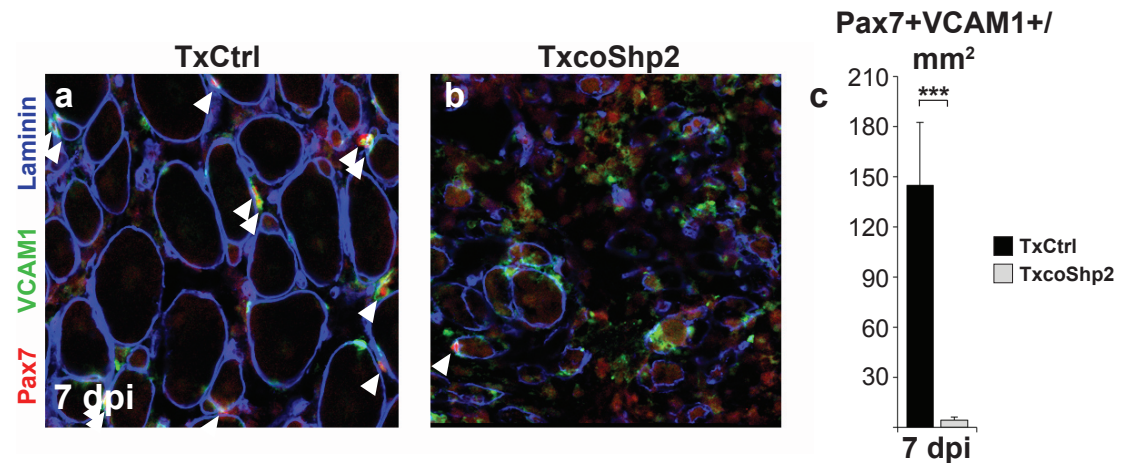
Fig. 3.13: TxcoShp2 Satellite cells are not maintained. (a-b) Immunohistological analysis of regenerating TA muscle using antibodies directed against Pax7, VCAM1 and Laminin 7 days after CTX injection. **c)** Quantification of Pax7+VCAM1+ cells per mm^2.
TxCtrl: control, Pax7$^{CreERT2/+}$; Shp2$^{flox/+}$
TxcoShp2: mutant, Pax7$^{CreERT2/+}$; Shp2$^{flox/flox}$

11. Shp2 is required for correct activation and proliferation of Satellite cells in culture

I used floating fiber cultures to study the activation of TxcoShp2 mutant Satellite cells. In this model, single myofibers with attached Satellite cells are isolated after enzymatic digestion from the *Extensor digitorum longus* (EDL) muscle. When such fibers are taken into culture, Satellite cells are activated, leave their niche to move on the outside surface and begin to proliferate. After 24 hours in culture, the Satellite cells displayed heterogeneous staining intensities for phosphorylated S6 protein (pS6) in fibers obtained from both TxCtrl (Pax7$^{CreERT2/+}$; Shp2$^{flox/+}$) and TxcoShp2 (Pax7$^{CreERT2/+}$; Shp2$^{flox/flox}$) muscle (Fig.3.14a,b). I noted a trend towards lower staining intensity in mutant Satellite cells, but the variability of background staining of fibers interfered with quantification. MyoD expression is quickly up-regulated upon Satellite cell activation (Zammit, 2004; Jones, 2005). More than 90% of Satellite cells on fibers from control and TxcoShp2 animals expressed MyoD after 24 hours (Fig. 3.14c,d,e). Thus, the lack of Shp2 does not interfere with the initial steps of Satellite cell activation.
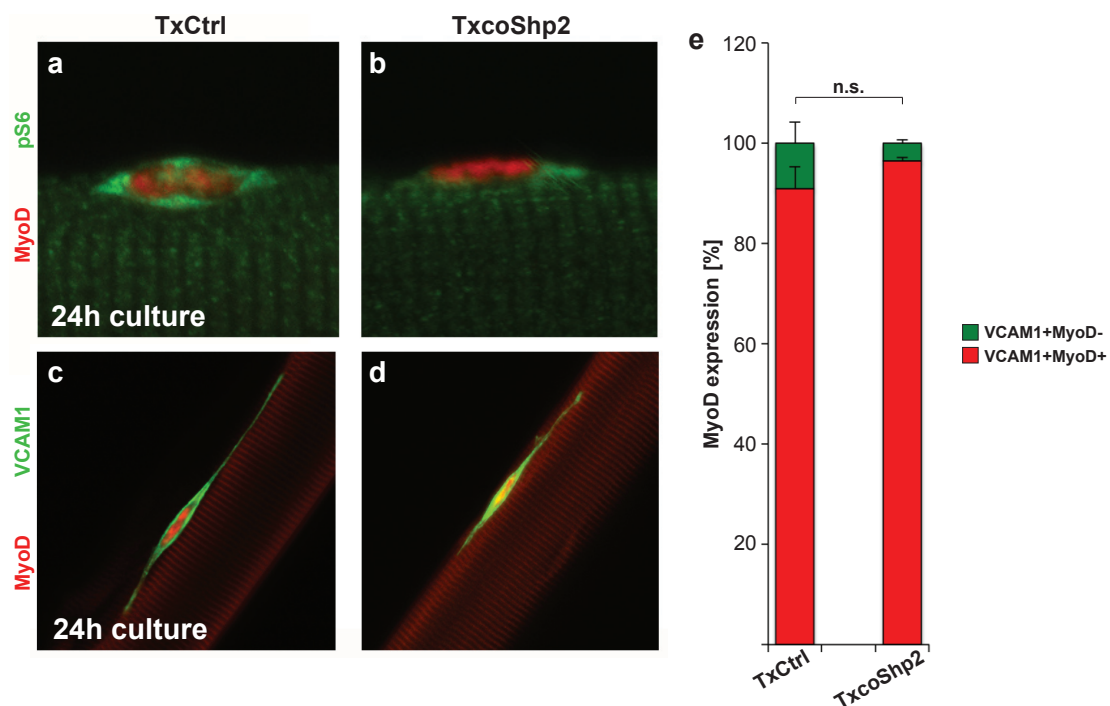
Fig. 3.14: Shp2 mutant Satellite cells activate protein synthesis and express the myogenic transcription factor MyoD. Immunohistological analysis of Satellite cells using **(a-b)** anti-phospho-S6, **(c-d)** anti-VCAM1 and anti-MyoD antibodies on myofibers cultured for 24 hours. **e)** Quantification of MyoD expression in VCAM1+ cells cultured for 24 hours. **TxCtrl:** control, Pax7$^{CreERT2/+}$; Shp2$^{flox/+}$
TxcoShp2: mutant, Pax7$^{CreERT2/+}$; Shp2$^{flox/flox}$

After 48 hours in culture, the majority of Satellite cells on control fibers had formed doublets (2 VCAM1+ cells per colony), but TxcoShp2 Satellite cells had only rarely divided (1.3 VCAM1+ cells per colony) (Fig.3.15a-c). After 72 hours, the difference was even more severe and I observed 5.5 VCAM1+ cells/colony on control fibers, and only 1.5 VCAM1+ cells/colony on the TxcoShp2 mutant fibers (Fig.3.15c-e). Pulse labeling (BrdU pulse between 24-48 hours) showed incorporation of BrdU in 93% and 60% of Satellite cells on control and TxcoShp2 mutant fibers (Fig.3.15a,b,f). Pulse labeling at later times showed again more severe deficits in proliferation. A BrdU pulse between 48-72 hours labeled 75% and 19% of control and TxcoShp2 mutant Satellite cells with BrdU, respectively (Fig.3.15d-f).
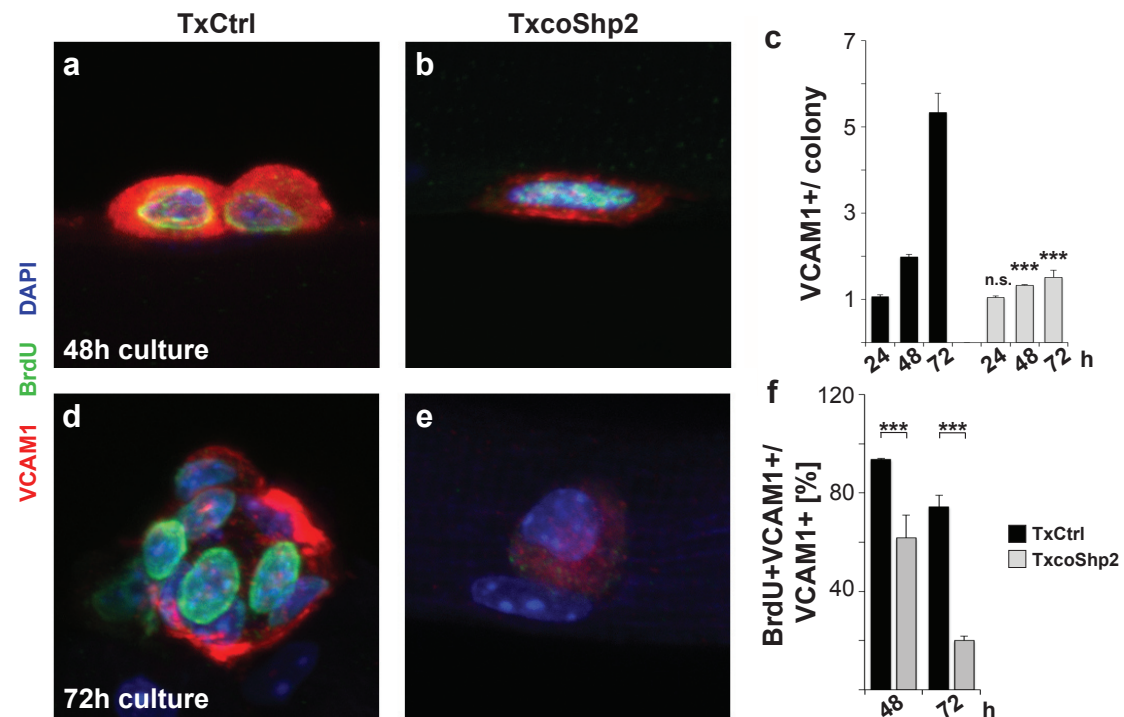
Fig. 3.15: Proliferation of TxcoShp2 Satellite cells is severely impaired. Immunohistological analysis of EDL fibers cultured for **(a -b)** 48 hours and **(d-e)** 72 hours with antibodies directed against VCAM1 and BrdU c) Quantification of VCAM1+ cells per colony after 24, 48 and 72 hours in culture **f)** Quantification of BrdU+VCAM1+ cells cultured for 48 and 72 hours. Fibers were incubated with BrdU for 24 hours. **TxCtrl:** control, Pax7$^{CreERT2/+}$; Shp2$^{flox/+}$ **TxcoShp2:** mutant, Pax7$^{CreERT2/+}$; Shp2$^{flox/flox}$

Next I tested whether Erk phosphorylation during adult Satellite cell activation depends on Shp2. Compared to the control, pErk staining intensity was strongly decreased in TxcoShp2 Satellite cells after 24h and 72h in culture (Fig. 3.17).
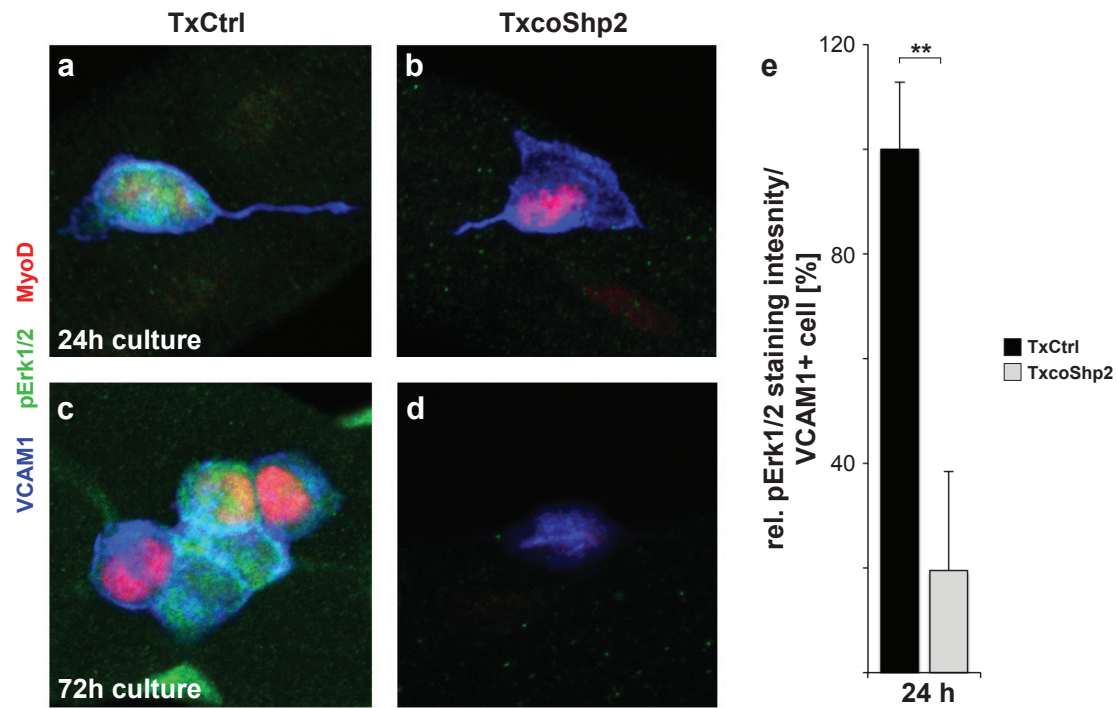
Fig. 3.16: Sustained phospho-Erk levels are decreased in TxcoShp2 Satellite cells. Immunohistological analysis of EDL fibers using antibodies against VCAM1 and pErk on fibers cultured for **(a-b)** 24 and **(c-d)** 72 hours. **e)** Quantification of phospho-Erk1/2 fluorescence in Satellite cells cultivated for 24 hours.
TxCtrl: control, Pax7$^{CreERT2/+}$; Shp2$^{flox/+}$
TxcoShp2: mutant, Pax7$^{CreERT2/+}$; Shp2$^{flox/flox}$

To assess cell cycle exit I analyzed Satellite cells for their Ki67 expression. After 48 hours of culture, 85% of control Satellite cells were positive for Ki67 and thus remained in the cell cycle, but only 55% of the TxcoShp2 mutant Satellite cells expressed Ki67 (Fig.3.17a-c). After 72 hours 65% and 25 % of the control and TxcoShp2 mutant cells expressed Ki67 (Fig.3.17d,e). Thus, in the absence of Shp2, Satellite cells proliferate less and many withdraw from the cell cycle.
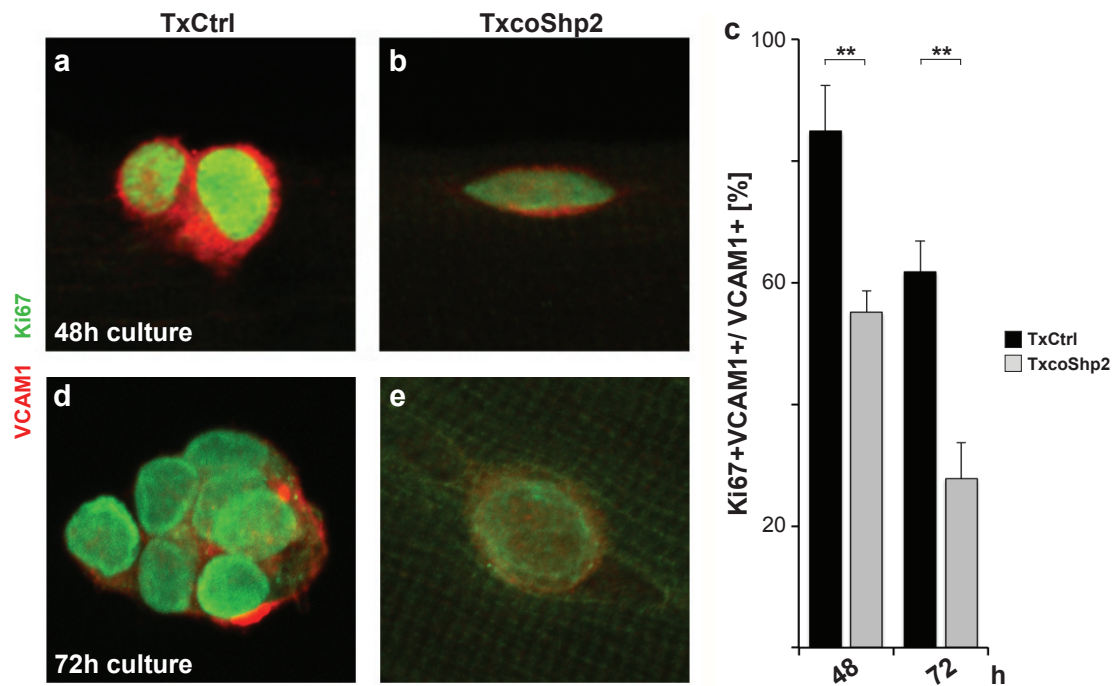
Fig. 3.17: Shp2 depleted Satellite cells quickly exit the cell cycle. Immunohistological analysis of EDL fibers using anti-VCAM1 and anti-Ki67 antibodies on fibers cultured for **(a-b)** 48 hours and **(d-e)** 72 hours. **c)** Quantification of Ki67+VCAM1+ cells on EDL fibers cultured for 48 and 72 hours.

TxCtrl: control, Pax7$^{CreERT2/+}$; Shp2$^{flox/+}$

**TxcoShp2:** mutant, Pax7$^{CreERT2/+}$; Shp2$^{flox/flox}$

12. Overexpression of a constitutively active MAPKK rescues proliferation of cultured coShp2 Satellite cells

To test whether activation of Mapk/Erk rescues proliferation in Shp2 mutant Satellite cells, I constitutively activated Mapk/Erk signaling using the Mek1DD allele. This allele encodes a constitutively active Mapkk variant that is expressed under the control of the ROSA locus after removal of a floxed translational stop cassette (Srinivasan, 2009; Cowley, 1994). Cre-dependent recombination can thus simultaneously introduce Shp2 mutation and Mapkk activation. I compared Satellite cell activation and proliferation in fiber cultures using control (TxCtrl: Pax7$^{CreERT2/+}$; Shp2$^{flox/+}$) and TxMek1DD single mutant (Pax7$^{CreERT2/+}$; Shp2$^{flox/+}$; Mek1DD$^{+/-}$) mice as well as TxcoShp2 (Pax7$^{CreERT2/+}$; Shp2$^{flox/flox}$) single and TxcoShp2; Mek1DD double (Pax7$^{CreERT2/+}$; Shp2$^{flox/flox}$; Mek1DD$^{+/-}$) mutant mice. At all tested time points (24h, 48h and 72h), I observed similar numbers of VCAM1+ cells in Satellite cell colonies from TxcoShp2; Mek1DD cells and control mice (Fig.3.18a,b,d,e). Similarly, when I tested for BrdU incorporation, I observed that activation of Mek1DD rescued the deficit observed in Shp2 mutants (Fig.3.18f). Thus, activated Mapkk was able to rescue the

proliferation deficit of Shp2 mutant Satellite cells. In contrast, when Shp2 was present, Mapkk activation had little effect on Satellite cell numbers or BrdU incorporation (Fig.3.18a,c,e). This became apparent when I compared fibers from TxCtrl animals and TxMek1DD mutants.
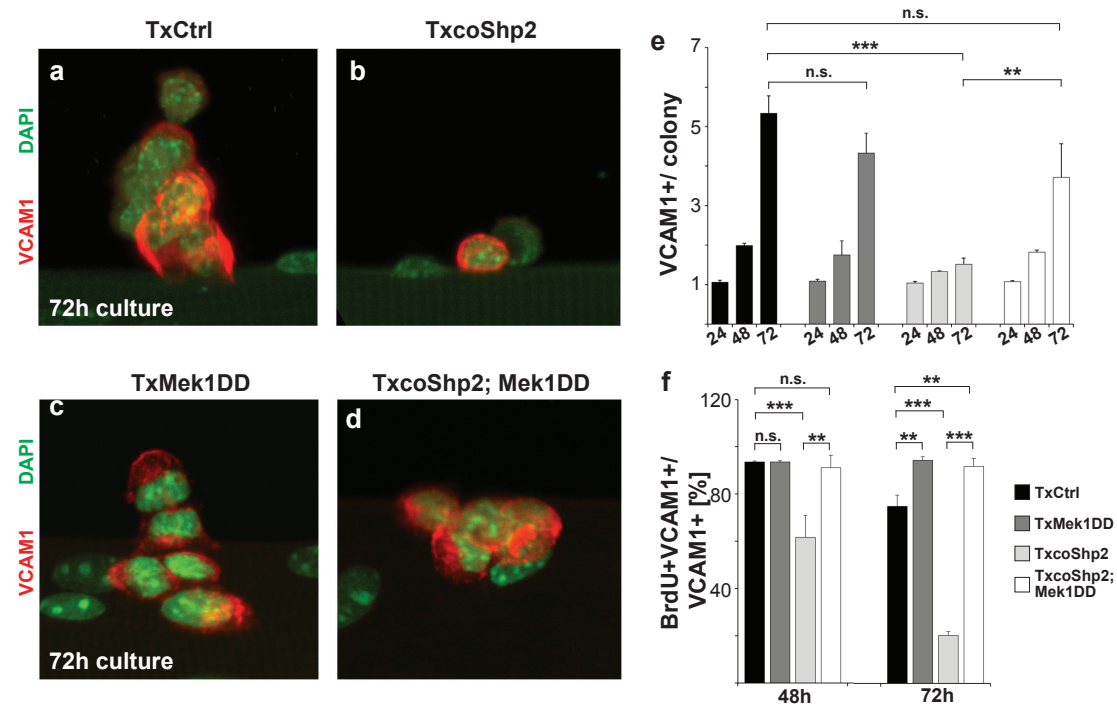
Fig. 3.18: Mek1DD expression in Shp2 mutant Satellite cells rescues proliferation.
(**a-d**) Immunohistological analysis of VCAM1 expressing cells on fibers cultured for 72 hours.
e) Quantification of VCAM1+ cells per colony after 24, 48 and 72 hours of culture.
f) Quantification of BrdU+VCAM1+ cells cultured for 48 and 72 hours. Fibers were incubated with BrdU for 24 hours.
TxCtrl: control, Pax7$^{CreERT2/+}$; Shp2$^{flox/+}$
TxMek1DD: activated Mapk/Erk, Pax7$^{CreERT2/+}$; Shp2$^{flox/+}$; Mek1DD$^{+/-}$
TxcoShp2: Shp2 mutant, Pax7$^{CreERT2/+}$; Shp2$^{flox/flox}$
TxcoShp2; Mek1DD: Shp2 mutant, activated Mapk/Erk Pax7$^{CreERT2/+}$; Shp2$^{flox/flox}$; Mek1DD$^{+/-}$

13. Shp2/Mapk/Erk signaling controls MyoD and MyoG expression

I next asked whether the Shp2 mutation affected myogenic differentiation. For this, Satellite cells in fiber culture from control and TxcoShp2 mice were analyzed for MyoD and MyoG expression at 72 hours in culture. This demonstrated that MyoD and MyoG were down-regulated in Shp2 mutant Satellite cells (Fig.3.19). Interestingly, MyoD, but not MyoG expression was rescued in TxcoShp2; Mek1DD double mutants (Fig.3.19a,d,e). Comparison of single TxMek1DD mutants and control mice demonstrated that Mapkk activation had only mild effects on MyoD

expression, but down-regulated MyoG. (Fig.3.19a-d&e-g). Thus, Mapkk activation as well as Shp2 mutation interfere with MyoG expression and thus with entry into terminal differentiation.
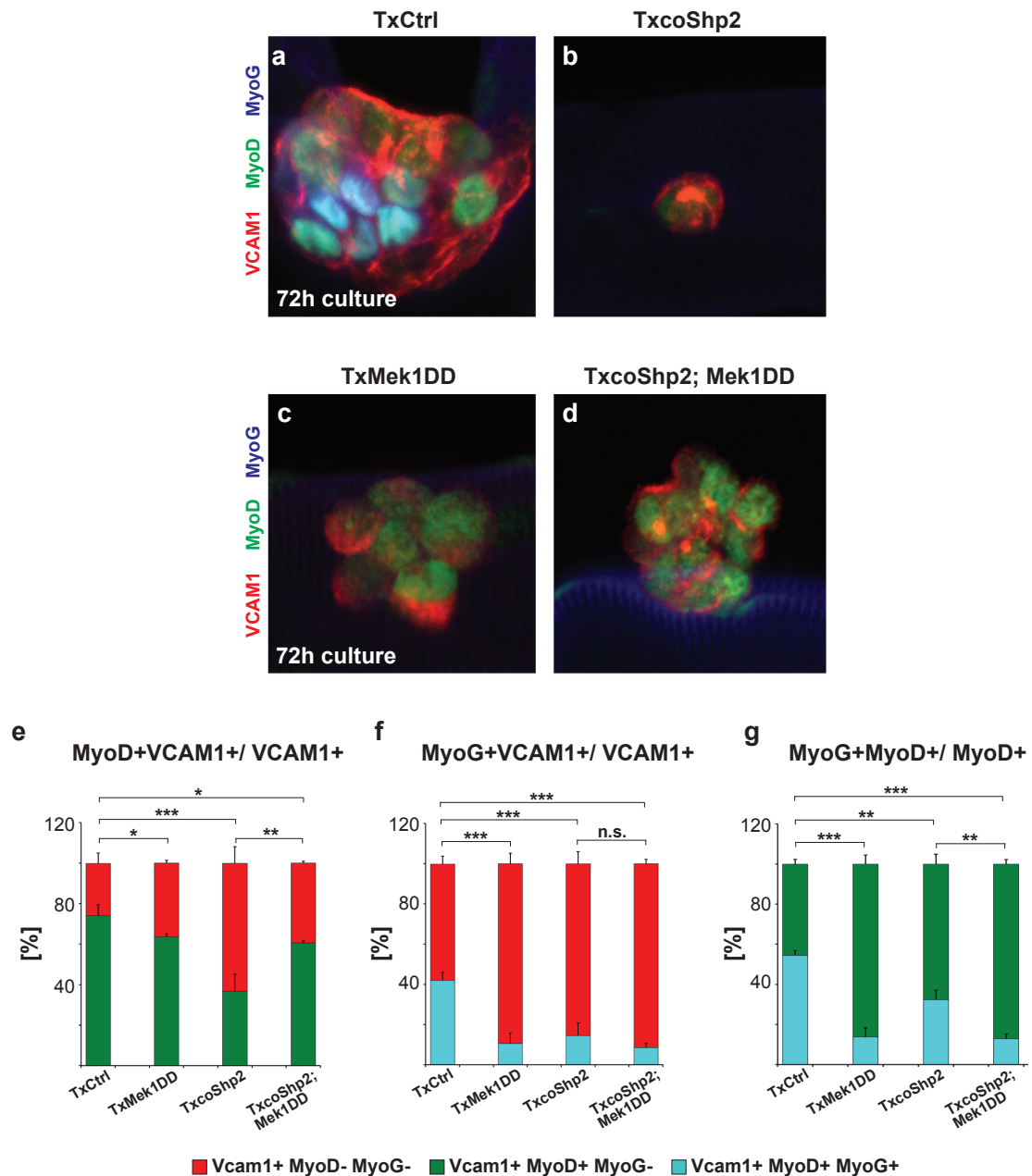
Fig. 3.19: Shp2/Mapk/Erk signaling regulates MyoD and MyoG expression. **(a-d)** Immunohistological analysis of activated Satellite cells on cultured EDL fibers with anti-VCAM1, anti-MyoD and anti-MyoG antibodies cultured for 72 hours. **e-f)** Quantification of **e)** MyoD and **f)** MyoG expression in VCAM1+ cells cultured for 72 hours. **g)** Quantification of MyoG expression in MyoD+ cells cultured for 72 hours.

TxCtrl: control, Pax7$^{CreERT2/+}$; Shp2$^{flox/+}$

TxMek1DD: activated Mapk/Erk, Pax7$^{CreERT2/+}$; Shp2$^{flox/+}$; Mek1DD$^{+/-}$

TxcoShp2: Shp2 mutant, Pax7$^{CreERT2/+}$; Shp2$^{flox/flox}$

TxcoShp2; Mek1DD: Shp2 mutant, activated Mapk/Erk Pax7$^{CreERT2/+}$; Shp2$^{flox/flox}$; Mek1DD$^{+/-}$

IV. Discussion

Newborn mice grow extensively and increase their weight 7-8-fold in the first three weeks of their life (White, 2010). Similarly, skeletal muscle grows more than 3-fold (Gokhin, 2008). During this three-week period, skeletal muscles mass increases by fusion of new cells, which are descendants of proliferating Satellite cells. Satellite cells enter quiescence in the adult but can be re-activated after injury and strongly proliferate to generate daughters that either differentiate to repair the muscle or self-renew to replenish the Satellite cell pool (Collins, 2005). These processes are highly regulated to control the balance in between differentiation, proliferation and re-entry into quiescence. Hence, deregulation of signals that control this balance has severe consequences for the maintenance of Satellite cells and skeletal muscle (Lepper, 2011; Sambasivan, 2011; Shea, 2010; Price, 2014; Gillespie, 2009; Fukada, 2011; Bröhl, 2012; Li; 2012).

In this work, I analyzed the functions of the tyrosine phosphatase Shp2 in Satellite cells during early skeletal muscle development and in the adult. Mutation of Shp2 in fetal and adult Satellite cells leads to severely impaired postnatal muscle growth and muscle regeneration, respectively. I show that Shp2 is essential for proliferation of Satellite cells, and that Shp2 depletion leads to a premature cell cycle exit. Further analysis showed that adult Shp2 mutant Satellite cells can enter an alert state but do not proliferate and instead quickly return to quiescence. My biochemical analyses demonstrated that Shp2 is essential for full activation of the Mapk/Erk pathway in proliferating Satellite cells of neonatal and adult animals. Interestingly, expression of Mek1DD suffices to overcome the proliferation deficits of Shp2 mutant Satellite cells, demonstrating that the major role of Shp2 is the activation of the Mapk/Erk-pathway.

1. Impaired postnatal muscle growth

Robin Schneider had already performed initial analysis of Shp2 mutant mice in postnatal development (Schneider, doctoral thesis, FU Berlin, 2011). Shp2-Gab1 interactions are essential for HGF/Met-initiated migration of myogenic progenitor cells into the developing limb buds (Schaeper, 2007). Robin therefore tested migration of myogenic precursor cells into the limbs but did not observe any deficits. This demonstrates that Pax7^{ICNm}-dependent recombination occurs after the cells have reached their target. Thus, Cre expression in the Pax7^{ICNm} allele reproduces the expression of the endogenous Pax7 gene in the limb (Hutcheson, 2009; Biressi, 2013).

To define the developmental stage when the Pax7^{ICNm} allele introduces robust recombination in myogenic precursor cells, I used a Rosa26-lox-stop-lox-EYFP (RYFP) reporter allele (Srinivas, 2001). Cells that express Cre eliminate the stop cassette and initiate YFP expression (Fig.3.1). FACS isolation of YFP+ and YFP- cells confirmed that the majority of myogenic precursor cells had recombined at E14.5. Similarly, levels of Shp2 were strongly reduced in YFP+ cells from coShp2 compared to control animals at E14.5 and P0. Thus, Shp2^{flox} recombination occurred after migration but during early fetal development.

Robin Schneider and I observed no obvious phenotype in newborn coShp2 mice. However, postnatal muscle growth is severely impaired, which is accompanied by a decrease in the number of nuclei per muscle fiber and a change in the minimal Feret's fiber diameter (Fig.3.2). Mutation of Shp2 occurs during early fetal muscle development but a phenotype of the Shp2 mutation becomes apparent only during the postnatal phase. Thus, Shp2 is dispensable for fetal myogenesis but postnatal muscle growth strongly depends on it.

The impaired postnatal muscle growth of coShp2 mice might be caused by a loss of the Pax7+ progenitor pool. Indeed, Robin Schneider observed an impaired proliferation of Pax7+ progenitors. This resulted in a depletion of progenitors and their derivatives, Myf5+ and MyoG+ myogenic cells, in postnatal muscle. I verified this result and analyzed additional genotypes to exclude dosage-dependent effects of Shp2 and changes caused by the Pax7^{ICNm} allele (Fig.3.3). The latter was tested because my data indicated that the presence of the Pax7^{CreERT2} allele already causes phenotypes in the adult muscle (see also below). During development, neither heterozygous Shp2 mutations nor the Pax7^{ICNm} allele interfered with proliferation and/or differentiation.

Interestingly, the onset of the proliferative deficit in Shp2 mutant Satellite cells correlates with their localizations to the Satellite cell niche (Fig.3.4). Before E16, myogenic precursor cells only loosely attach to developing muscle fibers, which do not yet posses a basal lamina. By E18, most Satellite cells localize in their niche (Kassar-Duchossoy, 2005). Impaired proliferation of Shp2 mutant Satellite cells and their homing thus correlate approximately in time. I analyzed whether proliferation of Pax7+ cells in the interstitium and in the niche differ in control and coShp2 mutant mice. I had chosen E16.5 for this analysis, because at this stage half of the Satellite cells are inside the niche and half outside. Pax7+ cells proliferated in the interstitium to comparable extents in control and coShp2 animals; in the niche, proliferation was moderately but significantly lower in Shp2 mutants. It should be noted that I did not observe significant differences when I analyzed the bulk of Satellite cells. These data support the notion that Satellite cells switch from Shp2-independent to Shp2-dependent proliferation when they enter their niche. Cre-mediated recombination with the Pax7^{ICNm} allele is induced in myogenic progenitor cells and persists in their derivatives, the muscle fiber. Therefore, the progenitors might be affected indirectly, for instance by a lack of muscle fiber-derived secreted factor(s) that controls proliferation. To assess directly whether Shp2 functions in a cell-autonomous or non-autonomous manner, I isolated control and coShp2 mutant myogenic progenitor cells by FACS and cultured them in growth medium (Fig.3.7). BrdU incorporation demonstrated that also in culture coShp2 mutant cells proliferated less. The fact that the majority of these cells no longer express Ki67 suggests that they withdraw from the cell cycle. Interestingly, this was observed for cells isolated from P0 but not from E14.5 mice. Consistently, *in vivo* the mutant Satellite cells exited the cell cycle around P0 but not during fetal myogenesis (Fig.3.5). Thus, the proliferation deficit observed *in vivo* is caused by cell autonomous mechanisms.

A genome-wide transcription analysis of neonatal Shp2 mutant Satellite cells also supported the notion that the lack of proliferation but not other mechanisms causes the Satellite cell loss. Several transcripts typical for cycling cells were down-regulated in neonatal Shp2 mutant cells, e.g. CyclinD1, CyclinB1 and PCNA. CyclinD1 is an important cyclin that promotes G_1 progression and entry into the S-phase, whereas PCNA functions as a subunit for DNA polymerase and is required during replication (Moldovan, 2007). In conclusion, mutation of Shp2 leads to a cell-autonomous proliferative deficit in neonatal Satellite cells, whereas fetal myogenic progenitor cells are little dependent on Shp2. Fetal and neonatal cells retain this differential

dependence on Shp2 in culture indicating that proliferation is controlled by distinct mechanisms.

Myogenic progenitor cells of different developmental stages are known to have distinct characteristics. Biressi and colleagues compared the transcripts of embryonic (E11) and fetal (E16) progenitors and found major differences, for instance in expression of Nfix, Pax3 and Pax7 (Biressi, 2007). Culture of Myf5-GFP cells isolated from mice at these stages demonstrated intrinsic differences in the cell behavior. Embryonic progenitors differentiate faster in culture than fetal progenitors. In addition, Tgfβ1 and Bmp4 interfered with differentiation of fetal but not embryonic progenitors. These differences were attributed to a changed expression of components of the Tgfβ/BMP pathway. Furthermore, several components of the Notch pathway were up-regulated in fetal progenitors. The transcription factor Nfix identified in this analysis was later shown to be a master regulator that controls the switch between fetal and embryonic progenitors (Messina, 2010).

Fetal and postnatal progenitors typically respond to growth factors in a similar manner, but recently the first differences between these cells were identified. For instance, in the postnatal muscle, a label retaining (non-proliferative) and a non-label retaining (i.e. proliferative) progenitor population exists (Chakkalakal, 2014). Apparently, in mice the majority of label retaining cells are specified shortly after birth. Postnatal and early fetal progenitors differ also in their association with muscle fibers, and cells in their niche might receive signals not encountered outside. My data provides evidence for a cell-autonomous difference in the proliferation control in fetal and postnatal progenitors that goes beyond such a possible signal switch. Cell autonomous differences during fetal and postnatal myogenesis were also noted for the high mobility group protein HMGA2. HMGA2 is a transcriptional co-activator that becomes essential for Satellite cell proliferation only during postnatal myogenesis despite the fact that it is present already in fetal progenitors (Li, 2012).

2. Shp2 controls Mapk/Erk activation in myogenic cells

Shp2 is important for full activation of the Mapk/Erk cascade in several cell types (Grossmann, 2009; Heuberger, 2014; Araki, 2003; Grossmann, 2010; Dance, 2008; Neel, 2003). I tested whether this is also correct in myogenic cells using pharmacological inhibition of Shp2 in C2C12 cells, or in cultured neonatal Satellite cells derived from control and Shp2 mutant animals. Mapk/Erk activation was strongly impaired when the cells were treated with inhibitor or when Shp2 was

ablated (Fig.8). Other tested signaling pathways like p38 or Akt were unaffected (Zhang, 2002; He, 2013). Thus, the major function of Shp2 in myogenic cells is the regulation of Mapk/Erk signaling. This is supported by my genome-wide expression analysis comparing control and Shp2 mutant Satellite cells. Immediate early genes respond very fast to RTK signaling and their expression is regulated by Mapk/Erk activity (Murphy, 2002; Li, 2007; Bradley, 2008; Chandra, 2013). Several immediate early genes, i.e. Egr2, Egr4 and Erm, were expressed at reduced levels in coShp2 Satellite cells (Tab.3.1). Mapk/Erk signaling has important functions in promoting proliferation and enhances expression of positive cell cycle regulators, like CyclinD1 which was also down-regulated in coShp2 Satellite cells. The observed changes in proliferation *in vitro* and *in vivo* are thus in accordance to previously described functions of Shp2/Mapk/Erk signaling.

3. Shp2 functions in adult Satellite cells

Shp2 is not only important during postnatal myogenesis but also in the adult. When I introduced Shp2 mutations in adult animals, a very substantial proportion (55%) of Shp2 mutant Satellite cells (TxcoShp2: $Pax7^{CreERT2/+}$; $Shp2^{flox/flox}$) got lost over the next three months when I compared this to control (TxCtrl: $Pax7^{CreERT2/+}$; $Shp2^{flox/+}$) mice (Fig.3.11). Thus, Shp2 is required for the maintenance of Satellite cells in the uninjured muscle. I noted that Satellite cells numbers in control animals were also decreased, but to a lesser extent. This indicates that heterozygous Shp2 mutation and/or the presence of the $Pax7^{CreERT2}$ allele affects Satellite cells numbers (Günther, 2013; von Maltzahn, 2013). As yet, I did not directly compare Satellite cell numbers in all possible genotypes and wildtype animals, and I need to investigate this further. Reports in the literature indicate that Satellite cell numbers in adult mice are stable and do not decrease until mice reach an old age (White, 2010; Keefe, 2015, Sousa-Victor, 2014). Thus, the heterozygous Shp2 mutation and/or the presence of the $Pax7^{CreERT2}$ allele appear to affect the Satellite cell pool in the adult but not in early postnatal development. Further work is needed to assess to what extent this effect is caused by the heterozygous Shp2 mutation or by the presence of the $Pax7^{CreERT2}$ allele.

Injury by cardiotoxin injection serves as a model to study muscle regeneration (Bentzinger, 2013; Rodgers, 2014; Günther, 2013). Tamoxifen-induced mutation of Shp2 did not affect Satellite cell numbers in sedentary muscle over a short period. Therefore, I analyzed muscle regeneration shortly after the introduction of the Shp2

mutation (TxCtrl: Pax7$^{CreERT2/+}$; Shp2$^{flox/+}$; TxcoShp2: Pax7$^{CreERT2/+}$; Shp2$^{flox/flox}$). Muscle regeneration was completely abrogated in TxcoShp2 animals 7 and 21 days after injury muscle. At both time points, I observed fibrotic tissue and fat inclusions instead of regenerating muscle fibers, which is similar to the response to injury when muscle is depleted of Satellite cells (Sambasivan, 2011; Lepper, 2011). Thus, without Shp2 adult Satellite cells are unable to regenerate injured muscle.

In regenerating muscle, Satellite cells proliferate extensively and increase in numbers (Ogawa, 2015; Lepper, 2011). However, 7 days after injury almost no Satellite cells were present in TxcoShp2 muscle, and their numbers declined even below the one observed before injury. Thus, mutant Satellite cells were lost during the regeneration process, which might be due to a deficit in proliferation and/or self-renewal. To address the mechanisms more carefully, I used the floating fiber assay, i.e. culture of isolated muscle fibers with the attached Satellite cells. When such fibers are cultivated, Satellite cells are activated, proliferate, and subpopulations differentiate or self-renew in a defined time-dependent manner (Zammit, 2004). I was unable to detect Pax7 by immunohistology in VCAM1+ Satellite cells on cultured fibers of mice carrying the Pax7^{CreERT2} allele; Pax7^{CreERT2} corresponds to a null allele and might reduce Pax7 expression levels. I used therefore VCAM1 as a marker to identify myogenic cells.

Upon injury, Satellite cells enter an alert state that is characterized by increased phosphorylation of the ribosomal protein S6, the first known response to activation (Rodgers, 2014). Thus, at early stages of activation, protein synthesis is induced. I tested this by analyzing phospho-S6 levels by immunohistology that can be done on a single cell level, and does not rely on the isolation of thousands of cells required for Western blotting. In addition, MyoD protein can be detected early in activated Satellite cells. After 24 hours in fiber culture, Shp2 mutant Satellite cells displayed strong pS6 staining and MyoD expression, indicating that the entry into the alert state does not depend on Shp2. Further analysis of the colony forming capacity showed a severely impaired proliferation of mutant cells which rarely divided during 3 days of culture (1.5 VCAM1+ cells per colony). In contrast, control cells had generated colonies that contained on average 5.5 cells. Similarly, BrdU incorporation or Ki67 expression were strongly decreased and, in particular, after 3 days in culture the majority of mutant cells had exited the cell cycle. Thus, Shp2 is essential for proliferation of Satellite cells, but does not interfere with entry into the alert state and early activation.

Shp2 is required for activation of Mapk/Erk in neonatal Satellite cells. I tested whether this is also observed in adult Satellite cells in fiber culture by immunohistology. pErk1/2 levels were strongly reduced at all time points analyzed. Continuous activation of Mapkk signaling (Mek1DD expression) in Shp2 mutant cells did suffice to overcome the proliferative deficit of TxcoShp2 Satellite cells. Thus, Shp2 controls activation of Mapk/Erk signaling in both neonatal and adult Satellite cells. In addition, Shp2 is essential for Mapk/Erk activation and activation of the signaling pathway suffices to replace Shp2 during Satellite cell proliferation.

What are the upstream signals that rely on Shp2? Satellite cells in regenerating muscle receive mitogenic signals that are potent Mapk/Erk activators, like hepatocyte growth factor (HGF) and fibroblast growth factors (Fgf) (overview in Bentzinger, 2010). Shp2 is an important mediator of the signals evoked by these growth factors (Schaeper, 2000; Schaeper, 2007; Hadari, 1998; Agazie, 2003; Gotoh, 2004; Li, 2014). HGF controls pre-activation (G_{Alert}) of Satellite cells and promotes their proliferation in culture (Allen, 1995; Sheehan, 1999; Li, 2009; Tatsumi, 1998; Rodgers, 2014). Rodgers and colleagues proposed that Met/PI3K signaling regulates the entry into the alert state, i.e. the earliest step in Satellite cell activation. Met/Mapk signaling might also participate in the control of proliferation and cooperate with other tyrosine kinase receptors like FGFR1/4 that have also been implicated in muscle regeneration. FGF growth factors are potent stimulators of Satellite cell proliferation in culture and mutations of FGFR1/2 or FGFR4 impair muscle regeneration (Sheehan, 1999; Jones, 2001; Fedorov, 2001; Yablonka-Reuveni, 2015; Zhao, 2006). The Fgf receptor substrate 2 (FRS2) is an important mediator of Fgf receptor signaling, and FRS2α-Shp2 interactions are essential for full Map/Erk activation (Hadari, 1998; Gotoh, 2004). Thus, converging inputs of several receptors provide mitogenic signals during muscle regeneration, and mutations of none of the single receptors cause the strong phenotypes that I observe in TxcoShp2 mutants. This indicates that many receptors active during muscle regeneration rely on Shp2 to activate Mapk/Erk.

4. Shp2 controls myogenic differentiation of adult but not early postnatal Satellite cells

Pharmacological inhibition of Mapk/Erk signaling enhances differentiation of cultured adult Satellite cells and embryonic myogenic progenitor cells (Michailovici, 2014; Jones, 2001). Conversely, modest elevation of Erk1/2 activity in Sprouty1-/-;

Sprouty2-/- mice results in decreased differentiation and expansion of the Pax7+ progenitor population in embryonic myogenesis (Michailovici, 2014). Thus, increased differentiation might account for the cell cycle exit and loss of neonatal and adult Shp2 mutant Satellite cells. I therefore analyzed expression of MyoD and MyoG in freshly isolated neonatal Shp2 mutant Satellite cells, and found that the numbers of Pax7+ cells that co-expressed MyoD were mildly reduced, and that the MyoD staining intensity appeared to be diminished. The number of MyoG+ cells were however unchanged. In addition, differentiation proceeded efficiently when the neonatal coShp2 Satellite cells were cultured in low serum (data not shown).

Compared to these subtle changes, the differentiation of adult TxcoShp2 Satellite cells was strongly affected. In particular, MyoD protein appeared upon activation of the cells in fiber culture, but was not correctly maintained and after 3 days only few of the cells were still MyoD-positive. Activation of Mapk/Erk by MEK1DD rescued cell numbers and ameliorated but not completely rescued MyoD expression. Mapk-dependent control of MyoD expression was previously described for Mapk/p38 signaling but not for Mapk/Erk (Jones, 2005; Troy, 2012). The distal regulatory region (DRR) of MyoD contains a conserved serum response element (SRE), which controls MyoD expression in proliferating C2C12 cells is bound by the serum response factor (SRF) (Gauthier-Rouviere, 1996; L'Honore; 2003; L'Honore, 2007). SRF functions as a heterodimeric complex with pElk-1, which is phosphorylated by Erk1/2 (Besnard, 2011; Janknecht, 1993; Gille, 1996). This mechanism might also be used to control MyoD expression in activated Satellite cells.

Despite the fact that MyoD expression was initiated, *MyoG* was not expressed in TxcoShp2 mutant Satellite cells in fiber culture. MyoD directly binds regulatory regions of the *MyoG* gene, but MyoG expression is not initiated until the cells receive a postulated 'differentiation cue' and exit the cell cycle (overview in Buckingham, 2014). Previous studies provided mechanistic insight into this regulation. For instance, in proliferating myoblasts, MyoD is associated with histone deacetylases (HDAC), which inhibits trans-activation of muscle differentiation-specific genes (overview in Buckingham, 2014). Furthermore, the transcriptional repressor complexes Snail-HDAC1/2 or Zeb1-Ctbp (zinc finger E-Box binding homeobox 1 & C-terminal binding protein) co-occupy regulatory sequences with MyoD in differentiation-specific genes and prevent MyoD-dependent activation (Soleimani, 2012; Siles, 2013). Mapk/Erk signaling might also impinge on these complex regulatory circuits that can modulate or delay MyoG activation.

Not only loss of Shp2, but also sustained activation of Mapk/Erk signaling interfered with MyoG expression in adult Satellite cells. MyoG is expressed when cells exit the cell cycle, and sustained activation of Mapk/Erk might force the cells to remain in a proliferative phase and prevent MyoG expression. Together, my data indicate that Mapk/Erk activity has to be tightly controlled to allow entry into terminal differentiation, and reduced Mapk/Erk activity (TxcoShp2 cells), or increased Mapk/Erk (TxMek1DD cells or TxcoShp2; Mek1DD) are unable to undergo myogenic differentiation.

V. Summary/ Zusammenfassung

1. Summary

Shp2 is a tyrosine phosphatase that mediates signals provided by many tyrosine kinase receptors. The experiments performed in this study revealed an important role for Shp2 in early postnatal muscle growth and adult muscle regeneration. Shp2 mutation in fetal myogenic progenitors and adult Satellite cells resulted in major changes in their proliferative capacities. I used pharmacological inhibitors, as well as genetics to show that Mapk/Erk activity depends on Shp2 in myogenic C2C12 cells or in neonatal and adult Satellite cells.

I introduced a conditional Shp2 mutation using different Cre lines. When Shp2 was ablated during early fetal myogenesis, changes in proliferation were only observed in the postnatal period. Cultures of isolated Shp2 mutant Satellite cells demonstrated that the proliferative deficit is cell-autonomous and observed in postnatal but not fetal cells. This suggests that Satellite cell proliferation is regulated by distinct mechanisms in the pre- and postnatal period.

I also introduced the conditional Shp2 mutation in adult Satellite cells and observed that these mutant Satellite cells are unable to repair muscle upon injury. *In vivo*, it can be difficult to follow the cells during the repair process. I therefore used cultures of myofibers and adherent Satellite cells to study the activation, proliferation and differentiation of adult Satellite cells in the absence of Shp2. This demonstrated that early steps in Satellite cell activation were Shp2-independent, but the cells were unable to proliferate and quickly withdrew from the cell cycle. I was able to rescue this proliferative deficit by expression of a constitutively active Mapkk (Mek1DD). This is in accordance with my biochemical analyses that had indicated that Shp2 is mainly necessary for Mapk/Erk activity.

Various growth factors have been implicated in muscle regeneration. Several of these growth factors activate Mapk/Erk signaling by their tyrosine kinase receptors in Satellite cells. Nevertheless, mutations of single receptors in Satellite cells do not impair muscle regeneration as severe as mutation of Shp2. Thus, Shp2 likely regulates the converging inputs of several receptor tyrosine kinases into the Mapk/Erk cascade (Fig.4.1).

2. Zusammenfassung

Shp2 ist eine Tyrosinphosphatase, die die Signale vieler Rezeptor-Tyrosinkinasen vermittelt. In dieser Studie konnte gezeigt werden, dass Shp2 postnatales Muskelwachstums und Muskelregeneration im adulten Tier reguliert. Mutation von Shp2 in fötalen Muskelvorläuferzellen oder adulten Satellitenzellen führte zu stark reduzierter Proliferation. Mittels pharmakologischer Inhibitoren und mit genetischen Studien konnte ich zeigen, dass Shp2 den Mapk/Erk Signalweg in myogenen C2C12 Zellen sowie neonatalen und adulten Satellitenzellen kontrolliert.

Ich setzte unterschiedliche Cre Linien ein, um Shp2 in Muskelvorläuferzellen in fötalen oder adulten Mäusen zu mutieren. Mutation von Shp2 in der fötalen Myogenese führte zu einem starken Proliferationsdefizit von Satellitenzellen im postnatalen Muskel. Kulturen isolierter myogener Vorläuferzellen zeigten, dass es sich um ein zell-autonomes Defizit handelt das in postnatalen, nicht aber in fötalen Zellen auftritt. Dies legt den Schluss nahe, dass unterschiedliche molekulare Mechanismen genutzt werden um Proliferation von prä- und postnatalen myogenen Vorläuferzellen zu steuern.

Zusätzlich führte ich eine konditionelle Shp2 Mutation in adulten Satellitenzellen ein und konnte eine stark beeinträchtigte Muskelregeneration beobachten. Es ist sehr aufwändig, solche Effekte und die verantwortlichen Mechanismen *in vivo* zu untersuchen. Ich setze deshalb Kulturen isolierter Muskelfasern und der assoziierten Satellitenzellen ein, um Aktivierung, Proliferation und Differenzierung der Stammzellen im Detail zu untersuchen. Während die initialen Schritte der Aktivierung unabhängig von Shp2 sind, war die Proliferation der Satellitenzellen stark beeinträchtigt und die Zellen traten verfrüht aus dem Zellzyklus aus. Expression einer konstitutiv aktiven Mapkk (MEK1DD) glich die defizitäre Proliferation aus. Dies war in Übereinstimmung mit meinen biochemischen Analysen, die darauf hinwiesen, dass Shp2 hauptsächlich die Aktivierung des Mapk/Erk Signalwegs reguliert.

Viele Wachstumsfaktoren regulieren die Muskelregeneration. Einige dieser Faktoren aktivieren Rezeptor-Tyrosinkinasen und den Mapk/Erk Signalweg. Die Mutationen dieser Rezeptoren führen allerdings zu weniger starken Defiziten in der Muskelregeneration als die Mutation von Shp2. Dies legt den Schluss nahe, das Shp2 die Signale verschiedener Rezeptoren während der Muskelregeneration weiterleitet (Fig.4.2).
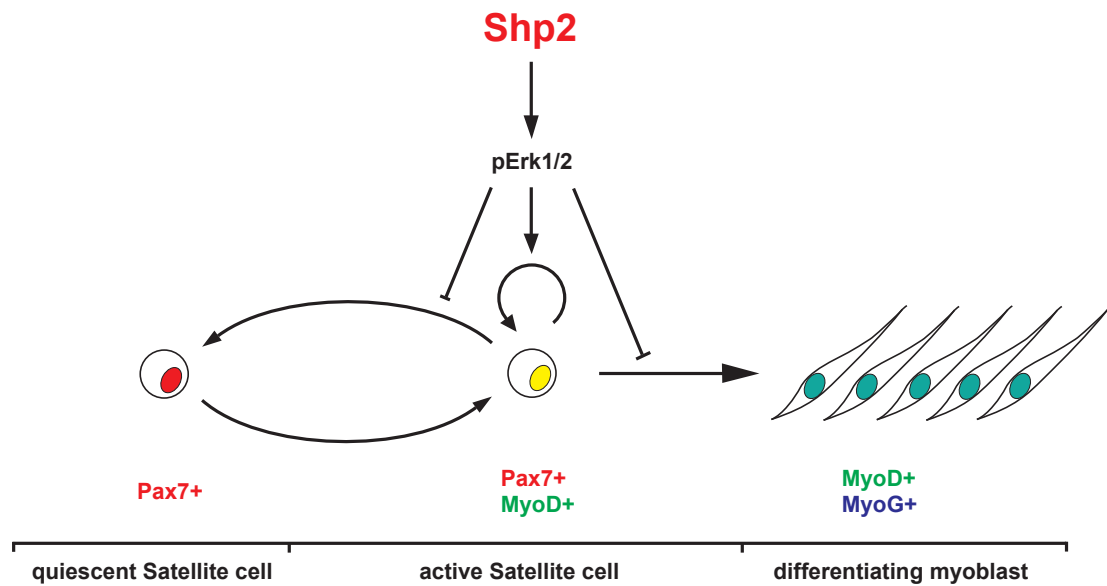
Fig.4.1: Shp2 functions in postnatal myogenesis and muscle regeneration. Mapk/Erk signaling maintains proliferating/active Satellite cells. In order to re-enter quiescence or initiate terminal differentiation Mapk/Erk signaling has to be down-regulated. Shp2 signaling indirectly promotes Mapk/Erk signaling and thereby maintains a proliferating Satellite cell population. pErk1/2: activated, phosphorylated Erk1/2 arrowhead: activating influence, blunt head: inhibiting influence
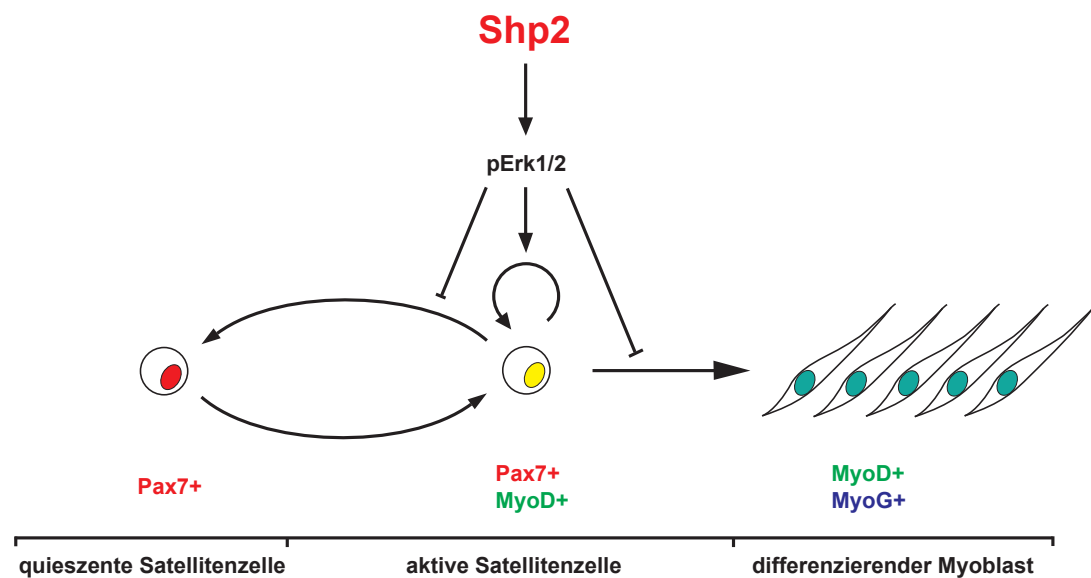
Fig.4.2: Shp2 Funktionen in der postnatalen Myogenese und der Muskelregeneration. Die Mapk/Erk Signalkaskade steuert aktive/ proliferierende Satellitenzellen. Für die Einleitung der terminalen Differenzierung oder die Rückkehr zur Quieszenz muss der Mapk/Erk Signalweg herunterreguliert werden. Shp2 aktiviert den Signalweg indirekt und erhält so eine proliferierende Satellitenzellpopulation. pErk1/2: aktiviertes, phosphoryliertes Erk1/2; Pfeilspitzen: positiver Einfluss; stumpfes Ende: inhibierender Einfluss

VI. References

Adachi, M., Sekiya, M., Miyachi, T., Matsuno, K., Hinoda, Y., Imai, K., and Yachi, A. (1992). Molecular cloning of a novel protein-tyrosine phosphatase SH-PTP3 with sequence similarity to the src-homology region 2. FEBS Lett. *314*, 335–339.

Agazie, Y.M., Movilla, N., Ischenko, I., and Hayman, M.J. (2003). The phosphotyrosine phosphatase SHP2 is a critical mediator of transformation induced by the oncogenic fibroblast growth factor receptor 3. Oncogene *22*, 6909–6918.

Ahmad, S., Banville, D., Zhao, Z., Fischer, E.H., and Shen, S.H. (1993). A widely expressed human protein-tyrosine phosphatase containing src homology 2 domains. Proc. Natl. Acad. Sci. U.S.A. *90*, 2197–2201.

Alberola-Ila, J., Forbush, K.A., Seger, R., Krebs, E.G., and Perlmutter, R.M. (1995). Selective requirement for MAP kinase activation in thymocyte differentiation. Nature *373*, 620–623.

Allbrook, D.B., Han, M.F., and Hellmuth, A.E. (1971). Population of muscle satellite cells in relation to age and mitotic activity. Pathology *3*, 223–243.

Allen, R.E., Sheehan, S.M., Taylor, R.G., Kendall, T.L., and Rice, G.M. (1995). Hepatocyte growth factor activates quiescent skeletal muscle satellite cells in vitro. J. Cell. Physiol. *165*, 307–312.

Araki, T., Nawa, H., and Neel, B.G. (2003). Tyrosyl phosphorylation of Shp2 is required for normal ERK activation in response to some, but not all, growth factors. J. Biol. Chem. *278*, 41677–41684.

Araki, T., Mohi, M.G., Ismat, F.A., Bronson, R.T., Williams, I.R., Kutok, J.L., Yang, W., Pao, L.I., Gilliland, D.G., Epstein, J.A., et al. (2004). Mouse model of Noonan syndrome reveals cell type- and gene dosage-dependent effects of Ptpn11 mutation. Nat. Med. *10*, 849–857.

Bajard, L., Relaix, F., Lagha, M., Rocancourt, D., Daubas, P., and Buckingham, M.E. (2006). A novel genetic hierarchy functions during hypaxial myogenesis: Pax3 directly activates Myf5 in muscle progenitor cells in the limb. Genes Dev. *20*, 2450–2464.

Barford, D., and Neel, B.G. (1998). Revealing mechanisms for SH2 domain mediated regulation of the protein tyrosine phosphatase SHP-2. Structure *6*, 249–254.

Bennett, A.M., Tang, T.L., Sugimoto, S., Walsh, C.T., and Neel, B.G. (1994). Protein-tyrosine-phosphatase SHPTP2 couples platelet-derived growth factor receptor beta to Ras. Proc. Natl. Acad. Sci. U.S.A. *91*, 7335–7339.

Bentzinger, C.F., Maltzahn, J. von, and Rudnicki, M.A. (2010). Extrinsic regulation of satellite cell specification. Stem Cell Res Ther *1*, 27.

Bentzinger, C.F., Wang, Y.X., Maltzahn, J. von, Soleimani, V.D., Yin, H., and Rudnicki, M.A. (2013). Fibronectin regulates Wnt7a signaling and satellite cell expansion. Cell Stem Cell *12*, 75–87.

Besnard, A., Galan-Rodriguez, B., Vanhoutte, P., and Caboche, J. (2011). Elk-1 a transcription factor with multiple facets in the brain. Front Neurosci *5*, 35.

Biressi, S., Tagliafico, E., Lamorte, G., Monteverde, S., Tenedini, E., Roncaglia, E., Ferrari, S., Ferrari, S., Cusella-De Angelis, M.G., Tajbakhsh, S., et al. (2007). Intrinsic phenotypic diversity of embryonic and fetal myoblasts is revealed by genome-wide gene expression analysis on purified cells. Dev. Biol. *304*, 633–651.

Biressi, S., Bjornson, C.R.R., Carlig, P.M.M., Nishijo, K., Keller, C., and Rando, T.A. (2013). Myf5 expression during fetal myogenesis defines the developmental progenitors of adult satellite cells. Dev. Biol. *379*, 195–207.

Bischoff, R. (1986). A satellite cell mitogen from crushed adult muscle. Dev. Biol. *115*, 140–147.

Bischoff, R. (1990). Cell cycle commitment of rat muscle satellite cells. J. Cell Biol. *111*, 201–207.

Bjornson, C.R.R., Cheung, T.H., Liu, L., Tripathi, P.V., Steeper, K.M., and Rando, T.A. (2012). Notch signaling is necessary to maintain quiescence in adult muscle stem cells. Stem Cells *30*, 232–242.

Bladt, F., Riethmacher, D., Isenmann, S., Aguzzi, A., and Birchmeier, C. (1995). Essential role for the c-met receptor in the migration of myogenic precursor cells into the limb bud. Nature *376*, 768–771.

Borello, U., Berarducci, B., Murphy, P., Bajard, L., Buffa, V., Piccolo, S., Buckingham, M., and Cossu, G. (2006). The Wnt/beta-catenin pathway regulates Gli-mediated Myf5 expression during somitogenesis. Development *133*, 3723–3732.

Boulton, T.G., Yancopoulos, G.D., Gregory, J.S., Slaughter, C., Moomaw, C., Hsu, J., and Cobb, M.H. (1990). An insulin-stimulated protein kinase similar to yeast kinases involved in cell cycle control. Science *249*, 64–67.

Boulton, T.G., Nye, S.H., Robbins, D.J., Ip, N.Y., Radziejewska, E., Morgenbesser, S.D., DePinho, R.A., Panayotatos, N., Cobb, M.H., and Yancopoulos, G.D. (1991). ERKs: a family of protein-serine/threonine kinases that are activated and tyrosine phosphorylated in response to insulin and NGF. Cell *65*, 663–675.

Bradley, E.W., Ruan, M.M., and Oursler, M.J. (2008). Novel pro-survival functions of the Kruppel-like transcription factor Egr2 in promotion of macrophage colony-stimulating factor-mediated osteoclast survival downstream of the MEK/ERK pathway. J. Biol. Chem. *283*, 8055–8064.

Braun, T., Rudnicki, M.A., Arnold, H.H., and Jaenisch, R. (1992). Targeted inactivation of the muscle regulatory gene Myf-5 results in abnormal rib development and perinatal death. Cell *71*, 369–382.

Bröhl, D., Vasyutina, E., Czajkowski, M.T., Griger, J., Rassek, C., Rahn, H.-P., Purfürst, B., Wende, H., and Birchmeier, C. (2012). Colonization of the satellite cell niche by skeletal muscle progenitor cells depends on Notch signals. Dev. Cell *23*, 469–481.

Brohmann, H., Jagla, K., and Birchmeier, C. (2000). The role of Lbx1 in migration of muscle precursor cells. Development *127*, 437–445.

Buckingham, M., and Rigby, P.W.J. (2014). Gene regulatory networks and transcriptional mechanisms that control myogenesis. Dev. Cell *28*, 225–238.

Carlson, M.E., Hsu, M., and Conboy, I.M. (2008). Imbalance between pSmad3 and Notch induces CDK inhibitors in old muscle stem cells. Nature *454*, 528–532.

Chakkalakal, J.V., Jones, K.M., Basson, M.A., and Brack, A.S. (2012). The aged niche disrupts muscle stem cell quiescence. Nature *490*, 355–360.

Chakkalakal, J.V., Christensen, J., Xiang, W., Tierney, M.T., Boscolo, F.S., Sacco, A., and Brack, A.S. (2014). Early forming label-retaining muscle stem cells require p27kip1 for maintenance of the primitive state. Development *141*, 1649–1659.

Chan, G., Gu, S., and Neel, B.G. (2013). Erk1 and Erk2 are required for maintenance of hematopoietic stem cells and adult hematopoiesis. Blood *121*, 3594–3598.

Chandra, A., Lan, S., Zhu, J., Siclari, V.A., and Qin, L. (2013). Epidermal growth factor receptor (EGFR) signaling promotes proliferation and survival in osteoprogenitors by increasing early growth response 2 (EGR2) expression. J. Biol. Chem. *288*, 20488–20498.

Chen, R.H., Chung, J., and Blenis, J. (1991). Regulation of pp90rsk phosphorylation and S6 phosphotransferase activity in Swiss 3T3 cells by growth factor-, phorbol ester-, and cyclic AMP-mediated signal transduction. Mol. Cell. Biol. *11*, 1861–1867.

Christ, B., Huang, R., and Scaal, M. (2007). Amniote somite derivatives. Dev. Dyn. *236*, 2382–2396.

Collins, C.A., Olsen, I., Zammit, P.S., Heslop, L., Petrie, A., Partridge, T.A., and Morgan, J.E. (2005). Stem cell function, self-renewal, and behavioral heterogeneity of cells from the adult muscle satellite cell niche. Cell *122*, 289–301.

Cornelison, D.D., Filla, M.S., Stanley, H.M., Rapraeger, A.C., and Olwin, B.B. (2001). Syndecan-3 and syndecan-4 specifically mark skeletal muscle satellite cells and are implicated in satellite cell maintenance and muscle regeneration. Dev. Biol. *239*, 79–94.

Cowley, S., Paterson, H., Kemp, P., and Marshall, C.J. (1994). Activation of MAP kinase kinase is necessary and sufficient for PC12 differentiation and for transformation of NIH 3T3 cells. Cell *77*, 841–852.

Crist, C.G., Montarras, D., and Buckingham, M. (2012). Muscle satellite cells are primed for myogenesis but maintain quiescence with sequestration of Myf5 mRNA targeted by microRNA-31 in mRNP granules. Cell Stem Cell *11*, 118–126.

Crompton, T., Gilmour, K.C., and Owen, M.J. (1996). The MAP kinase pathway controls differentiation from double-negative to double-positive thymocyte. Cell *86*, 243–251.

Dance, M., Montagner, A., Salles, J.-P., Yart, A., and Raynal, P. (2008). The molecular functions of Shp2 in the Ras/Mitogen-activated protein kinase (ERK1/2) pathway. Cell. Signal. *20*, 453–459.

Darzynkiewicz, Z., Halicka, H.D., and Zhao, H. (2010). Analysis of cellular DNA content by flow and laser scanning cytometry. Adv. Exp. Med. Biol. *676*, 137–147.

Deak, M., Clifton, A.D., Lucocq, L.M., and Alessi, D.R. (1998). Mitogen- and stress-activated protein kinase-1 (MSK1) is directly activated by MAPK and SAPK2/p38, and may mediate activation of CREB. EMBO J. *17*, 4426–4441.

Denetclaw, W.F., and Ordahl, C.P. (2000). The growth of the dermomyotome and formation of early myotome lineages in thoracolumbar somites of chicken embryos. Development *127*, 893–905.

Dietrich, S., Abou-Rebyeh, F., Brohmann, H., Bladt, F., Sonnenberg-Riethmacher, E., Yamaai, T., Lumsden, A., Brand-Saberi, B., and Birchmeier, C. (1999). The role of SF/HGF and c-Met in the development of skeletal muscle. Development *126*, 1621–1629.

Eck, M.J., Pluskey, S., Trüb, T., Harrison, S.C., and Shoelson, S.E. (1996). Spatial constraints on the recognition of phosphoproteins by the tandem SH2 domains of the phosphatase SH-PTP2. Nature *379*, 277–280.

Emanuel, P.D., Shannon, K.M., and Castleberry, R.P. (1996). Juvenile myelomonocytic leukemia: molecular understanding and prospects for therapy. Mol Med Today *2*, 468–475.

Epstein, J.A., Shapiro, D.N., Cheng, J., Lam, P.Y., and Maas, R.L. (1996). Pax3 modulates expression of the c-Met receptor during limb muscle development. Proc. Natl. Acad. Sci. U.S.A. *93*, 4213–4218.

Fan, C.M., Lee, C.S., and Tessier-Lavigne, M. (1997). A role for WNT proteins in induction of dermomyotome. Dev. Biol. *191*, 160–165.

Fedorov, Y.V., Rosenthal, R.S., and Olwin, B.B. (2001). Oncogenic Ras-induced proliferation requires autocrine fibroblast growth factor 2 signaling in skeletal muscle cells. J. Cell Biol. *152*, 1301–1305.

Feng, G.S., Hui, C.C., and Pawson, T. (1993). SH2-containing phosphotyrosine phosphatase as a target of protein-tyrosine kinases. Science *259*, 1607–1611.

Fornaro, M., Burch, P.M., Yang, W., Zhang, L., Hamilton, C.E., Kim, J.H., Neel, B.G., and Bennett, A.M. (2006). SHP-2 activates signaling of the nuclear factor of activated T cells to promote skeletal muscle growth. J. Cell Biol. *175*, 87–97.

Fragale, A., Tartaglia, M., Wu, J., and Gelb, B.D. (2004). Noonan syndrome-associated SHP2/PTPN11 mutants cause EGF-dependent prolonged GAB1 binding and sustained ERK2/MAPK1 activation. Hum. Mutat. *23*, 267–277.

Freeman, R.M., Plutzky, J., and Neel, B.G. (1992). Identification of a human src homology 2-containing protein-tyrosine-phosphatase: a putative homolog of Drosophila corkscrew. Proc. Natl. Acad. Sci. U.S.A. *89*, 11239–11243.

Fukada, S., Uezumi, A., Ikemoto, M., Masuda, S., Segawa, M., Tanimura, N., Yamamoto, H., Miyagoe-Suzuki, Y., and Takeda, S. (2007). Molecular signature of quiescent satellite cells in adult skeletal muscle. Stem Cells *25*, 2448–2459.

Fukada, S., Yamaguchi, M., Kokubo, H., Ogawa, R., Uezumi, A., Yoneda, T., Matev, M.M., Motohashi, N., Ito, T., Zolkiewska, A., et al. (2011). Hesr1 and Hesr3 are essential to generate undifferentiated quiescent satellite cells and to maintain satellite cell numbers. Development *138*, 4609–4619.

Gauthier, A.S., Furstoss, O., Araki, T., Chan, R., Neel, B.G., Kaplan, D.R., and Miller, F.D. (2007). Control of CNS cell-fate decisions by SHP-2 and its dysregulation in Noonan syndrome. Neuron *54*, 245–262.

Gauthier-Rouviere, C., Vandromme, M., Tuil, D., Lautredou, N., Morris, M., Soulez, M., Kahn, A., Fernandez, A., and Lamb, N. (1996). Expression and activity of serum response factor is required for expression of the muscle-determining factor MyoD in both dividing and differentiating mouse C2C12 myoblasts. Mol. Biol. Cell *7*, 719–729.

Gille, H., Kortenjann, M., Strahl, T., and Shaw, P.E. (1996). Phosphorylation-dependent formation of a quaternary complex at the c-fos SRE. Mol. Cell. Biol. *16*, 1094–1102.

Gillespie, M.A., Le Grand, F., Scimè, A., Kuang, S., Maltzahn, J. von, Seale, V., Cuenda, A., Ranish, J.A., and Rudnicki, M.A. (2009). p38-{gamma}-dependent gene silencing restricts entry into the myogenic differentiation program. J. Cell Biol. *187*, 991–1005.

Ginsberg, J.P., Davis, R.J., Bennicelli, J.L., Nauta, L.E., and Barr, F.G. (1998). Up-regulation of MET but not neural cell adhesion molecule expression by the PAX3-FKHR fusion protein in alveolar rhabdomyosarcoma. Cancer Res. *58*, 3542–3546.

Gokhin, D.S., Ward, S.R., Bremner, S.N., and Lieber, R.L. (2008). Quantitative analysis of neonatal skeletal muscle functional improvement in the mouse. J. Exp. Biol. *211*, 837–843.

Gotoh, N., Ito, M., Yamamoto, S., Yoshino, I., Song, N., Wang, Y., Lax, I., Schlessinger, J., Shibuya, M., and Lang, R.A. (2004). Tyrosine phosphorylation sites on FRS2alpha responsible for Shp2 recruitment are critical for induction of lens and retina. Proc. Natl. Acad. Sci. U.S.A. *101*, 17144–17149.

Goulding, M., Lumsden, A., and Paquette, A.J. (1994). Regulation of Pax-3 expression in the dermomyotome and its role in muscle development. Development *120*, 957–971.

Le Grand, F., Jones, A.E., Seale, V., Scimè, A., and Rudnicki, M.A. (2009). Wnt7a activates the planar cell polarity pathway to drive the symmetric expansion of satellite stem cells. Cell Stem Cell *4*, 535–547.

Le Grand, F., Grifone, R., Mourikis, P., Houbron, C., Gigaud, C., Pujol, J., Maillet, M., Pagès, G., Rudnicki, M., Tajbakhsh, S., et al. (2012). Six1 regulates stem cell repair potential and self-renewal during skeletal muscle regeneration. J. Cell Biol. *198*, 815–832.

Grifone, R., Demignon, J., Houbron, C., Souil, E., Niro, C., Seller, M.J., Hamard, G., and Maire, P. (2005). Six1 and Six4 homeoproteins are required for Pax3 and Mrf expression during myogenesis in the mouse embryo. Development *132*, 2235–2249.

Grifone, R., Demignon, J., Giordani, J., Niro, C., Souil, E., Bertin, F., Laclef, C., Xu, P.-X., and Maire, P. (2007). Eya1 and Eya2 proteins are required for hypaxial somitic myogenesis in the mouse embryo. Dev. Biol. *302*, 602–616.

Gros, J., Manceau, M., Thomé, V., and Marcelle, C. (2005). A common somitic origin for embryonic muscle progenitors and satellite cells. Nature *435*, 954–958.

Grosskopf, S., Eckert, C., Arkona, C., Radetzki, S., Böhm, K., Heinemann, U., Wolber, G., Kries, J.-P. von, Birchmeier, W., and Rademann, J. (2015). Selective inhibitors of the protein tyrosine phosphatase SHP2 block cellular motility and growth of cancer cells in vitro and in vivo. ChemMedChem *10*, 815–826.

Grossmann, K.S., Wende, H., Paul, F.E., Cheret, C., Garratt, A.N., Zurborg, S., Feinberg, K., Besser, D., Schulz, H., Peles, E., et al. (2009). The tyrosine phosphatase Shp2 (PTPN11) directs Neuregulin-1/ErbB signaling throughout Schwann cell development. Proc. Natl. Acad. Sci. U.S.A. *106*, 16704–16709.

Grossmann, K.S., Rosário, M., Birchmeier, C., and Birchmeier, W. (2010). The tyrosine phosphatase Shp2 in development and cancer. Adv. Cancer Res. *106*, 53–89.

Gu, H., Marth, J.D., Orban, P.C., Mossmann, H., and Rajewsky, K. (1994). Deletion of a DNA polymerase beta gene segment in T cells using cell type-specific gene targeting. Science *265*, 103–106.

Günther, S., Kim, J., Kostin, S., Lepper, C., Fan, C.-M., and Braun, T. (2013). Myf5-positive satellite cells contribute to Pax7-dependent long-term maintenance of adult muscle stem cells. Cell Stem Cell *13*, 590–601.

Gustafsson, M.K., Pan, H., Pinney, D.F., Liu, Y., Lewandowski, A., Epstein, D.J., and Emerson, C.P. (2002). Myf5 is a direct target of long-range Shh signaling and Gli regulation for muscle specification. Genes Dev. *16*, 114–126.

Hadari, Y.R., Kouhara, H., Lax, I., and Schlessinger, J. (1998). Binding of Shp2 tyrosine phosphatase to FRS2 is essential for fibroblast growth factor-induced PC12 cell differentiation. Mol. Cell. Biol. *18*, 3966–3973.

Hanafusa, H., Torii, S., Yasunaga, T., and Nishida, E. (2002). Sprouty1 and Sprouty2 provide a control mechanism for the Ras/MAPK signalling pathway. Nat. Cell Biol. *4*, 850–858.

Hanafusa, H., Torii, S., Yasunaga, T., Matsumoto, K., and Nishida, E. (2004). Shp2, an SH2-containing protein-tyrosine phosphatase, positively regulates receptor tyrosine kinase signaling by dephosphorylating and inactivating the inhibitor Sprouty. J. Biol. Chem. *279*, 22992–22995.

Hanke, S., and Mann, M. (2009). The phosphotyrosine interactome of the insulin receptor family and its substrates IRS-1 and IRS-2. Mol. Cell Proteomics *8*, 519–534.

Hanna, N., Montagner, A., Lee, W.H., Miteva, M., Vidal, M., Vidaud, M., Parfait, B., and Raynal, P. (2006). Reduced phosphatase activity of SHP-2 in LEOPARD syndrome: consequences for PI3K binding on Gab1. FEBS Lett. *580*, 2477–2482.

Hasty, P., Bradley, A., Morris, J.H., Edmondson, D.G., Venuti, J.M., Olson, E.N., and Klein, W.H. (1993). Muscle deficiency and neonatal death in mice with a targeted mutation in the myogenin gene. Nature *364*, 501–506.

He, Z., Zhu, H.H., Bauler, T.J., Wang, J., Ciaraldi, T., Alderson, N., Li, S., Raquil, M.-A., Ji, K., Wang, S., et al. (2013). Nonreceptor tyrosine phosphatase Shp2 promotes adipogenesis through inhibition of p38 MAP kinase. Proc. Natl. Acad. Sci. U.S.A. *110*, E79–E88.

Hellmuth, A.E., and Allbrook, D.B. (1971). Muscle satellite cell numbers during the postnatal period. J. Anat. *110*, 503.

Heuberger, J., Kosel, F., Qi, J., Grossmann, K.S., Rajewsky, K., and Birchmeier, W. (2014). Shp2/MAPK signaling controls goblet/paneth cell fate decisions in the intestine. Proc. Natl. Acad. Sci. U.S.A. *111*, 3472–3477.

Hochberg, Y., and Benjamini, Y. (1990). More powerful procedures for multiple significance testing. Stat Med *9*, 811–818.

L'honore, A., Lamb, N.J., Vandromme, M., Turowski, P., Carnac, G., and Fernandez, A. (2003). MyoD distal regulatory region contains an SRF binding CArG element required for MyoD expression in skeletal myoblasts and during muscle regeneration. Mol. Biol. Cell *14*, 2151–2162.

L'honore, A., Rana, V., Arsic, N., Franckhauser, C., Lamb, N.J., and Fernandez, A. (2007). Identification of a new hybrid serum response factor and myocyte enhancer factor 2-binding element in MyoD enhancer required for MyoD expression during myogenesis. Mol. Biol. Cell *18*, 1992–2001.

Horst, D., Ustanina, S., Sergi, C., Mikuz, G., Juergens, H., Braun, T., and Vorobyov, E. (2006). Comparative expression analysis of Pax3 and Pax7 during mouse myogenesis. Int. J. Dev. Biol. *50*, 47–54.

Hosoyama, T., Nishijo, K., Prajapati, S.I., Li, G., and Keller, C. (2011). Rb1 gene inactivation expands satellite cell and postnatal myoblast pools. J. Biol. Chem. *286*, 19556–19564.

Hubaud, A., and Pourquié, O. (2014). Signalling dynamics in vertebrate segmentation. Nat. Rev. Mol. Cell Biol. *15*, 709–721.

Hutcheson, D.A., Zhao, J., Merrell, A., Haldar, M., and Kardon, G. (2009). Embryonic and fetal limb myogenic cells are derived from developmentally distinct progenitors and have different requirements for beta-catenin. Genes Dev. *23*, 997–1013.

Janknecht, R., Ernst, W.H., Pingoud, V., and Nordheim, A. (1993). Activation of ternary complex factor Elk-1 by MAP kinases. EMBO J. *12*, 5097–5104.

Jarvis, L.A., Toering, S.J., Simon, M.A., Krasnow, M.A., and Smith-Bolton, R.K. (2006). Sprouty proteins are in vivo targets of Corkscrew/SHP-2 tyrosine phosphatases. Development *133*, 1133–1142.

Joe, A.W.B., Yi, L., Natarajan, A., Le Grand, F., So, L., Wang, J., Rudnicki, M.A., and Rossi, F.M.V. (2010). Muscle injury activates resident fibro/adipogenic progenitors that facilitate myogenesis. Nat. Cell Biol. *12*, 153–163.

Jones, N.C., Fedorov, Y.V., Rosenthal, R.S., and Olwin, B.B. (2001). ERK1/2 is required for myoblast proliferation but is dispensable for muscle gene expression and cell fusion. J. Cell. Physiol. *186*, 104–115.

Jones, N.C., Tyner, K.J., Nibarger, L., Stanley, H.M., Cornelison, D.D.W., Fedorov, Y.V., and Olwin, B.B. (2005). The p38alpha/beta MAPK functions as a molecular switch to activate the quiescent satellite cell. J. Cell Biol. *169*, 105–116.

Jostes, B., Walther, C., and Gruss, P. (1990). The murine paired box gene, Pax7, is expressed specifically during the development of the nervous and muscular system. Mech. Dev. *33*, 27–37.

Kahane, N., Cinnamon, Y., and Kalcheim, C. (1998a). The origin and fate of pioneer myotomal cells in the avian embryo. Mech. Dev. *74*, 59–73.

Kahane, N., Cinnamon, Y., and Kalcheim, C. (1998b). The cellular mechanism by which the dermomyotome contributes to the second wave of myotome development. Development *125*, 4259–4271.

Kardon, G., Harfe, B.D., and Tabin, C.J. (2003). A Tcf4-positive mesodermal population provides a prepattern for vertebrate limb muscle patterning. Dev. Cell *5*, 937–944.

Kassar-Duchossoy, L., Gayraud-Morel, B., Gomès, D., Rocancourt, D., Buckingham, M., Shinin, V., and Tajbakhsh, S. (2004). Mrf4 determines skeletal muscle identity in Myf5:Myod double-mutant mice. Nature *431*, 466–471.

Kassar-Duchossoy, L., Giacone, E., Gayraud-Morel, B., Jory, A., Gomès, D., and Tajbakhsh, S. (2005). Pax3/Pax7 mark a novel population of primitive myogenic cells during development. Genes Dev. *19*, 1426–1431.

Katz, M., Amit, I., and Yarden, Y. (2007). Regulation of MAPKs by growth factors and receptor tyrosine kinases. Biochim. Biophys. Acta *1773*, 1161–1176.

Ke, Y., Zhang, E.E., Hagihara, K., Wu, D., Pang, Y., Klein, R., Curran, T., Ranscht, B., and Feng, G.-S. (2007). Deletion of Shp2 in the brain leads to defective proliferation and differentiation in neural stem cells and early postnatal lethality. Mol. Cell. Biol. *27*, 6706–6717.

Keefe, A.C., Lawson, J.A., Flygare, S.D., Fox, Z.D., Colasanto, M.P., Mathew, S.J., Yandell, M., and Kardon, G. (2015). Muscle stem cells contribute to myofibres in sedentary adult mice. Nat Commun *6*, 7087.

Keller, C., Hansen, M.S., Coffin, C.M., and Capecchi, M.R. (2004). Pax3:Fkhr interferes with embryonic Pax3 and Pax7 function: implications for alveolar rhabdomyosarcoma cell of origin. Genes Dev. *18*, 2608–2613.

Klinghoffer, R.A., and Kazlauskas, A. (1995). Identification of a putative Syp substrate, the PDGF beta receptor. J. Biol. Chem. *270*, 22208–22217.

Kolch, W. (2005). Coordinating ERK/MAPK signalling through scaffolds and inhibitors. Nat. Rev. Mol. Cell Biol. *6*, 827–837.

Kontaridis, M.I., Swanson, K.D., David, F.S., Barford, D., and Neel, B.G. (2006). PTPN11 (Shp2) mutations in LEOPARD syndrome have dominant negative, not activating, effects. J. Biol. Chem. *281*, 6785–6792.

Krenz, M., Gulick, J., Osinska, H.E., Colbert, M.C., Molkentin, J.D., and Robbins, J. (2008). Role of ERK1/2 signaling in congenital valve malformations in Noonan syndrome. Proc. Natl. Acad. Sci. U.S.A. *105*, 18930–18935.

Kuang, S., Kuroda, K., Le Grand, F., and Rudnicki, M.A. (2007). Asymmetric self-renewal and commitment of satellite stem cells in muscle. Cell *129*, 999–1010.

Lan, L., Holland, J.D., Qi, J., Grosskopf, S., Vogel, R., Györffy, B., Wulf-Goldenberg, A., and Birchmeier, W. (2015). Shp2 signaling suppresses senescence in PyMT-induced mammary gland cancer in mice. EMBO J. *34*, 1493–1508.

Lemmon, M.A., and Schlessinger, J. (2010). Cell signaling by receptor tyrosine kinases. Cell *141*, 1117–1134.

Lepper, C., Conway, S.J., and Fan, C.-M. (2009). Adult satellite cells and embryonic muscle progenitors have distinct genetic requirements. Nature *460*, 627–631.

Lepper, C., Partridge, T.A., and Fan, C.-M. (2011). An absolute requirement for Pax7-positive satellite cells in acute injury-induced skeletal muscle regeneration. Development *138*, 3639–3646.

Li, C., Scott, D.A., Hatch, E., Tian, X., and Mansour, S.L. (2007). Dusp6 (Mkp3) is a negative feedback regulator of FGF-stimulated ERK signaling during mouse development. Development *134*, 167–176.

Li, J., Reed, S.A., and Johnson, S.E. (2009). Hepatocyte growth factor (HGF) signals through SHP2 to regulate primary mouse myoblast proliferation. Exp. Cell Res. *315*, 2284–2292.

Li, S., Hsu, D.D.F., Li, B., Luo, X., Alderson, N., Qiao, L., Ma, L., Zhu, H.H., He, Z., Suino-Powell, K., et al. (2014). Cytoplasmic tyrosine phosphatase Shp2 coordinates hepatic regulation of bile acid and FGF15/19 signaling to repress bile acid synthesis. Cell Metab. *20*, 320–332.

Li, Z., Gilbert, J.A., Zhang, Y., Zhang, M., Qiu, Q., Ramanujan, K., Shavlakadze, T., Eash, J.K., Scaramozza, A., Goddeeris, M.M., et al. (2012). An HMGA2-IGF2BP2 axis regulates myoblast proliferation and myogenesis. Dev. Cell *23*, 1176–1188.

Lin Shiau, S.Y., Huang, M.C., and Lee, C.Y. (1976). Mechanism of action of cobra cardiotoxin in the skeletal muscle. J. Pharmacol. Exp. Ther. *196*, 758–770.

Lipton, B.H., and Schultz, E. (1979). Developmental fate of skeletal muscle satellite cells. Science *205*, 1292–1294.

Liu, L., Cheung, T.H., Charville, G.W., Hurgo, B.M.C., Leavitt, T., Shih, J., Brunet, A., and Rando, T.A. (2013). Chromatin modifications as determinants of muscle stem cell quiescence and chronological aging. Cell Rep *4*, 189–204.

Lopez, F., Belloc, F., Lacombe, F., Dumain, P., Reiffers, J., Bernard, P., and Boisseau, M.R. (1991). Modalities of synthesis of Ki67 antigen during the stimulation of lymphocytes. Cytometry *12*, 42–49.

Ma, X.M., and Blenis, J. (2009). Molecular mechanisms of mTOR-mediated translational control. Nat. Rev. Mol. Cell Biol. *10*, 307–318.

Maltzahn, J. von, Jones, A.E., Parks, R.J., and Rudnicki, M.A. (2013). Pax7 is critical for the normal function of satellite cells in adult skeletal muscle. Proc. Natl. Acad. Sci. U.S.A. *110*, 16474–16479.

Mansouri, A., Stoykova, A., Torres, M., and Gruss, P. (1996). Dysgenesis of cephalic neural crest derivatives in Pax7–/– mutant mice. Development *122*, 831–838.

Marcelle, C., Stark, M.R., and Bronner-Fraser, M. (1997). Coordinate actions of BMPs, Wnts, Shh and noggin mediate patterning of the dorsal somite. Development *124*, 3955–3963.

Maroto, M., Bone, R.A., and Dale, J.K. (2012). Somitogenesis. Development *139*, 2453–2456.

Maroun, C.R., Naujokas, M.A., Holgado-Madruga, M., Wong, A.J., and Park, M. (2000). The tyrosine phosphatase SHP-2 is required for sustained activation of extracellular signal-regulated kinase and epithelial morphogenesis downstream from the met receptor tyrosine kinase. Mol. Cell. Biol. *20*, 8513–8525.

Mathew, S.J., Hansen, J.M., Merrell, A.J., Murphy, M.M., Lawson, J.A., Hutcheson, D.A., Hansen, M.S., Angus-Hill, M., and Kardon, G. (2011). Connective tissue fibroblasts and Tcf4 regulate myogenesis. Development *138*, 371–384.

Mauro, A. (1961). Satellite cell of skeletal muscle fibers. J Biophys Biochem Cytol *9*, 493–495.

McKay, M.M., and Morrison, D.K. (2007). Integrating signals from RTKs to ERK/MAPK. Oncogene *26*, 3113–3121.

Meloche, S., and Pouysségur, J. (2007). The ERK1/2 mitogen-activated protein kinase pathway as a master regulator of the G1- to S-phase transition. Oncogene *26*, 3227–3239.

Mennerich, D., Schäfer, K., and Braun, T. (1998). Pax-3 is necessary but not sufficient for lbx1 expression in myogenic precursor cells of the limb. Mech. Dev. *73*, 147–158.

Merkus, H.G. (2009). Particle Size Measurements: Fundamentals, Practice, Quality (Springer Netherlands).

Messina, G., Biressi, S., Monteverde, S., Magli, A., Cassano, M., Perani, L., Roncaglia, E., Tagliafico, E., Starnes, L., Campbell, C.E., et al. (2010). Nfix regulates fetal-specific transcription in developing skeletal muscle. Cell *140*, 554–566.

Michailovici, I., Harrington, H.A., Azogui, H.H., Yahalom-Ronen, Y., Plotnikov, A., Ching, S., Stumpf, M.P.H., Klein, O.D., Seger, R., and Tzahor, E. (2014). Nuclear to cytoplasmic shuttling of ERK promotes differentiation of muscle stem/progenitor cells. Development *141*, 2611–2620.

Mohi, M.G., Williams, I.R., Dearolf, C.R., Chan, G., Kutok, J.L., Cohen, S., Morgan, K., Boulton, C., Shigematsu, H., Keilhack, H., et al. (2005). Prognostic, therapeutic, and mechanistic implications of a mouse model of leukemia evoked by Shp2 (PTPN11) mutations. Cancer Cell *7*, 179–191.

Moldovan, G.-L., Pfander, B., and Jentsch, S. (2007). PCNA, the maestro of the replication fork. Cell *129*, 665–679.

Moss, F.P., and Leblond, C.P. (1970). Nature of dividing nuclei in skeletal muscle of growing rats. J. Cell Biol. *44*, 459–462.

Moss, F.P., and Leblond, C.P. (1971). Satellite cells as the source of nuclei in muscles of growing rats. Anat. Rec. *170*, 421–435.

Mourikis, P., and Tajbakhsh, S. (2014). Distinct contextual roles for Notch signalling in skeletal muscle stem cells. BMC Dev. Biol. *14*, 2.

Mourikis, P., Gopalakrishnan, S., Sambasivan, R., and Tajbakhsh, S. (2012). Cell-autonomous Notch activity maintains the temporal specification potential of skeletal muscle stem cells. Development *139*, 4536–4548.

Murphy, L.O., Smith, S., Chen, R.-H., Fingar, D.C., and Blenis, J. (2002). Molecular interpretation of ERK signal duration by immediate early gene products. Nat. Cell Biol. *4*, 556–564.

Musarò, A. (2014). The Basis of Muscle Regeneration. Advances in Biology Article ID 612471.

Nabeshima, Y., Hanaoka, K., Hayasaka, M., Esumi, E., Li, S., Nonaka, I., and Nabeshima, Y. (1993). Myogenin gene disruption results in perinatal lethality because of severe muscle defect. Nature *364*, 532–535.

Noonan, J.A. (2006). Noonan syndrome and related disorders: alterations in growth and puberty. Rev Endocr Metab Disord *7*, 251–255.

O'Donnell, A., Odrowaz, Z., and Sharrocks, A.D. (2012). Immediate-early gene activation by the MAPK pathways: what do and don't we know? Biochem. Soc. Trans. *40*, 58–66.

Ogawa, R., Ma, Y., Yamaguchi, M., Ito, T., Watanabe, Y., Ohtani, T., Murakami, S., Uchida, S., De Gaspari, P., Uezumi, A., et al. (2015). Doublecortin marks a new population of transiently amplifying muscle progenitor cells and is required for myofiber maturation during skeletal muscle regeneration. Development *142*, 810.

Ontell, M., Feng, K.C., Klueber, K., Dunn, R.F., and Taylor, F. (1984). Myosatellite cells, growth, and regeneration in murine dystrophic muscle: a quantitative study. Anat. Rec. *208*, 159–174.

O'Reilly, A.M., Pluskey, S., Shoelson, S.E., and Neel, B.G. (2000). Activated mutants of SHP-2 preferentially induce elongation of Xenopus animal caps. Mol. Cell. Biol. *20*, 299–311.

Palacios, D., Mozzetta, C., Consalvi, S., Caretti, G., Saccone, V., Proserpio, V., Marquez, V.E., Valente, S., Mai, A., Forcales, S.V., et al. (2010). TNF/p38α/polycomb signaling to Pax7 locus in satellite cells links inflammation to the epigenetic control of muscle regeneration. Cell Stem Cell *7*, 455–469.

Patapoutian, A., Yoon, J.K., Miner, J.H., Wang, S., Stark, K., and Wold, B. (1995). Disruption of the mouse MRF4 gene identifies multiple waves of myogenesis in the myotome. Development *121*, 3347–3358.

Pérez-Cadahía, B., Drobic, B., and Davie, J.R. (2011). Activation and function of immediate-early genes in the nervous system. Biochem. Cell Biol. *89*, 61–73.

Perkins, L.A., Larsen, I., and Perrimon, N. (1992). corkscrew encodes a putative protein tyrosine phosphatase that functions to transduce the terminal signal from the receptor tyrosine kinase torso. Cell *70*, 225–236.

Pfaffl, M.W. (2001). A new mathematical model for relative quantification in real-time RT-PCR. Nucleic Acids Res. *29*, e45.

Picard, C.A., and Marcelle, C. (2013). Two distinct muscle progenitor populations coexist throughout amniote development. Dev. Biol. *373*, 141–148.

Price, F.D., Maltzahn, J. von, Bentzinger, C.F., Dumont, N.A., Yin, H., Chang, N.C., Wilson, D.H., Frenette, J., and Rudnicki, M.A. (2014). Inhibition of JAK-STAT signaling stimulates adult satellite cell function. Nat. Med. *20*, 1174–1181.

Qu, C.K., Shi, Z.Q., Shen, R., Tsai, F.Y., Orkin, S.H., and Feng, G.S. (1997). A deletion mutation in the SH2-N domain of Shp-2 severely suppresses hematopoietic cell development. Mol. Cell. Biol. *17*, 5499–5507.

Qu, C.K., Yu, W.M., Azzarelli, B., Cooper, S., Broxmeyer, H.E., and Feng, G.S. (1998). Biased suppression of hematopoiesis and multiple developmental defects in chimeric mice containing Shp-2 mutant cells. Mol. Cell. Biol. *18*, 6075–6082.

Qu, C.K., Nguyen, S., Chen, J., and Feng, G.S. (2001). Requirement of Shp-2 tyrosine phosphatase in lymphoid and hematopoietic cell development. Blood *97*, 911–914.

Relaix, F., Rocancourt, D., Mansouri, A., and Buckingham, M. (2005). A Pax3/Pax7-dependent population of skeletal muscle progenitor cells. Nature *435*, 948–953.

Relaix, F., Montarras, D., Zaffran, S., Gayraud-Morel, B., Rocancourt, D., Tajbakhsh, S., Mansouri, A., Cumano, A., and Buckingham, M. (2006). Pax3 and Pax7 have distinct and overlapping functions in adult muscle progenitor cells. J. Cell Biol. *172*, 91–102.

Relaix, F., Demignon, J., Laclef, C., Pujol, J., Santolini, M., Niro, C., Lagha, M., Rocancourt, D., Buckingham, M., and Maire, P. (2013). Six homeoproteins directly activate Myod expression in the gene regulatory networks that control early myogenesis. PLoS Genet. *9*, e1003425.

Ren, Y., Meng, S., Mei, L., Zhao, Z.J., Jove, R., and Wu, J. (2004). Roles of Gab1 and SHP2 in paxillin tyrosine dephosphorylation and Src activation in response to epidermal growth factor. J. Biol. Chem. *279*, 8497–8505.

Rocheteau, P., Gayraud-Morel, B., Siegl-Cachedenier, I., Blasco, M.A., and Tajbakhsh, S. (2012). A subpopulation of adult skeletal muscle stem cells retains all template DNA strands after cell division. Cell *148*, 112–125.

Rodgers, J.T., King, K.Y., Brett, J.O., Cromie, M.J., Charville, G.W., Maguire, K.K., Brunson, C., Mastey, N., Liu, L., Tsai, C.-R., et al. (2014). mTORC1 controls the adaptive transition of quiescent stem cells from G0 to G(Alert). Nature *510*, 393–396.

Rosen, G.D., Sanes, J.R., LaChance, R., Cunningham, J.M., Roman, J., and Dean, D.C. (1992). Roles for the integrin VLA-4 and its counter receptor VCAM-1 in myogenesis. Cell *69*, 1107–1119.

Rudnicki, M.A., Braun, T., Hinuma, S., and Jaenisch, R. (1992). Inactivation of MyoD in mice leads to up-regulation of the myogenic HLH gene Myf-5 and results in apparently normal muscle development. Cell *71*, 383–390.

Rudnicki, M.A., Schnegelsberg, P.N., Stead, R.H., Braun, T., Arnold, H.H., and Jaenisch, R. (1993). MyoD or Myf-5 is required for the formation of skeletal muscle. Cell *75*, 1351–1359.

Sachs, M., Brohmann, H., Zechner, D., Müller, T., Hülsken, J., Walther, I., Schaeper, U., Birchmeier, C., and Birchmeier, W. (2000). Essential role of Gab1 for signaling by the c-Met receptor in vivo. J. Cell Biol. *150*, 1375–1384.

Sadeh, M., Czyewski, K., and Stern, L.Z. (1985). Chronic myopathy induced by repeated bupivacaine injections. J. Neurol. Sci. *67*, 229–238.

Sambasivan, R., Yao, R., Kissenpfennig, A., Van Wittenberghe, L., Paldi, A., Gayraud-Morel, B., Guenou, H., Malissen, B., Tajbakhsh, S., and Galy, A. (2011). Pax7-expressing satellite cells are indispensable for adult skeletal muscle regeneration. Development *138*, 3647–3656.

Sato, T., Rocancourt, D., Marques, L., Thorsteinsdóttir, S., and Buckingham, M. (2010). A Pax3/Dmrt2/Myf5 regulatory cascade functions at the onset of myogenesis. PLoS Genet. *6*, e1000897.

Satoh, Y., Kobayashi, Y., Takeuchi, A., Pagès, G., Pouysségur, J., and Kazama, T. (2011). Deletion of ERK1 and ERK2 in the CNS causes cortical abnormalities and neonatal lethality: Erk1 deficiency enhances the impairment of neurogenesis in Erk2-deficient mice. J. Neurosci. *31*, 1149–1155.

Schaeper, U., Gehring, N.H., Fuchs, K.P., Sachs, M., Kempkes, B., and Birchmeier, W. (2000). Coupling of Gab1 to c-Met, Grb2, and Shp2 mediates biological responses. J. Cell Biol. *149*, 1419–1432.

Schaeper, U., Vogel, R., Chmielowiec, J., Huelsken, J., Rosario, M., and Birchmeier, W. (2007). Distinct requirements for Gab1 in Met and EGF receptor signaling in vivo. Proc. Natl. Acad. Sci. U.S.A. *104*, 15376–15381.

Schienda, J., Engleka, K.A., Jun, S., Hansen, M.S., Epstein, J.A., Tabin, C.J., Kunkel, L.M., and Kardon, G. (2006). Somitic origin of limb muscle satellite and side population cells. Proc. Natl. Acad. Sci. U.S.A. *103*, 945–950.

Schlessinger, J. (2000). Cell signaling by receptor tyrosine kinases. Cell *103*, 211–225.

Schultz, E., Gibson, M.C., and Champion, T. (1978). Satellite cells are mitotically quiescent in mature mouse muscle: an EM and radioautographic study. J. Exp. Zool. *206*, 451–456.

Schneider, R., Birchmeier, C.; (2011). Funktionelle Analyse des Shp2 Gens in der Entwicklung der Muskulatur der Maus. Freie Universität Berlin. FUDISS_derivate_000000010205

Seale, P., Sabourin, L.A., Girgis-Gabardo, A., Mansouri, A., Gruss, P., and Rudnicki, M.A. (2000). Pax7 is required for the specification of myogenic satellite cells. Cell *102*, 777–786.

Sears, R., Nuckolls, F., Haura, E., Taya, Y., Tamai, K., and Nevins, J.R. (2000). Multiple Ras-dependent phosphorylation pathways regulate Myc protein stability. Genes Dev. *14*, 2501–2514.

Shea, K.L., Xiang, W., LaPorta, V.S., Licht, J.D., Keller, C., Basson, M.A., and Brack, A.S. (2010). Sprouty1 regulates reversible quiescence of a self-renewing adult muscle stem cell pool during regeneration. Cell Stem Cell *6*, 117–129.

Sheean, M.E., McShane, E., Cheret, C., Walcher, J., Müller, T., Wulf-Goldenberg, A., Hoelper, S., Garratt, A.N., Krüger, M., Rajewsky, K., et al. (2014). Activation of MAPK overrides the termination of myelin growth and replaces Nrg1/ErbB3 signals during Schwann cell development and myelination. Genes Dev. *28*, 290–303.

Sheehan, S.M., and Allen, R.E. (1999). Skeletal muscle satellite cell proliferation in response to members of the fibroblast growth factor family and hepatocyte growth factor. J. Cell. Physiol. *181*, 499–506.

Siegel, A.L., Kuhlmann, P.K., and Cornelison, D.D.W. (2011). Muscle satellite cell proliferation and association: new insights from myofiber time-lapse imaging. Skelet Muscle *1*, 7.

Siles, L., Sánchez-Tilló, E., Lim, J.-W., Darling, D.S., Kroll, K.L., and Postigo, A. (2013). ZEB1 imposes a temporary stage-dependent inhibition of muscle gene expression and differentiation via CtBP-mediated transcriptional repression. Mol. Cell. Biol. *33*, 1368–1382.

Soleimani, V.D., Yin, H., Jahani-Asl, A., Ming, H., Kockx, C.E.M., van Ijcken, W.F.J., Grosveld, F., and Rudnicki, M.A. (2012). Snail regulates MyoD binding-site occupancy to direct enhancer switching and differentiation-specific transcription in myogenesis. Mol. Cell *47*, 457–468.

Sousa-Victor, P., Gutarra, S., García-Prat, L., Rodriguez-Ubreva, J., Ortet, L., Ruiz-Bonilla, V., Jardí, M., Ballestar, E., González, S., Serrano, A.L., et al. (2014). Geriatric muscle stem cells switch reversible quiescence into senescence. Nature *506*, 316–321.

Spörle, R. (2001). Epaxial-adaxial-hypaxial regionalisation of the vertebrate somite: evidence for a somitic organiser and a mirror-image duplication. Dev. Genes Evol. *211*, 198–217.

Srinivas, S., Watanabe, T., Lin, C.S., William, C.M., Tanabe, Y., Jessell, T.M., and Costantini, F. (2001). Cre reporter strains produced by targeted insertion of EYFP and ECFP into the ROSA26 locus. BMC Dev. Biol. *1*, 4.

Srinivasan, L., Sasaki, Y., Calado, D.P., Zhang, B., Paik, J.H., DePinho, R.A., Kutok, J.L., Kearney, J.F., Otipoby, K.L., and Rajewsky, K. (2009a). PI3 kinase signals BCR-dependent mature B cell survival. Cell *139*, 573–586.

Srinivasan, R., Zabuawala, T., Huang, H., Zhang, J., Gulati, P., Fernandez, S., Karlo, J.C., Landreth, G.E., Leone, G., and Ostrowski, M.C. (2009b). Erk1 and Erk2 regulate endothelial cell proliferation and migration during mouse embryonic angiogenesis. PLoS ONE *4*, e8283.

Stahl, N., Farruggella, T.J., Boulton, T.G., Zhong, Z., Darnell, J.E., and Yancopoulos, G.D. (1995). Choice of STATs and other substrates specified by modular tyrosine-based motifs in cytokine receptors. Science *267*, 1349–1353.

Sukhatme, V.P. (1990). Early transcriptional events in cell growth: the Egr family. J. Am. Soc. Nephrol. *1*, 859–866.

Swat, W., Shinkai, Y., Cheng, H.L., Davidson, L., and Alt, F.W. (1996). Activated Ras signals differentiation and expansion of CD4+8+ thymocytes. Proc. Natl. Acad. Sci. U.S.A. *93*, 4683–4687.

Tajbakhsh, S., and Buckingham, M. (2000). The birth of muscle progenitor cells in the mouse: spatiotemporal considerations. Curr. Top. Dev. Biol. *48*, 225–268.

Tajbakhsh, S., Rocancourt, D., Cossu, G., and Buckingham, M. (1997). Redefining the genetic hierarchies controlling skeletal myogenesis: Pax-3 and Myf-5 act upstream of MyoD. Cell *89*, 127–138.

Takahashi, A., Tsutsumi, R., Kikuchi, I., Obuse, C., Saito, Y., Seidi, A., Karisch, R., Fernandez, M., Cho, T., Ohnishi, N., et al. (2011). SHP2 tyrosine phosphatase converts parafibromin/Cdc73 from a tumor suppressor to an oncogenic driver. Mol. Cell *43*, 45–56.

Tartaglia, M., Martinelli, S., Iavarone, I., Cazzaniga, G., Spinelli, M., Giarin, E., Petrangeli, V., Carta, C., Masetti, R., Aricò, M., et al. (2005). Somatic PTPN11 mutations in childhood acute myeloid leukaemia. Br. J. Haematol. *129*, 333–339.

Tatsumi, R., Anderson, J.E., Nevoret, C.J., Halevy, O., and Allen, R.E. (1998). HGF/SF is present in normal adult skeletal muscle and is capable of activating satellite cells. Dev. Biol. *194*, 114–128.

Tefft, D., Lee, M., Smith, S., Crowe, D.L., Bellusci, S., and Warburton, D. (2002). mSprouty2 inhibits FGF10-activated MAP kinase by differentially binding to upstream target proteins. Am. J. Physiol. Lung Cell Mol. Physiol. *283*, L700–L706.

Tefft, D., De Langhe, S.P., Del Moral, P.-M., Sala, F., Shi, W., Bellusci, S., and Warburton, D. (2005). A novel function for the protein tyrosine phosphatase Shp2 during lung branching morphogenesis. Dev. Biol. *282*, 422–431.

Troy, A., Cadwallader, A.B., Fedorov, Y., Tyner, K., Tanaka, K.K., and Olwin, B.B. (2012). Coordination of satellite cell activation and self-renewal by Par-complex-dependent asymmetric activation of p38α/β MAPK. Cell Stem Cell *11*, 541–553.

Tsutsumi, R., Masoudi, M., Takahashi, A., Fujii, Y., Hayashi, T., Kikuchi, I., Satou, Y., Taira, M., and Hatakeyama, M. (2013). YAP and TAZ, Hippo signaling targets, act as a rheostat for nuclear SHP2 function. Dev. Cell *26*, 658–665.

Turner, A.M. (2014). Noonan syndrome. J Paediatr Child Health *50*, E14–E20.

Uezumi, A., Fukada, S., Yamamoto, N., Takeda, S., and Tsuchida, K. (2010). Mesenchymal progenitors distinct from satellite cells contribute to ectopic fat cell formation in skeletal muscle. Nat. Cell Biol. *12*, 143–152.

Uezumi, A., Ito, T., Morikawa, D., Shimizu, N., Yoneda, T., Segawa, M., Yamaguchi, M., Ogawa, R., Matev, M.M., Miyagoe-Suzuki, Y., et al. (2011). Fibrosis and adipogenesis originate from a common mesenchymal progenitor in skeletal muscle. J. Cell. Sci. *124*, 3654–3664.

Vasyutina, E., Stebler, J., Brand-Saberi, B., Schulz, S., Raz, E., and Birchmeier, C. (2005). CXCR4 and Gab1 cooperate to control the development of migrating muscle progenitor cells. Genes Dev. *19*, 2187–2198.

Vasyutina, E., Lenhard, D.C., Wende, H., Erdmann, B., Epstein, J.A., and Birchmeier, C. (2007). RBP-J (Rbpsuh) is essential to maintain muscle progenitor cells and to generate satellite cells. Proc. Natl. Acad. Sci. U.S.A. *104*, 4443–4448.

Vogel, W., and Ullrich, A. (1996). Multiple in vivo phosphorylated tyrosine phosphatase SHP-2 engages binding to Grb2 via tyrosine 584. Cell Growth Differ. *7*, 1589–1597.

Vogel, W., Lammers, R., Huang, J., and Ullrich, A. (1993). Activation of a phosphotyrosine phosphatase by tyrosine phosphorylation. Science *259*, 1611–1614.

Wagner, J., Schmidt, C., Nikowits, W., and Christ, B. (2000). Compartmentalization of the somite and myogenesis in chick embryos are influenced by wnt expression. Dev. Biol. *228*, 86–94.

Waskiewicz, A.J., Flynn, A., Proud, C.G., and Cooper, J.A. (1997). Mitogen-activated protein kinases activate the serine/threonine kinases Mnk1 and Mnk2. EMBO J. *16*, 1909–1920.

Watson, J.V., Chambers, S.H., and Smith, P.J. (1987). A pragmatic approach to the analysis of DNA histograms with a definable G1 peak. Cytometry *8*, 1–8.

Wellbrock, C., Karasarides, M., and Marais, R. (2004). The RAF proteins take centre stage. Nat. Rev. Mol. Cell Biol. *5*, 875–885.

White, R.B., Biérinx, A.-S., Gnocchi, V.F., and Zammit, P.S. (2010). Dynamics of muscle fibre growth during postnatal mouse development. BMC Dev. Biol. *10*, 21.

Williams, B.A., and Ordahl, C.P. (1994). Pax-3 expression in segmental mesoderm marks early stages in myogenic cell specification. Development *120*, 785–796.

Winer, J., Jung, C.K., Shackel, I., and Williams, P.M. (1999). Development and validation of real-time quantitative reverse transcriptase-polymerase chain reaction for monitoring gene expression in cardiac myocytes in vitro. Anal. Biochem. *270*, 41–49.

Yablonka-Reuveni, Z., Danoviz, M.E., Phelps, M., and Stuelsatz, P. (2015). Myogenic-specific ablation of Fgfr1 impairs FGF2-mediated proliferation of satellite cells at the myofiber niche but does not abolish the capacity for muscle regeneration. Front Aging Neurosci *7*, 85.

Yamamoto, S., Yoshino, I., Shimazaki, T., Murohashi, M., Hevner, R.F., Lax, I., Okano, H., Shibuya, M., Schlessinger, J., and Gotoh, N. (2005). Essential role of Shp2-binding sites on FRS2alpha for corticogenesis and for FGF2-dependent proliferation of neural progenitor cells. Proc. Natl. Acad. Sci. U.S.A. *102*, 15983–15988.

Yang, W., Klaman, L.D., Chen, B., Araki, T., Harada, H., Thomas, S.M., George, E.L., and Neel, B.G. (2006). An Shp2/SFK/Ras/Erk signaling pathway controls trophoblast stem cell survival. Dev. Cell *10*, 317–327.

Yang, W., Wang, J., Moore, D.C., Liang, H., Dooner, M., Wu, Q., Terek, R., Chen, Q., Ehrlich, M.G., Quesenberry, P.J., et al. (2013). Ptpn11 deletion in a novel progenitor causes metachondromatosis by inducing hedgehog signalling. Nature *499*, 491–495.

Yusuf, F., and Brand-Saberi, B. (2006). The eventful somite: patterning, fate determination and cell division in the somite. Anat. Embryol. *211 Suppl 1*, 21–30.

Zalc, A., Hayashi, S., Auradé, F., Bröhl, D., Chang, T., Mademtzoglou, D., Mourikis, P., Yao, Z., Cao, Y., Birchmeier, C., et al. (2014). Antagonistic regulation of p57kip2 by Hes/Hey downstream of Notch signaling and muscle regulatory factors regulates skeletal muscle growth arrest. Development *141*, 2780–2790.

Zammit, P.S., Heslop, L., Hudon, V., Rosenblatt, J.D., Tajbakhsh, S., Buckingham, M.E., Beauchamp, J.R., and Partridge, T.A. (2002). Kinetics of myoblast proliferation show that resident satellite cells are competent to fully regenerate skeletal muscle fibers. Exp. Cell Res. *281*, 39–49.

Zammit, P.S., Golding, J.P., Nagata, Y., Hudon, V., Partridge, T.A., and Beauchamp, J.R. (2004). Muscle satellite cells adopt divergent fates: a mechanism for self-renewal? J. Cell Biol. *166*, 347–357.

Zhang, S.Q., Tsiaras, W.G., Araki, T., Wen, G., Minichiello, L., Klein, R., and Neel, B.G. (2002). Receptor-specific regulation of phosphatidylinositol 3'-kinase activation by the protein tyrosine phosphatase Shp2. Mol. Cell. Biol. *22*, 4062–4072.

Zhang, W., Behringer, R.R., and Olson, E.N. (1995). Inactivation of the myogenic bHLH gene MRF4 results in up-regulation of myogenin and rib anomalies. Genes Dev. *9*, 1388–1399.

Zhao, P., Caretti, G., Mitchell, S., McKeehan, W.L., Boskey, A.L., Pachman, L.M., Sartorelli, V., and Hoffman, E.P. (2006). Fgfr4 is required for effective muscle regeneration in vivo. Delineation of a MyoD-Tead2-Fgfr4 transcriptional pathway. J. Biol. Chem. *281*, 429–438.

VII. Appendix

1. Supplementary figures
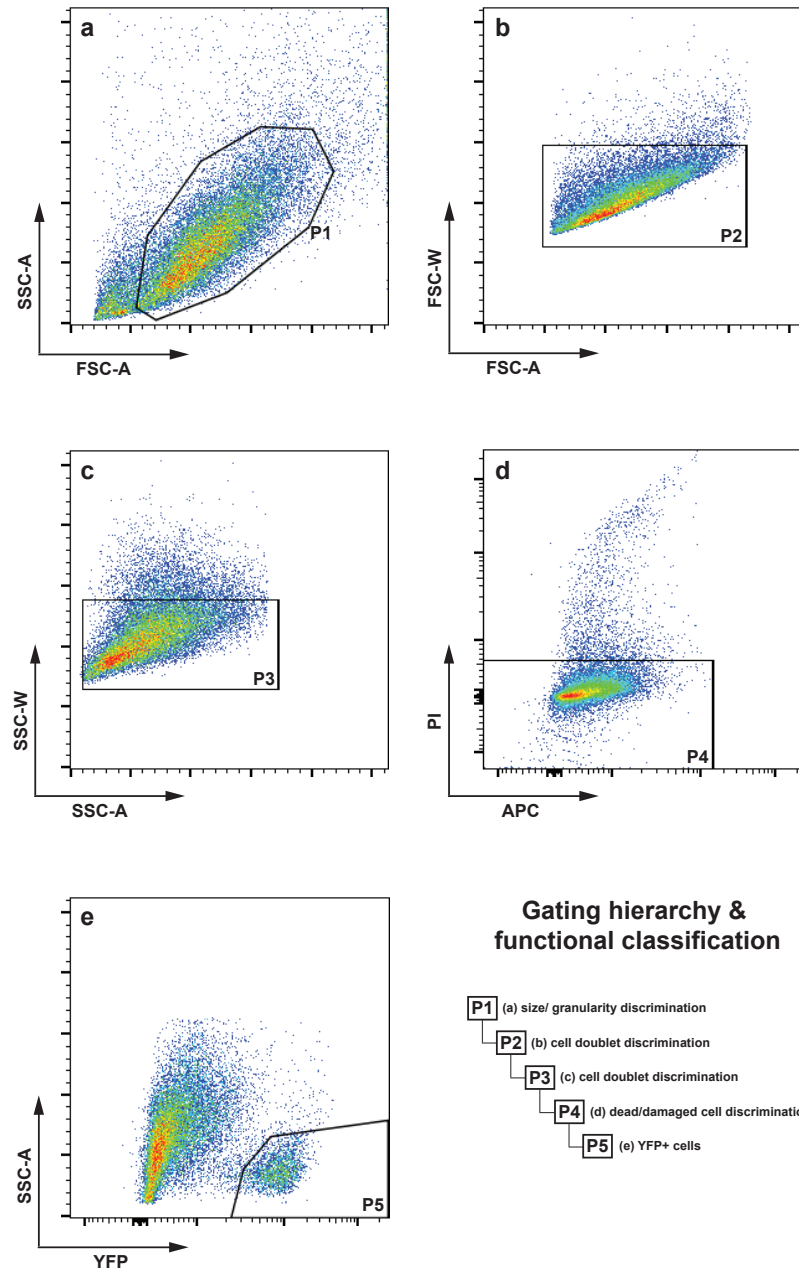
Fig.A1: Isolation of YFP-positive cells by FACS. Isolation of YFP+ myogenic cells from limb muscles of Pax7$^{ICNm/+}$; RYFP$^{+/-}$ mice at P0. Debris and cell doublets were excluded by forward scatter (FSC) and side scatter (SSC) parameters. Dead and damaged cells were excluded by propidium iodide (PI) staining. Population P5 was collected/ analyzed for further down-stream applications. YFP+ cells of E14.5 and E18.5 fetuses were isolated using the same procedure. A: Area, integration of detected laser intensity; W: width, pulse width of one event
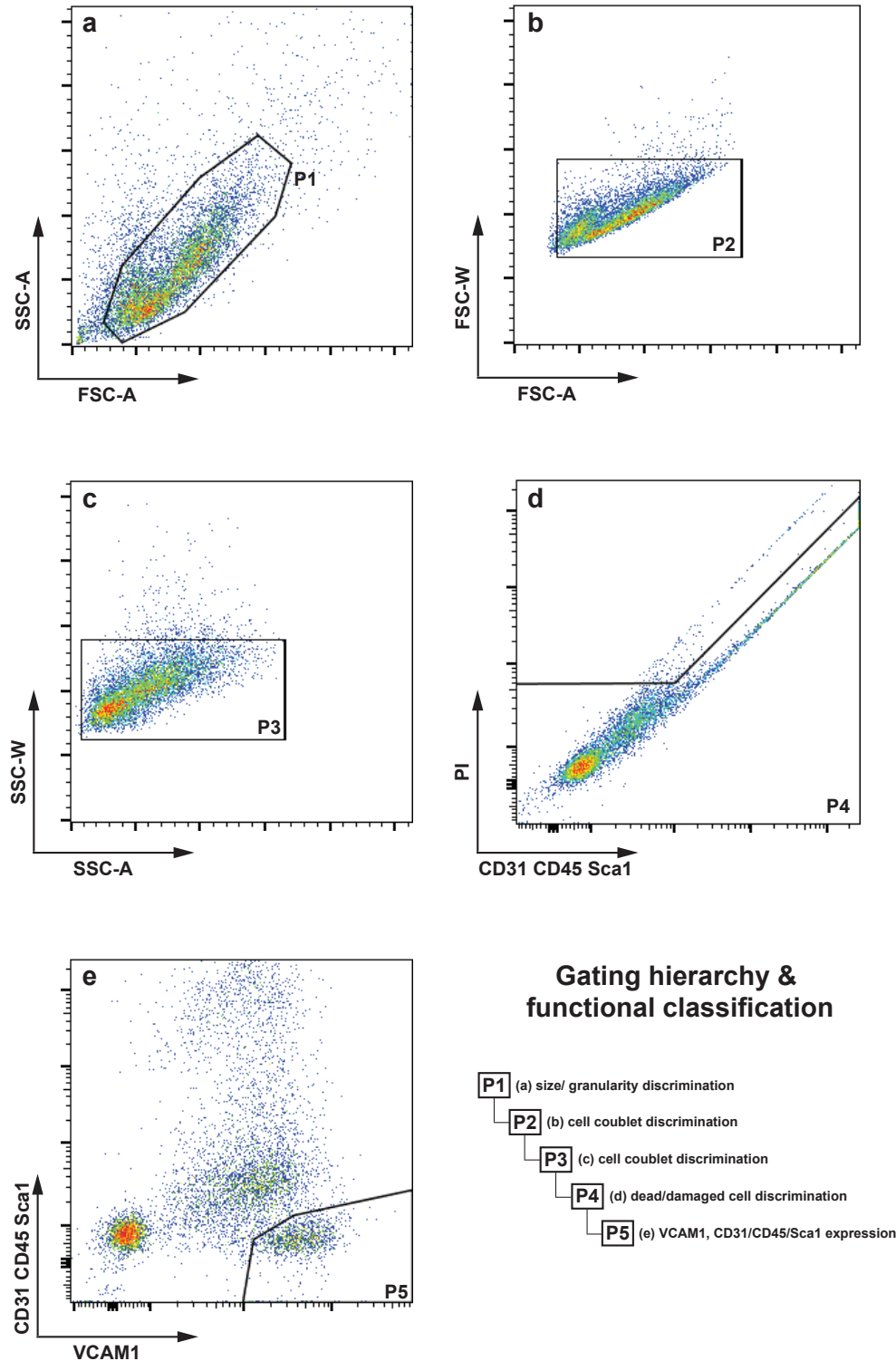
Fig.A2: Isolation of neonatal VCAM1+CD31-CD45-Sca1- cells by FACS. Cells were stained with PE-conjugated CD31, CD45, Sca1 and an anti-VCAM1 antibody combined with a Cy5-conjugated secondary antibody. Debris and cell doublets were excluded by FSC and SSC parameters. Dead and damaged cells were excluded by PI staining. Population P5 was collected/analyzed for further down-stream applications.
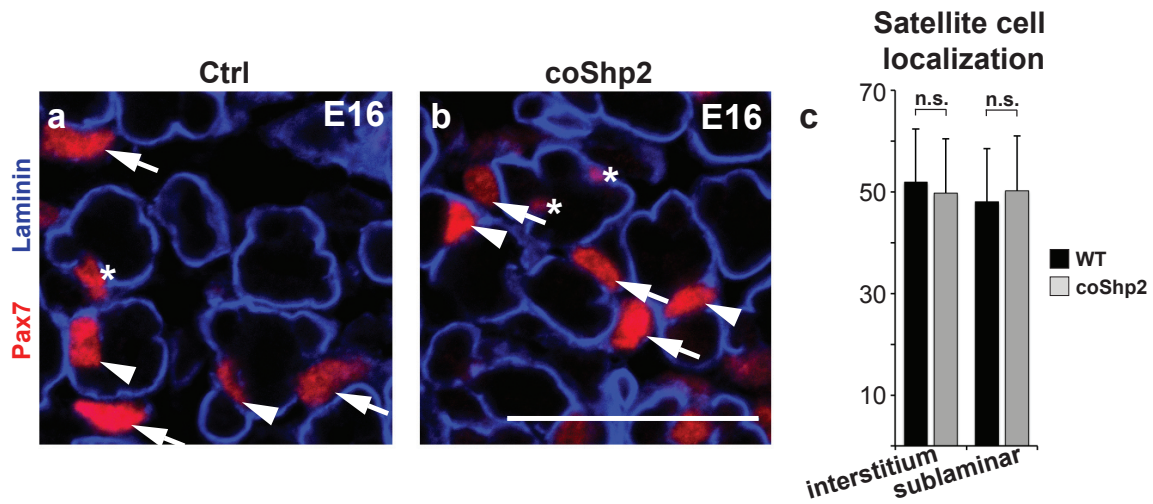
Fig.A3: Satellite cell homing is not impaired in Shp2 mutant Satellite cells. (a-b) Immunohistological analysis of forelimb muscle at E16.5 using an anti-Pax7 and anti-Laminin antibody. arrowheads: Satellite cells in a sublaminar position; arrows: Satellite cells in the interstitial space; star: Satellite cells with an unclear position were excluded from the quantification in Fig.A3c and Fig.3.4f. **c)** Quantification of Satellite cells in the interstitial space or located in between the muscle fiber and the developing basal lamina. Scale bar: 30 μm

Gating hierarchy & functional classification

P1 (a) size/ granularity discrimination
P2 (b) cell doublet discrimination
P3 (c) cell doublet discrimination
P4 (d) cell doublet discrimination
P5 (e) PI fluorescence
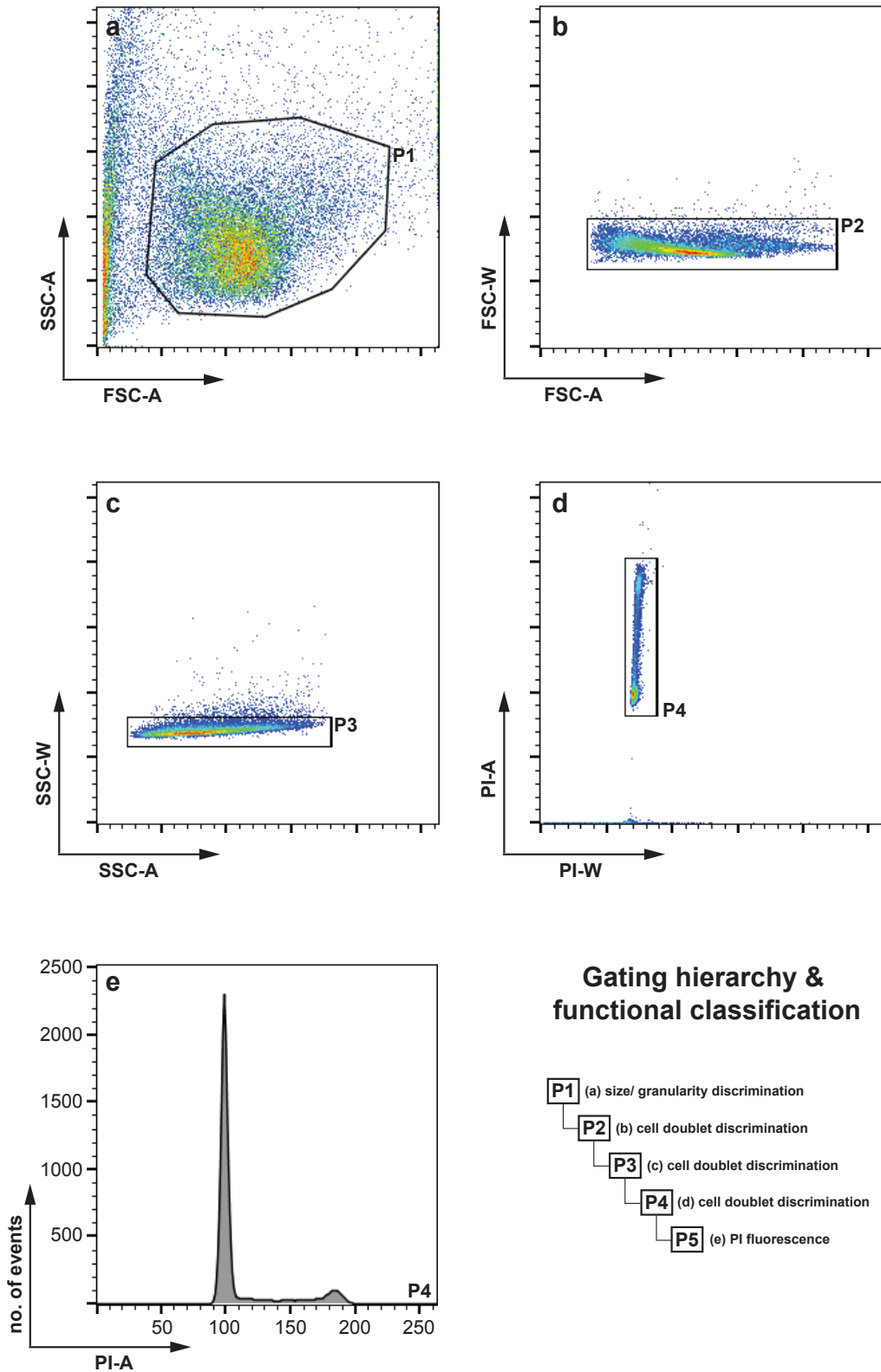
Fig. A4: Gating strategy to quantify propidium iodide fluorescence in YFP+ myogenic cells. Fixed YFP+ cells isolated from E18.5 fetuses according to Fig.A1 were stained with an excess of PI. FSC, SSC and PI parameters were used to exclude debris and cell doublets.
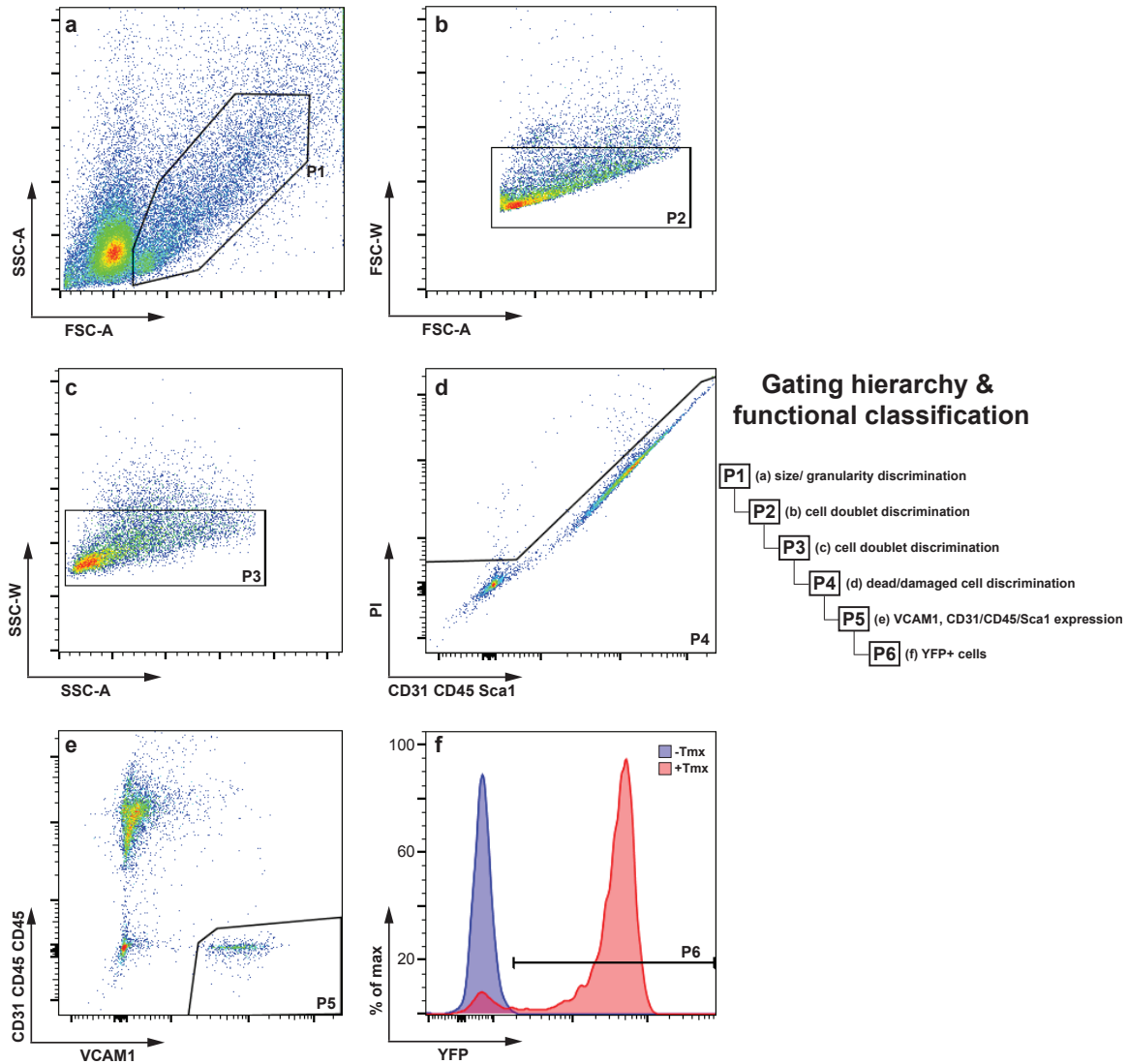
Fig.A5: Gating strategy to quantify YFP fluorescence of adult VCAM1+CD31-CD45-Sca1-cells from Pax7$^{CreERT2/+}$; RYFP$^{+/-}$ mice by flow cytometry. Cells were isolated from TA muscle 10 days after the last of 5 consecutive intraperitoneal Tamoxifen injections and stained with PE-conjugated anti-CD31, anti-CD45, anti-Sca1 and an anti-VCAM1 antibody combined with a Cy5-conjugated secondary antibody. Debris and cell doublets were excluded by FSC and SSC parameters. Dead and damaged cells were excluded by PI staining. Population P5 was analyzed for YFP expression.

Tab.A1: Down-regulated genes in neonatal Shp2 mutant Satellite cells. Differentially expressed transcripts in FACS-sorted VCAM1+CD31-CD45-Sca1- coShp2 (Pax7$^{ICNm/+}$; Shp2$^{flox/flox}$) and control (Pax7$^{ICNm/+}$; Shp2$^{flox/+}$) cells were determined by an ANOVA variance analysis. Shown are genes with a **fold-change < -1.5** and an **FDR < 0.075**.

SYMBOL	Definition	Fold-change coShp2 vs. Ctrl
Egr4	early growth response 4	-3.02
Kif18a	kinesin family member 18A	-2.97
Ccnd1	cyclin D1	-2.78
Iqsec3		-2.68
Clspn	claspin homolog	-2.67
Tnfrsf12a	tumor necrosis factor receptor superfamily, member 12a	-2.63
Plk2	polo-like kinase 2	-2.62
Egr2	early growth response 2	-2.59
Plk4	polo-like kinase 4	-2.44
Dek	DEK oncogene (DNA binding)	-2.44
Ndc80	NDC80 homolog, kinetochore complex component	-2.44
Klhl6	kelch-like 6 (Drosophila)	-2.42
Sdc3	syndecan 3	-2.36
Arbp	ribosomal protein, large, P0	-2.35
C79407	expressed sequence C79407	-2.34
F630043A04Rik	RIKEN cDNA F630043A04 gene	-2.31
Cdc2a	cell division cycle 2 homolog A	-2.28
Esco2	establishment of cohesion 1 homolog 2	-2.27
5830411K18Rik	WD repeat domain 76	-2.23
Zfp367	zinc finger protein 367	-2.23
2610300B10Rik	centromere protein L	-2.22
Ccnb1	cyclin B1	-2.22
5830426I05Rik	non-SMC condensin II complex, subunit G2	-2.19
Rnaset2	ribonuclease T2B	-2.17
F2rl1	coagulation factor II (thrombin) receptor-like 1	-2.16
Clspn	claspin homolog	-2.14
Thyn1	thymocyte nuclear protein 1	-2.14
Cacng5	calcium channel, voltage-dependent, gamma subunit 5	-2.14
Upp1	uridine phosphorylase 1	-2.12
Cenpl	centromere protein L	-2.11
Ranbp1	RAN binding protein 1	-2.11
Zfp131	PREDICTED: similar to putative transcription factor ZNF131, transcript variant 1	-2.11
Upp1	uridine phosphorylase 1	-2.10
Cdca4	cell division cycle associated 4	-2.09
Cenph	centromere protein H	-2.04
Ccrn4l	CCR4 carbon catabolite repression 4-like	-2.04
Eif1a	eukaryotic translation initiation factor 1A	-2.02
Pcna	proliferating cell nuclear antigen	-2.02
Etv5	ets variant gene 5	-2.01
Icsbp1	interferon regulatory factor 8	-2.00
Ssb4	splA/ryanodine receptor domain and SOCS box containing 4	-2.00
Nol5	nucleolar protein 5	-2.00
4930452B06Rik	RIKEN cDNA 4930452B06 gene	-1.99
Dbf4	DBF4 homolog	-1.97
Kif11	kinesin family member 11	-1.96
Jam2	junction adhesion molecule 2	-1.93
2610016F04Rik	polybromo 1	-1.90
Emid2	EMI domain containing 2	-1.89
Tyms	thymidylate synthase	-1.88
Map3k14	mitogen-activated protein kinase kinase kinase 14	-1.87
Fen1	flap structure specific endonuclease 1	-1.87
2700084L22Rik	ubiquitin-conjugating enzyme E2T	-1.86
5830426I05Rik	non-SMC condensin II complex, subunit G2	-1.86
Psip1	PC4 and SFRS1 interacting protein 1	-1.82
Vcam1	vascular cell adhesion molecule 1	-1.81
Sertad1	SERTA domain containing 1	-1.80
Ndufa4	NADH dehydrogenase (ubiquinone) 1 alpha subcomplex, 4	-1.80
Pknox1	Pbx/knotted 1 homeobox	-1.80
Twistnb	TWIST neighbor	-1.79
Siah2	seven in absentia 2	-1.78
Vil2	PREDICTED: hypothetical protein LOC100044177	-1.77
Sdpr	serum deprivation response	-1.76

Continuation of Tab.A1

Popdc3	popeye domain containing 3	-1.76
Maff	v-maf musculoaponeurotic fibrosarcoma oncogene family, protein F	-1.76
Rab38	Rab38, member of RAS oncogene family	-1.76
Sec63	SEC63-like	-1.75
1810014F10Rik	nuclear autoantigenic sperm protein (histone-binding) transcript variant 2	-1.75
Timeless	timeless homolog transcript variant 2	-1.74
Trim59	tripartite motif-containing 59	-1.72
Hspca	heat shock protein 90, alpha (cytosolic), class A member 1	-1.72
Eed	embryonic ectoderm development	-1.72
Cacybp	calcyclin binding protein	-1.71
2410042D21Rik	RIKEN cDNA 2410042D21 gene	-1.70
C77032	guanine nucleotide binding protein-like 3 (nucleolar) transcript variant 1	-1.70
Midn	midnolin	-1.69
Pcf11	cleavage and polyadenylation factor subunit homolog	-1.68
Dek	DEK oncogene (DNA binding)	-1.68
Ssb	Sjogren syndrome antigen B	-1.67
Rbp7	retinol binding protein 7, cellular	-1.67
Hspd1	heat shock protein 1 (chaperonin)	-1.67
C87860	NMD3 homolog	-1.66
Taf5	TAF5 RNA polymerase II, TATA box binding protein (TBP)-associated factor	-1.66
Nup62	nucleoporin 62	-1.62
LOC654426	ATP synthase, H+ transporting, mitochondrial F0 complex, subunit F pseudogene	-1.61
Pkn2	protein kinase N2	-1.60
Shcbp1	Shc SH2-domain binding protein 1	-1.59
Kif4	kinesin family member 4	-1.58
Ddx6	DEAD (Asp-Glu-Ala-Asp) box polypeptide 6	-1.58
Rnpc2		-1.56
Cdc25c	cell division cycle 25 homolog C	-1.56
Spcs3	signal peptidase complex subunit 3 homolog	-1.55
Smad5	MAD homolog 5	-1.54
Hccs	holocytochrome c synthetase	-1.53
4921537D05Rik	coiled-coil domain containing 41	-1.52
4930427A07Rik	RIKEN cDNA 4930427A07 gene	-1.50

Tab.A2: Up-regulated genes in neonatal Shp2 mutant Satellite cells. Differentially expressed transcripts in FACS-sorted VCAM1+CD31-CD45-Sca1- coShp2 (Pax7$^{ICNm/+}$; Shp2$^{flox/flox}$) and control (Pax7$^{ICNm/+}$; Shp2$^{flox/+}$) cells were determined by an ANOVA variance analysis. Shown are genes with a **fold-change > 1.5** and an **FDR < 0.075**.

SYMBOL	Definition	Fold-change coShp2 vs. Ctrl
Sln	sarcolipin	8.69
Adh1	alcohol dehydrogenase 1 (class I)	3.47
Adh1	alcohol dehydrogenase 1 (class I)	3.23
Igfbp6	insulin-like growth factor binding protein 6	3.06
Actn3	actinin alpha 3	3.04
Pdgfra	platelet derived growth factor receptor, alpha polypeptide (Pdgfra), transcript variant 1	2.97
Ppap2b	phosphatidic acid phosphatase type 2B	2.91
Adamts2	a disintegrin-like and metallopeptidase (reprolysin type) with thrombospondin type 1 motif, 2	2.90
Nfatc4	nuclear factor of activated T-cells, cytoplasmic, calcineurin-dependent 4	2.83
Mfap4	microfibrillar-associated protein 4	2.83
Fmod	fibromodulin	2.82
Meox1	mesenchyme homeobox 1	2.80
Myh8	myosin, heavy polypeptide 8, skeletal muscle, perinatal	2.80
Fmod	fibromodulin	2.75
Adamts2	a disintegrin-like and metallopeptidase (reprolysin type) with thrombospondin type 1 motif, 2	2.70
Mfap2	microfibrillar-associated protein 2	2.62
Scube2	signal peptide, CUB domain, EGF-like 2	2.55
Tnxb	tenascin XB	2.55
2610027C15Rik	RIKEN cDNA 2610027C15 gene	2.49
Dcn	decorin	2.49
Rasl11b	RAS-like, family 11, member B	2.48
Mip	major intrinsic protein of eye lens fiber	2.47
Htra1	HtrA serine peptidase 1	2.47
Kera	keratocan	2.43
Ctsf	cathepsin F	2.40
Tmem119	transmembrane protein 119	2.35
Adamts2	a disintegrin-like and metallopeptidase (reprolysin type) with thrombospondin type 1 motif, 2	2.34
Tnnc2	troponin C2, fast	2.33
Mfap2	microfibrillar-associated protein 2	2.33
Htra1	HtrA serine peptidase 1	2.32
Igfbp4	insulin-like growth factor binding protein 4	2.32
Cxcl14	chemokine (C-X-C motif) ligand 14	2.31
Dbx1	developing brain homeobox 1	2.29
Actn3	actinin alpha 3	2.28
Mfng	MFNG O-fucosylpeptide 3-beta-N-acetylglucosaminyltransferase	2.28
Etv4	ets variant gene 4 (E1A enhancer binding protein, E1AF)	2.27
Gja1	gap junction membrane channel protein alpha 1	2.25
Srpx	sushi-repeat-containing protein	2.25
Bmper	BMP-binding endothelial regulator	2.24
Serping1	serine (or cysteine) peptidase inhibitor, clade G, member 1	2.23
Col12a1	collagen, type XII, alpha 1	2.23
Akap12	A kinase (PRKA) anchor protein (gravin) 12	2.21
2610001E17Rik	coiled-coil domain containing 80	2.19
Col1a2	collagen, type I, alpha 2	2.18
2610027C15Rik	RIKEN cDNA 2610027C15 gene	2.18
Aqp1	aquaporin 1	2.18
Rasl11b	RAS-like, family 11, member B	2.14
Mmp23	matrix metallopeptidase 23	2.13
Myh2		2.11
E430002G05Rik	RIKEN cDNA E430002G05 gene	2.11
Ramp1	receptor (calcitonin) activity modifying protein 1	2.08
Fmo1	flavin containing monooxygenase 1	2.08
Loxl1	lysyl oxidase-like 1	2.07
BC054438	transmembrane protein 204	2.06
Ngfr	nerve growth factor receptor (TNFR superfamily, member 16)	2.05
Ccnd2	cyclin D2	2.05
Mrgprf	MAS-related GPR, member F	2.04
Slitl2	vasorin	2.04

Continuation of Tab.A2

Klf2	Kruppel-like factor 2 (lung)	2.03
Srpx	sushi-repeat-containing protein	2.03
Asb2	ankyrin repeat and SOCS box-containing 2	2.01
Espnl	espin-like	2.00
Stk23	serine/arginine-rich protein specific kinase 3	2.00
Mfap2	microfibrillar-associated protein 2	2.00
Pitx2	paired-like homeodomain transcription factor 2 transcript variant 3	1.99
Vtn	vitronectin	1.99
Vps33a	vacuolar protein sorting 33A	1.98
Nupr1	nuclear protein 1	1.92
Ldb2		1.91
Neu1	neuraminidase 1	1.90
1500015O10Rik	RIKEN cDNA 1500015O10 gene	1.90
Nrap	nebulin-related anchoring protein transcript variant 2	1.90
BC046404	cDNA sequence BC046404	1.90
1810054O13Rik	transmembrane protein 86A	1.90
Igfbp7	insulin-like growth factor binding protein 7	1.90
Rassf2	Ras association (RalGDS/AF-6) domain family member 2	1.89
Col14a1	collagen, type XIV, alpha 1	1.88
9130416N05Rik	ankyrin repeat domain 39	1.86
Abhd4	abhydrolase domain containing 4	1.85
Pgam2	phosphoglycerate mutase 2	1.84
Nrn1	neuritin 1 (	1.84
BC046404	cDNA sequence BC046404	1.83
C1qtnf6	C1q and tumor necrosis factor related protein 6	1.83
1110012D08Rik	RIKEN cDNA 1110012D08 gene	1.83
Postn	periostin, osteoblast specific factor	1.82
Gng7	guanine nucleotide binding protein (G protein), gamma 7 transcript variant 2	1.80
Ckm	creatine kinase, muscle	1.78
Eln	elastin	1.77
Cyhr1	cysteine and histidine rich 1 transcript variant 2	1.77
Tnnc1	troponin C, cardiac/slow skeletal	1.75
Gstt3	glutathione S-transferase, theta 3	1.75
Yipf3	Yip1 domain family, member 3	1.73
Col6a1	procollagen, type VI, alpha 1	1.71
Fcgrt	Fc receptor, IgG, alpha chain transporter	1.70
Gnb3	guanine nucleotide binding protein (G protein), beta 3	1.69
Vldlr	very low density lipoprotein receptor	1.68
Tex264	testis expressed gene 264 transcript variant 1	1.67
Rras	Harvey rat sarcoma oncogene, subgroup R	1.65
AI415330	adhesion molecule with Ig like domain 2	1.63
Myoz1	myozenin 1	1.61
C230075L19Rik	zer-1 homolog	1.61
Apbb1ip	amyloid beta (A4) precursor protein-binding, family B, member 1 interacting protein	1.59
Kazald1	Kazal-type serine peptidase inhibitor domain 1	1.59
Lrpap1	low density lipoprotein receptor-related protein associated protein 1	1.57
Ggtla1	gamma-glutamyltransferase 5	1.54
AI429612	integrin alpha FG-GAP repeat containing 3	1.54
Dnaja2	DnaJ (Hsp40) homolog, subfamily A, member 2	1.53
1110005A03Rik		1.53
Mir16	membrane interacting protein of RGS16	1.52
Bicc1	bicaudal C homolog 1	1.52
Ivd	isovaleryl coenzyme A dehydrogenase, nuclear gene encoding mitochondrial protein	1.51
Asb10	ankyrin repeat and SOCS box-containing protein 10	1.51
Dctn2	dynactin 2	1.50
Scg3	secretogranin III	1.50

2. Abbreviations

Adamts	a disintegrin and metalloproteinase with thrombospondin motifs
ANOVA	analysis of variance
bHLH	basic helix loop helix
BMP	bone morphogenetic protein
BrdU	5-Bromo-2'deoxyuridine
BSA	bovine serum albumin
cDNA	copy DNA
Col	collagen
coShp2	conditional Shp2
cRNA	copy DNA
csw	corkscrew
Ctbp	C-terminal binding protein
Ctrl	control
CTX	cardiotoxin
DAPI	4',6-diamidino-2-phenylindole
DMSO	dimethyl sulfoxide
DNA	desoxyribonucleic acid
DPBS	Dulbecco's phosphate buffered saline
DRR	distal regulatory region
E	embryonal day
ECRL	extensor carpi radialis longus
EDL	extensor digitorum l
EDTA	ethylenediaminetetraacetic acid
Egr	early growth response
EGTA	ethylene glycol tetraacetic acid
Elk	Ets like factor
Erk	extracellular signal-regulated kinase
EtOH	ethanol
Eya1/2	eyes absent 1/2
EYFP	enhanced yellow fluorescent protein
FACS	fluorescence activated cell sorting
FDR	false discovery rate
Fgf	fibroblast growth factor
Fgfr	fibroblast growth factor receptor
FLP	flipase
FRS	fibroblast growth factor receptor substrate
Fzd7	Frizzled 7
Gab1	Grb2-associated protein 1
GFP	green fluorescent protein
Grb2	growth factor receptor-bound protein 2
HDAC	histone deacetylase
Hes1	Hairy enhancer of split family bHLH transcription factor 1
Hey1	Hes-related family bHLH transcription factor with YRPW motif 1
HeyL	Hes-related family bHLH transcription factor with YRPW motif-like
HGF	hepatocyte growth factor
HMGA2	histone mobility group A2

HRP	horse radish peroxidase
IF	immunofluorescence
Igfbp	insulin growth factor binding protein
Igfr	insulin-like growth factor receptor
IRES	internal ribosome entry site
IRS	insulin-like growth factor receptor substrate
JMML	juvenile myelomonocytic leukemia
Jnk	c-Jun N-terminal kinase
KSR	kinase suppressor of Ras
Lbx1	Ladybird homeobox 1
LEOPARD	Noonan syndrome with multiple lentigenes
LRC	Label retaining
Mapk	mitogen activated kinase
Mapkk	mitogen activated kinase kinase
Mapkkk	mitogen activated kinase kinase kinase
MCK	muscle creatine kinase
MetOH	methanol
Mmp	matrix metallo proteinase
Mnk1/2	MAP kinase-activated protein kinase
MP1	MEK partner 1
Mrf4	myogenic regulatory factor 4
Msk1/2	mitogen and stress-activated protein kinase
mTORC1	mammalian target of rapamycin complex 1
Myf5	myogenic factor 5
MyoD	myogenic differentiation 1
MyoG	myogenin
NFAT	nuclear factor of activated T-cells
Nfix	nuclear factor 1 X-type
NICD	Notch intracellular domain
NLRC	non label retaining
P	postnatal day
Pax3/7	paired box gene 3/7
PCNA	proliferating cell nuclear antigen
PCR	polymerase chain reaction
Pdgf	platelet derived growth factor
Pdgfr	platelet derived growth factor receptor
PFA	para-formaldehyde
PSM	presomitic mesoderm
PTP	protein tyrosine phosphatase
PTPN11	protein tyrosine phosphatase 11
qPCR	quantitative polymerase chain reaction
RNA	ribonucleic acid
Rsk	ribosomal S6 kinase
RTK	receptor tyrosine kinase
SDF1	stromal derived factor 1
SH2	src homology domain containing

Shc	Src homology 2 domain containing 1
Shh	sonic hedgehog
Shp2	SH2-domain containing tyrosine phosphatase
Six1/4	sine oculis homeobox homolog 1/4
slowMyHC	slow myosin heavy chain
Sos	son of sevenless
SRE	serum response element
TA	Tibialis anterior
TCF	T-cell factor
Tgfb	transforming growth factor beta
Thr	threonine
Tmx	tamoxifen
Tyr	tyrosine
VCAM1	vascular cell adhesion molecule 1
Wnt7a	wingless-type MMTV integration site family member 7a
WT	wild type
YFP	yellow fluorescent protein
Zeb1	Zinc finger E-box binding homeobox 1

3. Eidesstattliche Erklärung

Hiermit versichere ich, die vorliegende Dissertation selbstständig und ohne unerlaubte Hilfe angefertigt zu haben.

Bei der Verfassung der Dissertation wurden keine anderen als die im Text angegebenen Quellen und Hilfsmittel verwendet.

Ein Promotionsverfahren wurde zu keinem früheren Zeitpunkt an einer anderen Hochschule oder bei einem anderen Fachbereich beantragt.

Berlin, den 27.07.2015

_____

Joscha Griger